(Phospho)regulation of kinetochore-microtubule attachment
and spindle checkpoint activity by the Mps1 kinase

by

John Maciejowski

A Dissertation

Presented to the Faculty of the Louis V. Gerstner, Jr.

Graduate School of Biomedical Sciences,

Memorial Sloan-Kettering Cancer Center

in Partial Fulfillment of the Requirements for the Degree of

Doctor of Philosophy

New York, NY

October, 2013

_____   _____
Prasad V. Jallepalli, MD, PhD   Date   10/14/2013
Dissertation Mentor

To my family and friends.

ABSTRACT

Accurate chromosome segregation during mitosis relies on the successful collaboration of a large set of mitotic kinases. Untangling the linear relationships between these kinases and their substrates is essential to understanding mitotic progression. The evolutionarily conserved kinase Mps1 protects genome stability by promoting chromosome bi-orientation and by enforcing the spindle assembly checkpoint, a surveillance pathway that restrains anaphase until all chromatids properly attach to the mitotic spindle (Foley and Kapoor, 2013; Lan and Cleveland, 2010; Musacchio and Salmon, 2007). Despite a central role for Mps1 in these processes few of its substrates have been identified in higher eukaryotes. Quantitation of over 20,000 phosphorylation sites revealed Mps1-regulated modifications on numerous kinetochore proteins including Mps1 itself, Histone H2A, the spindle checkpoint proteins Bub1, BubR1, and Mad1, and the outer kinetochore proteins Hec1,KNL1 and Ska3 (Santaguida and Musacchio, 2009). Analysis of the spatial and temporal distribution of Mps1-regulated phosphorylation events with modification-specific antibodies demonstrates that Mps1 targets its substrates within the outer kinetochore primarily when microtubule occupancy is weak to non-existent and does so under the regulation of the B56-PP2A phosphatase (Foley et al., 2011). Finally, we identify Ska3 as a direct Mps1 substrate that mediates efficient chromosome bi-orientation and K-fiber stability (Gaitanos et al., 2009; Schmidt et al., 2012; Welburn et al., 2009). Total internal reflection microscopy (TIRF-M) experiments indicate that this phosphorylation event increases the number of short-lived Ska complex particles

on microtubules and reduces the size of tracking complexes on dynamic microtubules. Our study has identified and functionally validated the first Mps1 substrate in higher eukaryotes and shows how this kinase monitors and regulates kinetochore activity to achieve high fidelity chromosome segregation. This partnership between chemical genetics and quantitative proteomics promises to be a potent tool in making accurate and direct links between kinases and their substrates.

VITAE

John was born in New York City where he remained for his graduate studies.

ACKNOWLEDGMENTS

TABLE OF CONTENTS

LIST OF FIGURES

LIST OF TABLES

LIST OF ABBREVIATIONS

AAV - adeno-associated virus

APC/C - anaphase promoting complex/cyclosome

as - analog sensitive

CH - calponin homology

CENP - centromere protein

CCAN - constitutive centromere associated network

Dam1 - Duo1 and Mps1 interacting

FDR - false discovery rate

G - gap

GMPCPP - guanylyl 5'-α,β-methylenediphosphonate

Hec1 - highly expressed in cancer 1

hTERT - human telomerase reverse transcriptase

IP – immunoprecipitation

KD – kinase dead

KMN - KNL1-Mis12-Ndc80

KNL1 - kinetochore null 1

KT - kinetochore

Mad1 - mitotic arrest deficient 1

Mad2 - mitotic arrest deficient 2

Mis12 - missegregation 12

Mps1 - monopolar spindle 1

ms - millisecond

MT - microtubule

Ndc80 - nuclear division cycle 80

NEBD - nuclear envelope breakdown

PP1 - protein phosphatase 1

PP2A - protein phosphatase 2A

RPE - retinal pigment epithelial

RZZ - Rod Zwilch Zw10

S - Svedberg

s - second

SAC - Spindle Assembly Checkpoint

SAM - statistical analysis of microarrays

Ska - spindle and kinetochore associated

SILAC - stable isotope labeling of amino acids in cell culture

STLC - S-trityl-L-cysteine

TFA - trifluoroacetic acid

wt - wild type

Zw10 - zeste white 10

CHAPTER ONE: Introduction

During mitosis the cell segregates its duplicated genome into two daughter cells. Chromosome segregation is powered by a dynamic, microtubule-based mitotic spindle that makes physical attachments to chromatids at a proteinaceous structure termed the kinetochore (Santaguida and Musacchio, 2009). In order to maintain fidelity during chromosome segregation, the cell monitors the presence and quality of these attachments, destabilizing improper attachments and selectively stabilizing correct attachments (Foley and Kapoor, 2013). In addition, a cell cycle checkpoint, named the spindle assembly checkpoint (SAC) delays anaphase until each kinetochore has made a proper attachment to the mitotic spindle (Musacchio and Salmon, 2007). Not surprisingly, unattached kinetochores are a major source of the SAC. Kinetochore-microtubule attachment and SAC signaling are both regulated by a large set of mitotic kinases, including Mps1. The precise contribution of many of these kinases, in particular Mps1, to these processes, their place in the signaling hierarchy, and relevant substrates are often unknown (Funabiki and Wynne, 2013; Zich and Hardwick, 2010). Phosphatases provide another regulatory control of kinetochore function helping to stabilize proper kinetochore-microtubule attachments and trigger the anaphase switch by extinguishing the SAC (Foley et al., 2011; Liu et al., 2010; Pinsky et al., 2009; Rosenberg et al., 2011). Thus, successful chromosome segregation during mitosis depends on the precise regulation of kinetochore function by mitotic kinases and phosphatases.

The Kinetochore

An Overview

The primary function of the kinetochore (KT) (from the Greek 'kineto-', meaning 'move', and '-chore', meaning 'means for distribution') is to ensure accurate chromosome segregation by establishing and maintaining an interaction between centromeric DNA and spindle microtubules (MTs) (Cheeseman and Desai, 2008). The KT provides a sturdy interface for force generated by the depolymerizing spindle MTs that power chromosome movement to daughter cells (Joglekar et al., 2010; Rago and Cheeseman, 2013). KTs assemble on centromeric chromatin immediately after nuclear envelope breakdown (NEBD) (Figure 1.1A) (Torras-Llort et al., 2009). Protein localization to and association with the kinetochore is dynamic, but roughly 100 proteins are known to associate with the kinetochore at some time during mitosis. KTs first make lateral attachments to spindle MTs (Figure 1.1B) that are converted to mature end-on attachments, in part by dynein (Li et al., 2007). KTs that have not yet made stable attachments to spindle MTs catalyze the production of an anaphase inhibitor, and provide a source of the spindle assembly checkpoint (SAC), which will be discussed in detail below(Musacchio and Salmon, 2007). Successful, end-on kinetochore-microtubule interactions are termed amphitelic and are produced as sister chromatids become bi-oriented on the metaphase plate (Figure 1.1A). Once every kinetochore has made productive attachments to spindle microtubules, the source of the SAC is extinguished, and chromatids separate towards opposite spindle poles.

The KMN Network

Studies in yeast, worms, fruit flies, and cultured cells as well as biochemical evidence have universally pointed to a large complex of proteins as the core MT-binding activity of the kinetochore.

The KMN network, comprised of Hec1 (Ndc80 complex) complexed with Mis12 (Mtw1 complex) and KNL1 (Spc105), serves as the central KT-MT face in all eukaryotes (Cheeseman et al., 2006; Ciferri et al., 2008; Wei et al., 2005). Inactivation of any component of the KMN network has deleterious consequences for the cell by leading to defective KT-MT attachment and chromosome missegregation at anaphase (DeLuca et al., 2005; Desai et al., 2003; Wigge and Kilmartin, 2001).

Hec1 (Ndc80) binds spindle MTs through conserved calponin homology (CH) domains. These positively charged domains directly interact electrostatically with spindle MTs (Ciferri et al., 2008). Mutations in these domains completely disrupt MT-binding *in vivo* and *in vitro* (Ciferri et al., 2008; Sundin et al., 2011; Tooley et al., 2011). These negatively charged CH domains work in concert with Hec1's positively charged, unstructured, N-terminal tail to capture spindle MTs.

a

Interphase (G2)

Prophase

Prometaphase

Metaphase

Anaphase

Telophase

Chromosome

Kinetochore

Microtubule

Sister chromatids

b

1
2
3
4
5
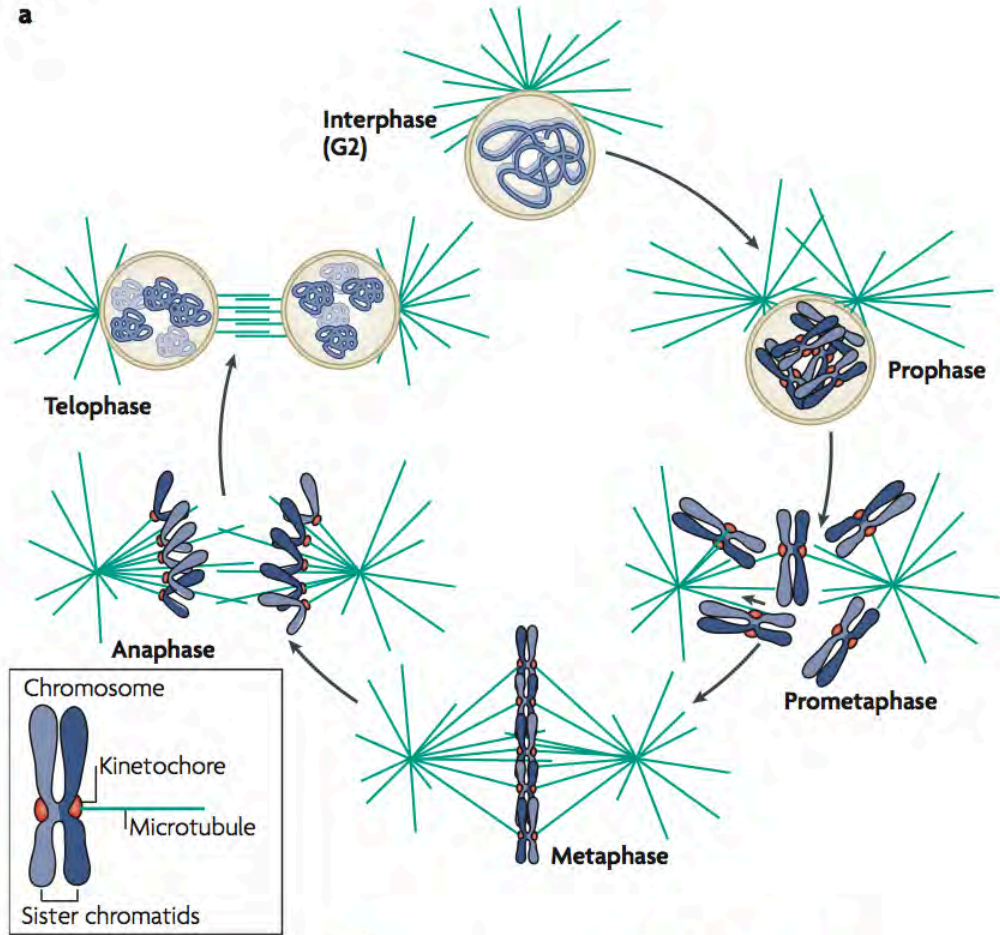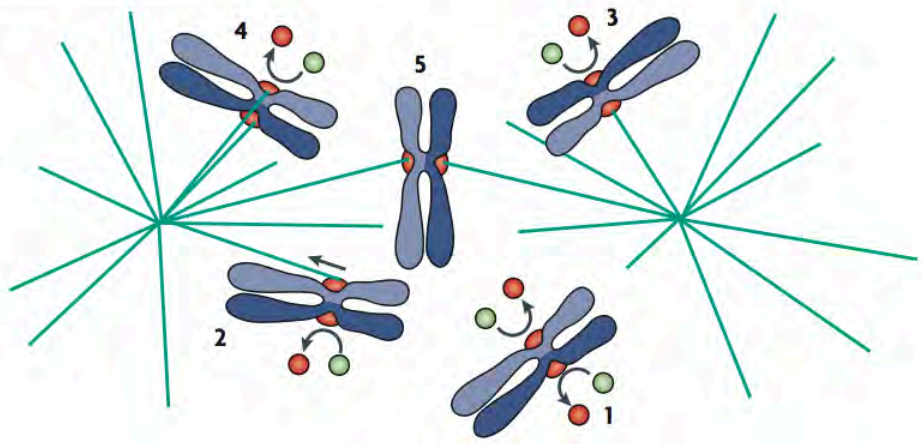
Figure 1.1 Kinetochores mediate chromatid attachment to the spindle to ensure accurate chromosome segregation in mitosis.
A. The journey of chromosomes and kinetochores during mitosis. Kinetochores assemble on condensed chromosomes after nuclear envelope breakdown (NEBD). After NEBD, during prometaphase, kinetochores interact with spindle microtubules. By metaphase chromosomes become bi-oriented and align at the metaphase plate. During anaphase separated sister chromatids move away from each other to opposite spindle poles. Finally, in telophase chromatids decondense and the nuclear envelope reforms producing two daughter cells. B. Detailed view of prometaphase. During prometaphase kinetochores progress from an unattached state **(1)** to a fully bi-oriented state **(5)**. Often, kinetochores first establish lateral attachments **(2)** before progressing to mature end-on attachments **(5).** Unattached kinetochores **(1,2,3)** catalyze the production of an anaphase inhibitor, a source of the SAC, which will be discussed later. Reprinted with permission(Cheeseman and Desai, 2008).
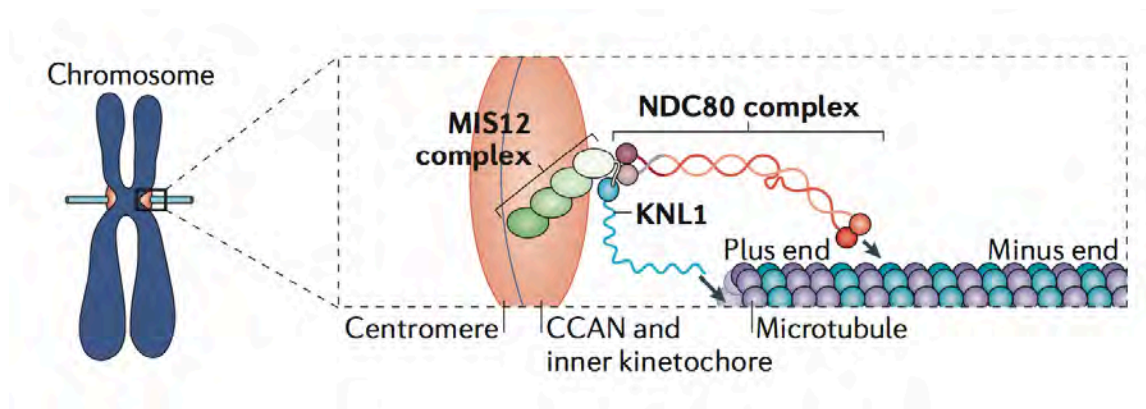
Figure 1.2 Schematic of the KMN (kinetochore null protein 1 (KNL1)-missegregation 12 (MIS12) complex-nuclear division cycle 80 (NDC80) complex) network.
The MIS12 complex connects the NDC80 complex and KNL1 to centromeric DNA. The NDC80 complex and KNL1 make direct contacts with spindle MTs. Arrows indicate MT-binding activities. Reprinted with permission (Foley and Kapoor, 2013).

In addition, this N-terminal tail may help facilitate Hec1 oligomerization and more robust MT-binding in humans (Alushin et al., 2012; 2010). Surprisingly, this N-terminal tail is dispensable in budding yeast(Akiyoshi et al., 2009). As discussed below, Hec1 is a known substrate of the mitotic kinase Aurora B(Alushin et al., 2012), and a suspected substrate of Mps1(Kemmler et al., 2009).

In addition to its MT-binding activity, Hec1 can also regulate MT dynamics. A reconstituted *in vitro* system has shown that the Ndc80 complex directly stabilizes the tips of disassembling MTs and promotes rescue, the transition from MT shortening to growth) (Umbreit et al., 2012). However, in other systems, truncated Ndc80, was not able to associate with depolymerizing MTs(Welburn et al., 2009). Aside from its role in MT-binding, the Hec1 complex is also thought to be a major factor in communicated kinetochore attachment status to the rest of the cell through the SAC (Martin-Lluesma et al., 2002).

KNL1 also possesses MT-binding activity and cooperates with Hec1 to form the core MT-binding site of the kinetochore (Cheeseman et al., 2006). Fewer details are known about KNL1's MT-binding activity, but this activity is subject to regulation by the mitotic kinase Aurora B (Cheeseman et al., 2006). Hec1 and KNL1 are thought to operate synergistically (Cheeseman et al., 2006). In addition, KNL1 helps position Hec1 at kinetochores (Cheeseman et al., 2008).

KNL1 also operates as a nexus of mitotic signaling events. KNL1 serves as a binding platform for the SAC proteins Bub1 and BubR1, a mitotic localization event that was recently shown to depend on Mps1, which will be discussed in more detail below (Kiyomitsu et al., 2011; 2007; London et al., 2012; Shepperd et al., 2012; Yamagishi et al., 2012). KNL1 also facilitates checkpoint silencing by recruiting the PP1 phosphatase (Liu et al., 2010; Rosenberg et al., 2011).

The Mis12 complex anchors Hec1 and KNL1 to centromeric DNA (Screpanti et al., 2011).

The Dam1 complex and the Ska1 complex

In *Saccharomyces cerevisiae,* the hetero-decameric Dam1 complex, also called DASH, is essential for accurate chromosome segregation (Cheeseman et al., 2001; Lampert et al., 2010; Tien et al., 2010). This complex is thought to be particularly important in the transition from lateral to end-on attachments (Tanaka et al., 2007). *In vitro,* the Dam1 complex forms a ring structure around MTs (Miranda et al., 2005; Westermann et al., 2005). Interestingly, the Dam1 complex can form load bearing-attachments, sustaining 2-3 pN on average when situated near the end of a depolymerizing MT (Asbury et al., 2006; Grishchuk et al., 2008). The Dam1 complex is also thought to work synergistically with Ndc80 (Tien et al., 2010) by conferring MT plus end tracking activity to the Ndc80 complex (Lampert et al., 2010). However, as discussed above the Ndc80 complex may possess its own MT tracking activity as well.

Although of paramount importance in yeast, the Dam1 complex is the rare example of a kinetochore module that is not conserved from yeast to humans. Instead, the Ska1 (Spindle and kinetochore associated) complex, which is composed of Ska1, Ska2, and Ska3 has been proposed to perform a functionally analogous role in higher eukaryotes (Chan et al., 2012; Daum et al., 2009; Gaitanos et al., 2009; Guimaraes and DeLuca, 2009; Hanisch et al., 2006; Raaijmakers et al., 2009; Theis et al., 2009; Welburn et al., 2009). Ska1 was the first subunit of the complex to be identified (Sauer et al., 2005), and subsequently, Ska2 and Ska3 were identified as binding partners (Daum et al., 2009; Gaitanos et al., 2009; Hanisch et al., 2006; Ohta et al., 2010; Theis et al., 2009; Welburn et al., 2009). Components of the Ska complex depend on one another for protein stability (Gaitanos et al., 2009). siRNA depletion of each subunit of the Ska complex leads to chromosome congression defects and mis-segregation events at anaphase (Daum et al., 2009; Gaitanos et al., 2009; Welburn et al., 2010). The outer kinetochore remains largely intact after Ska depletion; nevertheless, these defects in chromosome congression have been linked to problems in the generation of stable KT-MT attachments (Gaitanos et al., 2009; Raaijmakers et al., 2009; Welburn et al., 2010). These catastrophic consequences appear to be lethal in human cells, although a DT40 knockout of Ska3/RAMA1 is viable (Ohta et al., 2010).

Ska1 possesses the main MT-binding activity of this complex, with minor contributions from Ska2 and Ska3 (Welburn et al., 2009). Complex homodimerization, however, does provide some boost in MT-binding activity.

The affinity of the Ska1 complex for MT's places it in a similar category to other components of the outer kinetochore such as Hec1 and KNL1. However, the Cheeseman lab has recently demonstrated that the Ska complex can track with depolymerizing MTs, a property not previously seen for other components of the outer kinetochore (Schmidt et al., 2012). Moreover, the Ska1 complex was shown to increase the association of Hec1 with depolymerizing MTs (Schmidt et al., 2012). Interestingly, an interaction between Ndc80, a clear Hec1 homolog in budding yeast, and the Dam1 complex has also been shown (Lampert et al., 2013).

The crystal structure of a truncated core complex has provided insight into the mechanism of Ska1 complex function (Jeyaprakash et al., 2012). The Ska1 complex consists of a W shaped dimer of coiled coils, formed by the intertwined interaction of Ska1, Ska2, and Ska3 (Fig. 1.3). The hinge region of this W-shaped molecule is largely stabilized by Ska3. The truncated structure solved in this study omitted the C terminal MT-binding domain of Ska1, but this work was nicely complemented by an NMR structure of the C-terminal fragment of the MT-binding domain of *C. elegans* Ska1 (Schmidt et al., 2012). Several Aurora B phosphorylation sites can be mapped onto this MT-binding domain, revealing a

potential regulatory role for Aurora B in the MT-binding activity of the Ska1 complex. However, in other studies no affect was seen on the Ska1 complex's MT-binding affinity after *in vitro* phosphorylation by Aurora B (Chan et al., 2012). Instead, it was proposed that Aurora B regulates the kinetochore localization of the Ska1 complex.

The Spindle Assembly Checkpoint

An Overview

The Spindle Assembly Checkpoint (SAC) monitors KT attachments to the spindle to prevent aneuploidy and to maintain high fidelity chromosome segregation during mitosis (Foley and Kapoor, 2013; Musacchio and Salmon, 2007). In short, unattached kinetochores catalyze the production of a "wait anaphase" inhibitor, consisting of a complex of Mad2 and/or BubR1 bound to the APC/C mitotic activator Cdc20 (Chao et al., 2013; Han et al., 2013; Kulukian et al., 2009; Nilsson et al., 2008; Sudakin et al., 2001) (Fig. 1.4). Mad2 and BubR1 binding to Cdc20 inhibits APC/C activity, thus stabilizing the APC/C targets Cyclin B1, a co-activator of the mitotic kinase Cdk1, and securin, an inhibitor of the cysteine protease, separase. After all KTs have made productive attachments to spindle MTs, the APC/C is activated and mitotic exit is triggered by Cyclin B1 and securin ubiquitylation and proteolysis (Fig. 1.4).
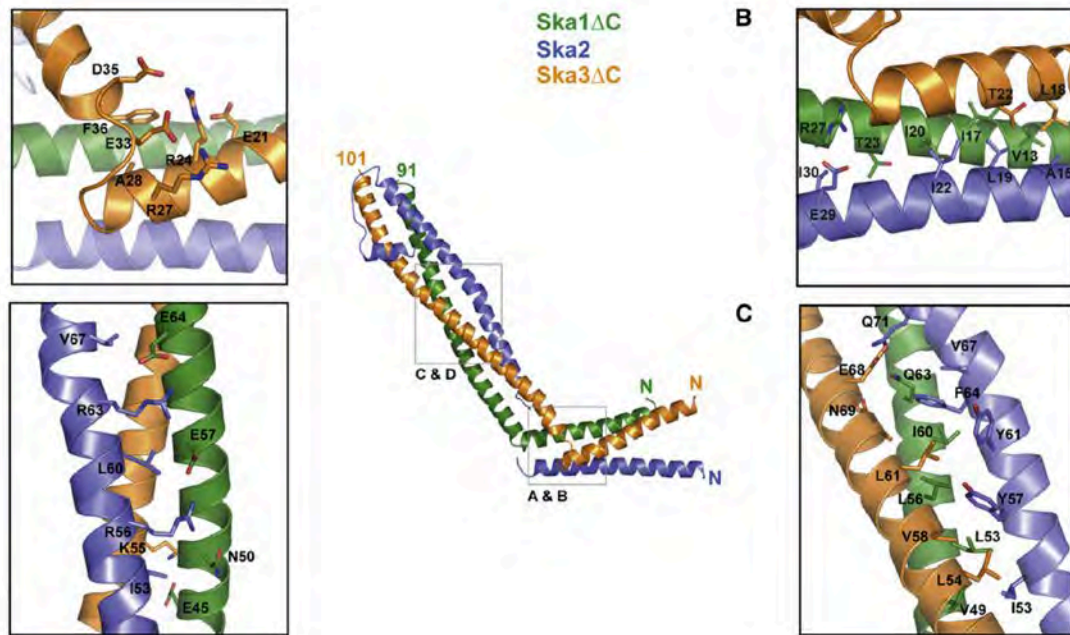
Figure 1.3 Crystal structure of the Ska1 complex.
The Ska1 complex forms a W-shaped homodimer, consisting of intertwined coiled coils of Ska1, Ska2, and Ska3. Extensive hydrophobic and electrostatic interactions are presented throughout the bundles. Reprinted with permission (Jeyaprakash et al., 2012).

The SAC depends on a network of proteins, originally identified in yeast screens (Hoyt et al., 1991; Li and Murray, 1991), which specifically localize to unattached kinetochores (Vigneron et al., 2004). Recent microscopy-based experiments position SAC proteins at the KMN network in checkpoint active metaphase cells (Varma et al., 2013).

The role of kinases in the SAC

A large number of kinases are thought to operate in the SAC (Funabiki and Wynne, 2013; Zich and Hardwick, 2010). Most studies have assigned roles for these kinases in the kinetochore recruitment of other SAC proteins (Ditchfield et al., 2003; Hauf et al., 2003; Morrow et al., 2005; Musacchio and Salmon, 2007; Vigneron et al., 2004), but the kinase(s) directly responsible for the phosphorylation event(s) that mediate the checkpoint arrested state and the ability of the MCC to inhibit the APC/C are not known. There are six kinases implicated in SAC signaling: Mps1, Aurora B, Bub1, BubR1. BubR1 kinase activity is not required for the SAC in any organism studied so far (Chan et al., 1999; Chen, 2002; Tang et al., 2001). In fact, its closest budding yeast homolog, MAD3, does not contain a kinase domain (Hardwick et al., 2000). Recently, BubR1 was identified as an unusual pseudokinase (Suijkerbuijk et al., 2012a; 2010) as residues in its kinase domain help stabilize BubR1 protein levels, but do not possess catalytic activity (Suijkerbuijk et al., 2012a).

Prophase

Active CDK1

Inactive separase

Prometaphase

MCC Checkpoint effector

CDC20

Metaphase

Active APC/C

Inactive APC/C

Anaphase

Active separase

Telophase

26S proteosome

G1

Inactive CDK1
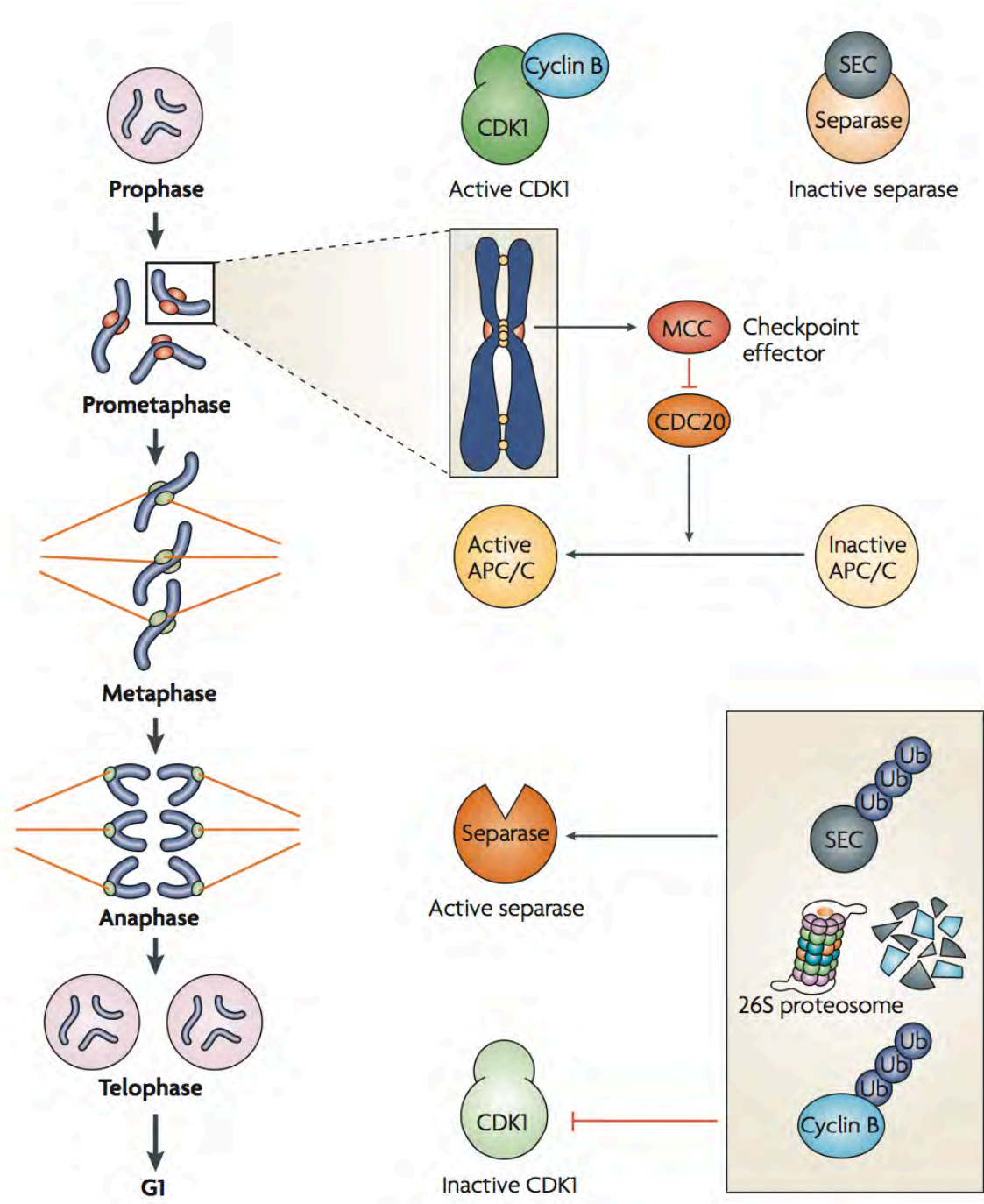
Figure 1.4 Unattached kinetochores inhibit APC/C activity by catalyzing the production of an anaphase inhibitor known as the mitotic checkpoint complex, or MCC.
After nuclear envelope breakdown (NEBD) unattached kinetochores catalyze the production of a checkpoint effector, known as the MCC. The MCC inactivates the APC/C by targeting its mitotic specificity factor Cdc20. After chromosome bi-orientation, the checkpoint is satisfied, and anaphase is triggered by degradation of the APC/C targets Cyclin B and securin. Separase, cleaves cohesin to split sister chromatids and Cyclin B degradation inactivates Cdk1, triggering mitotic exit. Reprinted with permission (Musacchio and Salmon, 2007).

Bub1 kinase activity plays a central role in regulating mitotic exit and promoting robust KT-MT attachment in prometaphase (Klebig et al., 2009a; Taylor and McKeon, 1997). This kinetochore kinase recruits Mad1, Mad2, BubR1, Bub3, Mps1, and Cdc20 to kinetochores (Musacchio and Salmon, 2007; Sharp-Baker and Chen, 2001; Taylor et al., 1998). In fission yeast, the stable kinetochore localization of BUB1 led researchers to propose that BUB1 acts as a scaffold for the recruitment of SAC signaling proteins (Rischitor et al., 2007). Bub1 phosphorylates Cdc20 to sensitize it to SAC inhibition (Morrow et al., 2005) (Tang et al., 2004; Vanoosthuyse and Hardwick, 2005; Yu and Tang, 2005). In addition to these SAC signaling functions, Bub1 also promotes efficient chromosome alignment (Meraldi and Sorger, 2005).

Plk1 is a kinase is not required for the SAC (Burkard et al., 2007; Steegmaier et al., 2007). PLK1 phosphorylates BUBR1 to regulate the stability of kinetochore-microtubule interactions (Elowe et al., 2007). This requires priming phosphorylation performed by the regulatory mitotic kinase CDK1 (Elowe et al., 2007).

Mps1

An Overview

The Mps1 gene encodes a dual specificity kinase that is conserved from yeast to humans (Lauzé et al., 1995; Stucke et al., 2002). The Mps1 kinase is a core component of the SAC (Abrieu et al., 2001; Liu and Winey, 2012; Weiss and

16

Winey, 1996). Although the precise molecular mechanisms of Mps1 are not well understood, several findings suggest that Mps1 has an upstream role in checkpoint initiation. First, Mps1 localizes to kinetochores and its depletion by siRNA or antibody microinjection disrupts the ability of a cell to arrest in response to microtubule depolymerization (Stucke et al., 2002). Second, Mps1 kinase activity is required for the kinetochore localization of other checkpoint proteins including Mad2 (Abrieu et al., 2001; Jelluma et al., 2008b; Liu et al., 2003; Stucke et al., 2002; Tighe et al., 2008). In addition, release of Mps1 from kinetochores is required for timely anaphase (Jelluma et al., 2010). Finally, in yeast, Mps1 has been shown to be sufficient to activate the SAC when temporally mis-expressed in anaphase and its destruction by an active APC/C inactivates the checkpoint (Palframan et al., 2006).

Initial Characterization

The original mutant allele of Mps1 in budding yeast, *mps1-1*, caused spindle pole body duplication defects at a restrictive temperature (Winey et al., 1991). Subsequent studies identified Mps1 as a kinase (Lauzé et al., 1995) and a player in the mitotic checkpoint (Weiss and Winey, 1996). Mps1 overexpression was found to induce a mitotic arrest and Mad1 was hypothesized to be a Mps1 substrate (Hardwick et al., 1996). Since these early studies Mps1 orthologs have been identified in many eukaryotes including fungi, vertebrates, invertebrates, plants, diatoms, and algae (Liu and Winey, 2012). Nematodes, including *Caenorhabditis elegans,* are a notable exception.

Mps1 and the Spindle Assembly Checkpoint

The observation that Mps1 localized to kinetochores during mitosis in yeast suggested that Mps1 was involved in kinetochore-catalyzed production of the "wait anaphase" inhibitor. (Castillo et al., 2002). Vertebrate studies confirmed that this localization and presumably Mps1 function were conserved (Abrieu et al., 2001). More recently, Mps1 was shown to catalyze its own removal from kinetochores, a feature required for timely anaphase onset (Jelluma et al., 2010; Santaguida et al., 2010; Tighe et al., 2008).

It is now clear that Mps1 kinase activity is required for checkpoint activity and targeting of many other SAC proteins, including Mad1, Mad2, Bub1, and BubR1 to unattached kinetochores (Abrieu et al., 2001; Hewitt et al., 2010; Kwiatkowski et al., 2010; Lan and Cleveland, 2010; Liu et al., 2003; Maciejowski et al., 2010; Santaguida et al., 2010; Sliedrecht et al., 2010; Stucke et al., 2002; Tighe et al., 2008; Vigneron et al., 2004).

Mps1 away from the kinetochore

Although a large body of data places Mps1 at the kinetochore in terms of SAC activity, compelling evidence also suggests that this is not the whole story. For example, Mps1 overexpression is capable of producing a mitotic arrest in yeast strains lacking a functional kinetochore (Fraschini et al., 2001). A truncated allele of Mps1 that cannot localize to kinetochores is also sufficient for mitotic arrest in
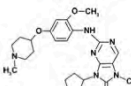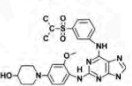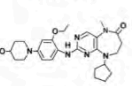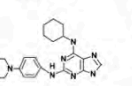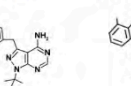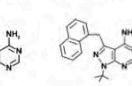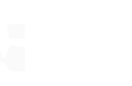
response to spindle poisons (Maciejowski et al., 2010). Mps1 kinase activity is also required to stabilize the MCC in interphase, in cell cycle time points where functional kinetochores do not exist (Maciejowski et al., 2010).

Mps1 substrates

Despite Mps1's central role in the SAC, few checkpoint relevant substrates have been identified. Once again budding yeast have paved the path forward in understanding Mps1 function. Mps1 was first suggested to target the Mad1 component of the Mad1, Mad2 heterodimer, however, this hypothesis awaits further experimental support (Hardwick et al., 1996). Another putative Mps1 substrate is Ndc80, the budding yeast ortholog of the outer kinetochore protein Hec1 (Kemmler et al., 2009). Mutating Mps1 phosphorylation sites to alanine was shown to compromise SAC signaling while phosphomimetic mutation was shown to constitutively engage the checkpoint (Kemmler et al., 2009). However, this study lacked *in vivo* verification of these phosphorylation events.

Three impactful papers published last year have pointed to KNL1 as a major SAC-relevant Mps1 target (London et al., 2012; Shepperd et al., 2012; Yamagishi et al., 2012). Mps1 phosphorylation of conserved MELT motifs in KNL1 was shown to be required to recruit the SAC effector Bub1 to kinetochores, an activity that can be reversed by the PP1 phosphatase (Fig. 1.5).

Table I. Summary of studies using chemical inhibitors of human Mps1 kinase activity

Property	Studies						
	Hewitt et al., 2010	Kwiatkowski et al., 2010		Santaguida et al., 2010	Maciejowski et al., 2010	Sliedrecht et al., 2010	Tighe et al., 2008
Inhibitor	AZ3146	Mps1-IN-1	Mps1-IN-2	Reversine	3MB-PP1	23-dMB-PP1	1-NM-PP1
Structure							
IC_{50} (nM)[a]	35	370	145	3/6[b]	ND	ND	ND
Conc. used in cell (µM)	2	10	10	0.5	10	1	10
Drug target	Endogenous Mps1	Endogenous Mps1	Endogenous Mps1[c]	Endogenous Mps1[d]	Mps1-as[e]	Mps1-as[e]	Mps1-as[e]
Approach	Inhibitor; siRNA	Inhibitor; stable shRNA	Inhibitor; stable shRNA	Inhibitor; siRNA	Gene knockout + stable transgene	stable shRNA + stable transgene	shRNA + transgene
Cell line used	HeLa	U2OS/HCT116/HeLa/RPE1	U2OS	HeLa	hTERT-RPE1	U2OS/HCT116	HeLa
$T_{Mitosis}$ (min)[f]	~90	ND	ND	~45	~42	~22/18	ND
$T_{Mitosis+Inhibitor}$ (min)	~32	~45	ND	~30	~12	~12/10	~36
Kinetochore localization inhibited[g]	O-Mad2/CENP-E	Mad2/Mad1	ND	Mad1/Spindly/Rod/Zw10/Zwilch	Mad2/Mad1/Bub1/BubR1/Zw10/Plk1/CENP-E/pH2A/Sgo1	Mad2/Mad1/Bub1/Cdc20	Mad2
Kinetochore localization not inhibited	Mad1[h]/Zwilch[h] pCENP-A/Aurora B/pAurora B/ACA	CREST	ND	Bub1/BubR1/KNL1/Mis12/Ndc80/Zwint/Aurora B/pCENP-A/CENP-C/CREST	Ska3/Ndc80/KNL1/Zwint/CENP-A/Aurora B/INCENP/CREST	CENP-E/BubR1/ACA	Mad1/ACA
Chromosome misalignment	ND	Yes	ND	Yes	Yes	Yes	ND
Defect in error correction	Yes	NA	ND	Yes	ND	Yes	ND
Affect Aurora B kinase activity	No	Yes	ND	No (at 0.5 µM)	No	Yes	ND

Conc., concentration.
[a]The half maximal inhibitory concentration.
[b]For full-length and kinase domain Mps1, respectively.
[c]Binds Plk1 with higher affinity.
[d]Inhibits Aurora B with an IC_{50} of 98 nM.
[e]Analogue-sensitive Mps1.
[f]Time cells spend in mitosis.
[g]Scoring >50% reduction of signal intensity.
[h]Depends on when drugs are applied.

Table 1.1 . Summary of Mps1 inhibition by several small molecule inhibitors.
Reprinted with permission (Lan and Cleveland, 2010).

20
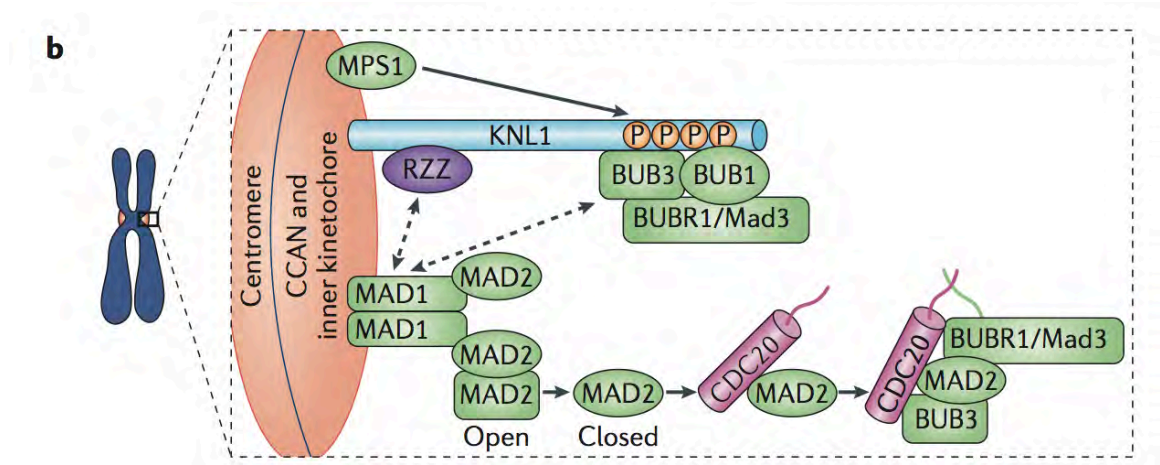
Figure 1.5 Mps1 phosphorylates KNL1 to recruit the Bubs to unattached kinetochores.

Mps1 phosphorylates conserved MELT motifs in KNL1 to recruit Bub1, BubR1/Mad3, and Bub3 to kinetochores. KNL1 also recruits the RZZ complex to kinetochores. At the kinetochores the Bub proteins, the RZZ, and the Mad1/2 heterodimer interact to produce a mature mitotic checkpoint inhibitor. Reprinted with permission (Foley and Kapoor 2013).

Mps1 and cancer

The increased frequency of aneuploidy in solid tumors has been proposed to open a therapeutic window for anti-mitotic agents and mitotic kinase inhibitors in the treatment of cancer. Indeed, partial Mps1 inhibition has been shown to sensitize various cancer cell lines to anti-mitotic drugs (Tannous et al., 2013; Janssen et al., 2009; Schmidt et al., 2005, Jemaa et al., 2012). However, a direct link between spindle assembly checkpoint activity, mitotic duration, and the effectiveness of anti-mitotic agents is not clear (Gascoigne et al., 2009). Future mouse models of Mps1, such as transgenic overexpression and partial inhibition, will provide necessary insights (Schvartzman et al., 2010).

Aurora B

The homolog of Aurora B in budding yeast, Ipl1, has been shown to play a tangential role in the SAC by sensing tensionless kinetochore-microtubule interactions and activating the checkpoint by creating unattached kinetochores (Pinsky and Biggins, 2005; Pinsky et al., 2006)[45]. Furthermore, Aurora B is not required to generate a mitotic arrest in response to nocodazole, whereas MCC formation is required for this arrest (Morrow et al., 2005; Santaguida et al., 2011). Instead, Aurora B may play a role in the SAC by aiding in the initial, rapid accumulation of SAC proteins to unattached kinetochores (Saurin et al., 2011).

Mps1 and Aurora B

In addition to its SAC function, Mps1 was also recently shown to promote chromosome bi-orientation (Jelluma et al., 2008b). It was suggested that Mps1 promoted efficient bi-orientation by phosphorylating a component of the chromosomal passenger complex, borealin, and thus boosting Aurora B activity (Hauf, 2008; Jelluma et al., 2008b). Aurora B is a kinase with well established roles in error correction, a quality control pathway that destabilizes improper KT-MT attachments, and chromosome bi-orientation (Ditchfield et al., 2003; Hauf et al., 2003; Lampson et al., 2004; Welburn et al., 2010). However, more recent studies have shown, using structurally unrelated inhibitors, that Aurora B activity is unaffected even by potent Mps1 inhibition (Hewitt et al., 2010; Lan and Cleveland, 2010; Maciejowski et al., 2010; Santaguida et al., 2010) (Table 1). There are two notable exceptions: Mps1-IN1, another small molecule inhibitor of Mps1, that does cause defects in Aurora B activity (Kwiatkowski et al., 2010) and a chemical genetic system for Mps1 inhibition built in HCT116 colon carcinoma cells, in which Mps1 inhibition by a rationally designed inhibitor also leads to disruptions in Aurora B activity (Sliedrecht et al., 2010). In any case Mps1 and Aurora B seem to be tightly linked as Aurora B activity has also been shown to potentially play a role in the SAC and to be required for efficient Mps1 activation (Santaguida et al., 2011; Saurin et al., 2011). It seems that an upstream and downstream model may be too simple to understand the complex relationship between these two kinases (Lan and Cleveland, 2010).

Mitotic Serine/Threonine Phosphatases

The role of kinases in regulating mitotic progression has been appreciated for a long time so it is not surprising that serine and threonine phosphatases are now being recognized as serving major regulatory roles as well. Indeed, recent studies have placed an emphasis on the importance of protein phosphatases in mitotic regulation (Foley and Kapoor, 2013). The majority of serine, threonine protein phosphatase activity is exerted by just two protein families: protein phosphatase 1 (PP1) and protein phosphatase 2A (PP2A) (Fig. 1.6).

The PP1 family of phosphatases has been recognized to play a conserved role in regulating mitotic exit, mostly by counteracting Aurora B and Ipl1 (Emanuele et al., 2008; Francisco and Chan, 1994). The Glc7/PP1 phosphatase was recently shown to target the kinetochore protein, KNL1, help trigger mitotic exit by inhibiting the SAC (Rosenberg et al., 2011). KNL1-mediated recruitment of PP1 has also been observed in human cells (Liu et al., 2010). Interestingly, PP1 was shown to counteract Mps1 phosphorylation of KNL1 at the kinetochore (London et al., 2012).

Our emerging understanding of the role of phosphatases has helped to resolve a paradox in the formation of KT-MT attachments. Although it has long been acknowledged that kinase activity, in general, severs KT-MT attachments, we did not have a clear understanding of how KT-MT attachments could overcome this regulation to form stable attachments. This discrepancy was resolved by the

24

identification of the B56-PP2A phosphatase as an enzyme required to counteract Aurora B and Plk1 and to stabilize KT-MT attachments during mitosis (Foley et al., 2011). B56-PP2A activity at the kinetochore is tightly regulated by Plk1 and BubR1 (Suijkerbuijk et al., 2012b).
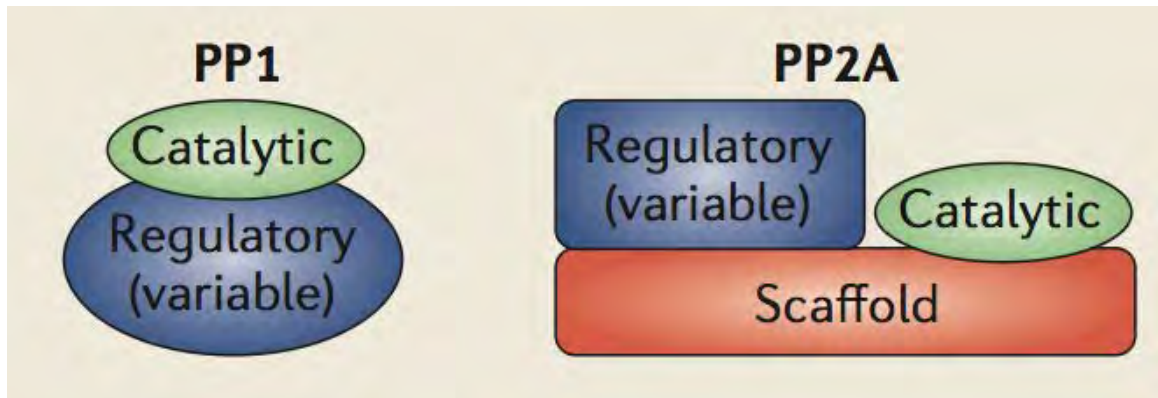
Figure 1.6 The PP1 and PP2A phosphatase families.
PP1 and PP2A enzymes contain a catalytic subunit and variable regulatory subunits that are responsible for targeting the holoenzymes to particular regions of the cell or to specific substrates. In addition, the PP2A family of enzymes also contains a scaffolding subunit. Reprinted with permission (Foley and Kapoor, 2013).

CHAPTER TWO: Mps1 directs the assembly of Cdc20 inhibitory complexes during interphase and mitosis to control M phase timing and spindle checkpoint signaling

Summary

The spindle assembly checkpoint (SAC) in mammals uses cytosolic and kinetochore-based signaling pathways to inhibit anaphase. Here we use chemical genetics to show that the protein kinase Mps1 regulates both aspects of the SAC. Human *MPS1*-null cells were generated via gene targeting and reconstituted with either the wildtype kinase (Mps1^{wt}) or a mutant version (Mps1^{as}) sensitized to bulky purine analogs. Mps1 inhibition sharply accelerated anaphase onset, such that cells completed mitosis in 12 minutes, and prevented Cdc20's association with either Mad2 or BubR1 during interphase, i.e., before the appearance of functional kinetochores. Furthermore, intramitotic Mps1 inhibition evicted Bub1 and all other known SAC transducers from the outer kinetochore, but contrary to a recent report, did not perturb Aurora B-dependent phosphorylation. We conclude that Mps1 has two complementary roles in SAC regulation: (i) initial cytoplasmic activation of Cdc20 inhibitor(s), and (ii) recruitment of factors that promote sustained anaphase inhibition and chromosome bi-orientation to unattached kinetochores.

Introduction

Accurate chromosome segregation is essential for cell viability, organismal development, and tumor suppression. Accordingly, eukaryotes have evolved a number of mechanisms to defend against chromosome segregation errors. Paramount among these is the so-called spindle assembly checkpoint (SAC), which inhibits anaphase onset until all kinetochore pairs have attached to microtubules (MTs) emanating from both spindle poles, generating a stable configuration termed chromosome bi-orientation (Musacchio and Salmon, 2007). In biochemical terms the SAC acts by inhibiting the Cdc20-bound form of the anaphase-promoting complex or cyclosome (APC/C), a large ubiquitin-protein ligase (Peters, 2006). Repression of APC/C^{Cdc20} activity stabilizes its downstream targets, including securin and cyclin B, which directly block sister chromatid separation and mitotic exit.

Early timelapse and laser ablation studies pointed to a central role for unattached kinetochores in checkpoint signaling (Li and Nicklas, 1995; Rieder et al., 1995; 1994). Consistent with this notion, all known SAC transducers – including the protein kinases Mps1, Bub1, and BubR1, and the non-kinase components Mad1, Mad2, and Bub3 – associate with unattached kinetochores in prometaphase (reviewed in (Musacchio and Salmon, 2007)). In particular, it is thought that kinetochore-localized Mad1/Mad2 heterodimers catalyze the conversion of soluble "open" Mad2 (O-Mad2) to a "closed" conformer (C-Mad2) that stably binds to and inhibits Cdc20 (De Antoni et al., 2005). However, other compelling

data argue that SAC signaling does not entirely depend on kinetochores. First, complexes of Cdc20 bound to Mad2 and/or BubR1 (sometimes referred to the mitotic checkpoint complex or MCC) have been detected in interphase mammalian cells and yeast strains that lack functional kinetochores (Fraschini et al., 2001; Sudakin et al., 2001). Second, Mad2 and BubR1 are required not only to prolong mitosis in the presence of unattached kinetochores, but also to specify the minimum length of M phase under unperturbed conditions (Malureanu et al., 2009; Meraldi et al., 2004). In contrast, inactivation of other SAC components or factors required for kinetochore-microtubule binding does not accelerate M phase. Third, BubR1's essential mitotic functions can be reconstituted with an N-terminal fragment that binds Cdc20 but cannot localize to kinetochores (Malureanu et al., 2009). Together these observations argue that Mad2 and BubR1 are components of a "cytosolic timer" that actively restrains anaphase onset, affording early mitotic cells time to mature their kinetochores and (if necessary) engage the kinetochore-dependent branch of the SAC. However, the upstream factor(s) that govern this timer remain elusive.

Although the SAC is conserved throughout Eukarya, efforts to define the order in which its components act relative to one another have yielded unexpectedly divergent results. For instance, studies in human cells have consistently positioned Mps1 near the distal end of the SAC, as depleting this kinase via RNAi results in the selective loss of Mad2 from kinetochores (Jelluma et al., 2008b; Liu et al., 2003; 2006; Stucke et al., 2002; Tighe et al., 2008). In contrast,

genetic analyses in yeast and immunodepletion experiments in *Xenopus* egg extracts place Mps1 at the apex of the SAC, upstream of not only Mad2 but also Bub1, BubR1/Mad3, and Mad1 (Abrieu et al., 2001; Hardwick et al., 1996; Vigneron et al., 2004; Wong et al., 2007). Similarly, whereas human Mps1 reportedly facilitates chromosome alignment by direct phosphorylation of the Aurora B kinase regulator Borealin, and hence is necessary to sustain full Aurora B activity in human cells (Jelluma et al., 2008b), the Aurora B-related kinase Ipl1 retains its normal localization and full activity in Mps1-deficient yeast strains (Maure et al., 2007). These findings have been interpreted as evidence of species-specific differences in kinetochore organization and SAC regulation, but other explanations (e.g., technical issues related to the completeness or specificity of Mps1 inactivation) have not been excluded.

To clarify these issues, we created human cells in which both copies of the *MPS1* locus could be deleted via gene targeting. The resulting *MPS1*-null cells were then complemented with versions of the kinase that differ at a single amino acid within the ATP-binding site, conferring resistance or sensitivity to bulky purine analogs. Using this chemical genetic system, we investigated the role of Mps1 in M phase progression and SAC signaling. Our studies identify a novel interphase function for Mps1, whereby it ensures that Cdc20 binds Mad2 and BubR1 before kinetochores have matured and can generate their own anaphase-inhibitory signals. Mps1 is also critical for the subsequent phase of SAC signaling, as its inhibition evicts all known SAC mediators from prometaphase

kinetochores. Furthermore, we find that although human Mps1 indeed controls chromosome bi-orientation, it does so independently of Aurora B regulation, as evidenced by undiminished phosphorylation of multiple Aurora B substrates in Mps1-inhibited cells. Taken together, these findings reveal new insights into the SAC response in mammalian cells and provide new tools for interrogating this response in a rapid and specific manner, without collateral inhibition of Aurora B.

Results

Chemical genetics reveals the M phase timing function of Mps1

To establish a tight genetic background for functional studies, we used adeno-associated virus (AAV)-mediated gene targeting (Berdougo et al., 2009) to conditionally delete *MPS1* from the human genome. Briefly, two vectors were constructed, such that exon 4 of the *MPS1* locus was either flanked by *loxP* sites or deleted outright (Fig. 2.1A). Conceptually, removal of this exon truncates the open reading frame at codon 121, upstream of sequences required for kinase activity and kinetochore localization (Stucke et al., 2004). Both vectors were used to sequentially infect telomerase-immortalized human retinal pigment epithelial (hTERT-RPE) cells, with targeting efficiencies of 6% and 3%, respectively. To initiate gene deletion, $MPS1^{flox/\Delta}$ cells were infected with adenoviruses expressing Cre recombinase (AdCre) or β-galactosidase (Adβgal) as a negative control. Mps1 expression ceased within 48 hours of AdCre infection, without the appearance of any new immunoreactive species (Fig.

2.1B). As anticipated, $MPS1^{\Delta/\Delta}$ clones could not be recovered by limiting dilution

(data not shown), indicating that this kinase is essential in mammals.

Next, $MPS1^{flox/\Delta}$ cells were transduced with retroviruses expressing either the

wildtype kinase (Mps1^{wt}) or an analog-sensitive mutant (M602A; hereafter

Mps1^{as}) fused to a localization and affinity purification (LAP) tag (Cheeseman

and Desai, 2005). *In vitro* Mps1^{as} was considerably less active than Mps1^{wt},

similar to other analog-sensitive kinases ((Bishop et al., 2000; Burkard et al.,

2007; Holland et al., 2010; Jones et al., 2005) ; Fig. 2.2). Nevertheless, both

Mps1^{as} and Mps1^{wt} supported the growth of *MPS1*-null cells (Fig. 2.1C,D) and

localized to kinetochores (Fig. 2.1E), demonstrating their functionality *in vivo*.

Crucially, Mps1^{as} cells alone were susceptible to growth inhibition by the bulky

purine analog 3-MB-PP1 ((Burkard et al., 2007); Fig. 2.1D). To evaluate the

integrity of these alleles with respect to SAC signaling, Mps1^{wt} and Mps1^{as} cells

were challenged with spindle poisons that either globally depolymerize MTs

(nocodazole) or prevent spindle bipolarization by targeting the kinesin Eg5

(monastrol and S-trityl-L-cysteine (STLC)). Afterwards, mitotic indices were

determined by MPM-2 staining and flow cytometry (Fig. 2.2). In the absence of

3-MB-PP1, cells of all genotypes arrested with comparably high efficiencies.

However, in the presence of 3-MB-PP1, Mps1^{as} cells demonstrated little if any

increase in the mitotic index relative to unchallenged controls. To complement

this endpoint assay, we measured the duration of M phase in individual

nocodazole-treated cells by timelapse phase-contrast microscopy. Strikingly,

Mps1[as] inhibition reduced the length of M phase (defined in this assay as the period of cell rounding) from 1651 ± 463 minutes to 18 ±12 minutes (Fig. 2.1F). Acceleration of M phase to this degree was noteworthy and unexpected, as both wildtype cells and those lacking the kinetochore-dependent arm of the SAC require about 30 minutes to complete mitosis (Meraldi et al., 2004). To score mitotic timing more precisely, we generated cells expressing a histone H2B-mCherry fusion protein and imaged them at higher temporal and spatial resolution using spinning-disk confocal microscopy (Fig. 2.3A). Mps1[wt] cells progressed from nuclear envelope breakdown (NEB) to anaphase in 34 ± 19 minutes, while untreated Mps1[as] cells exhibited slightly longer kinetics of 42 ± 26 minutes (Fig. 2.3B). Upon 3-MB-PP1 treatment, however, the NEB-to-anaphase interval in Mps1[as] cells fell to just 12 ± 2 minutes, as also occurs in Mad2- or BubR1-depleted HeLa cells (Meraldi et al., 2004). Because Mps1 is thought to regulate Aurora B (Jelluma et al., 2008b), we tested whether the latter is also required to sustain normal M phase timing. However, treating cells with the Aurora kinase inhibitor ZM447439 ((Ditchfield et al., 2003); hereafter ZM) actually delayed anaphase onset slightly, rather than accelerating it (Fig. 2.3B). Aurora B inhibition also failed to block Mps1's self-catalyzed phosphorylation and consequent upshift on SDS-PAGE (Fig. 2.3C). We conclude that Mps1 plays a key role in setting the basal length of mitosis, but does so by a mechanism that is independent of Aurora B.

A

MPS1*flox* vector

MPS1 locus

MPS1*Δ* vector

B

Mps1
(97 kD)

tubulin
(55 kD)

Adβgal   AdCre

1   2   3   4   1   2   3   4

days post infection

C

flox/Δ   Δ/Δ +
          wt   as

LAP-Mps1(130 kD)
Mps1 (97 kD)

tubulin (55 kD)

D

0   3-MB-PP1

wt

as

F

E

CREST   Mps1   merge

Mps1^{wt}

Mps1^{as}

34
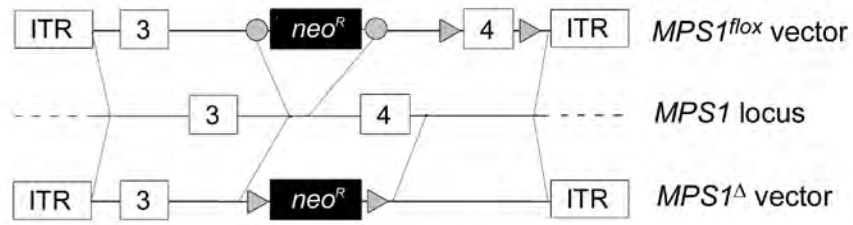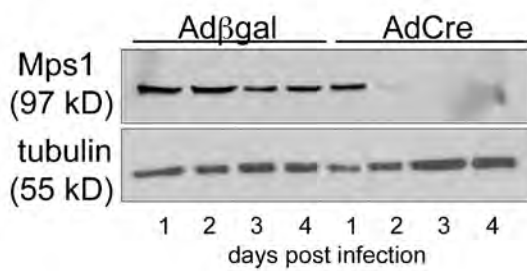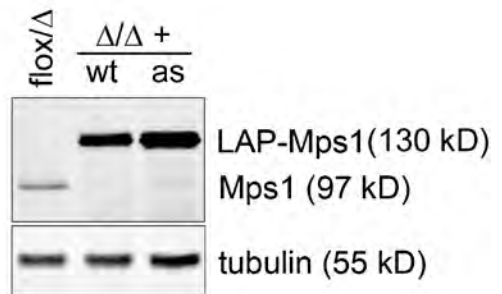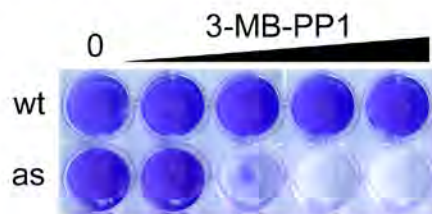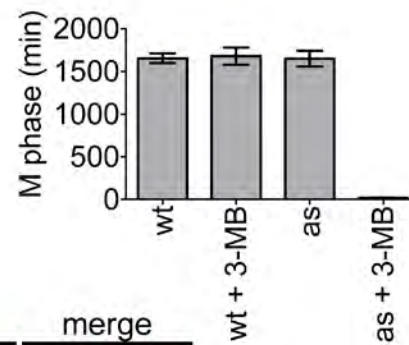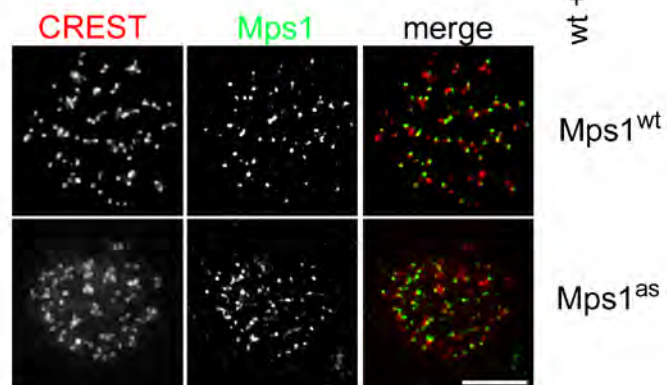
Figure 2.1 Generation of Mps1 conditional-null and analog-sensitive human cells.

(A) Schematic of adeno-associated virus vectors used to mutate the *MPS1* locus. Circles and triangles denote *FRT* and *loxP* sites respectively; ITR, inverted terminal repeat. (B) *MPS1*^{flox/Δ} cells were infected with the indicated adenoviruses and analyzed for Mps1 expression by immunoblotting. (C) $MPS1^{flox/\Delta}$ cells and $MPS1^{\Delta/\Delta}$ cells complemented by wildtype (wt) or analog-sensitive (as) Mps1 transgenes were analyzed by immunoblotting. (D) Allele-specific inhibition of $Mps1^{as}$. Cells were cultured in the presence of the bulky purine analog 3-MB-PP1 (from left to right: 0 µM, 0.078 µM, 0.313 µM, 1.25 µM, and 5 µM) for 7 days and stained with crystal violet. (E) Cells were fixed and stained with antibodies to centromere autoantigens (CREST, red) and transgene-encoded $Mps1^{wt}$ and $Mps1^{as}$ (green). Scale bar, 10 µm. (F) $Mps1^{as}$ inhibition overrides the SAC. Cells were filmed at 10-minute intervals during treatment with nocodazole in the presence or absence of 3-MB-PP1 (10 µM) to assess the length of M phase (defined here as the period of cell rounding by phase-contrast microscopy). Error bars indicate s.e.m.

A

Mps1^wt   Mps1^as

3MB   3MB

[^32P] LAP-Mps1   (130 kD)

IB: LAP-Mps1

100 90 100 70   6   6   5   1

specific activity (% of Mps1^wt control)

B

LAP-Mps1 construct: wt   as   kd   as
3-MB-PP1:   -   -   -   +

LAP-Mps1   (130 kD)

C

MPM2 positive cells

80%

60%

40%

20%

0%

nocodazole   monastrol   STLC

- Mps1^wt
- Mps1^wt + 3-MB
- Mps1^as
- Mps1^as + 3-MB
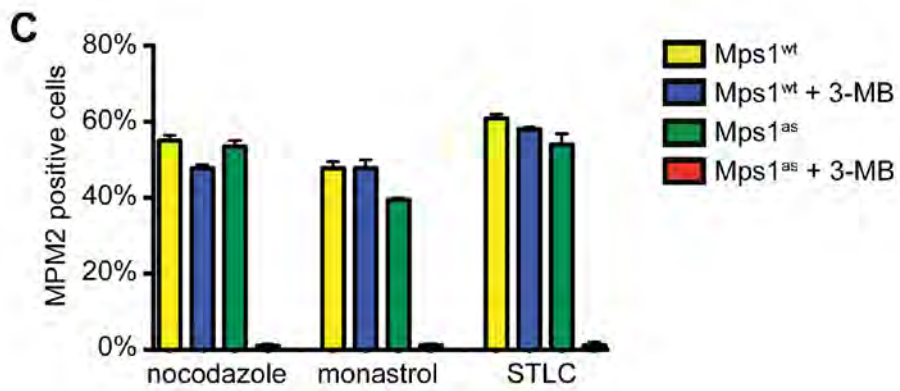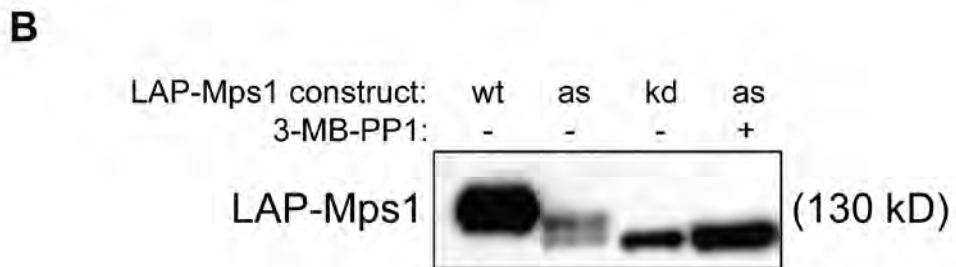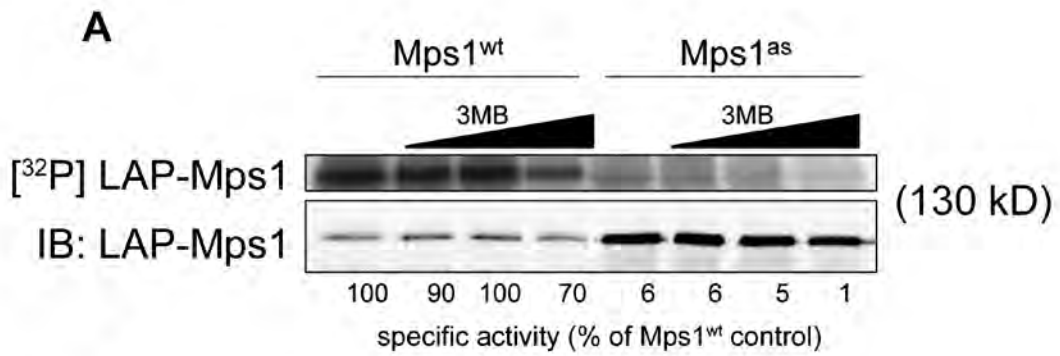
Figure 2.2 Mps1^{as} retains kinase activity and Mps1 kinase activity is required for mitotic arrest in response to several spindle poisons.

(A) Mps1 was immunoprecipitated from mitotic Mps1^{wt} or Mps1^{as} extracts and either immunoblotted (lower panel) or incubated with [γ^{32}P]-ATP. 3-MB-PP1 was added to the reaction at 0.1 µM, 1.0 µM or 10 µM where indicated. (B) Inhibition of Mps1^{as} prevents its autophosphorylation and electrophoretic upshift during mitosis. HEK293 cells were transfected with the indicated LAP-tagged forms of Mps1, synchronized in mitosis with nocodazole, and then treated for 2 hours with 3-MB-PP1. Lysates were resolved by SDS-PAGE and immunoblotted with GFP-specific antibodies (reactive with the LAP tag). (C) Mps1^{as} inhibition overrides SAC arrest caused by MT-destabilizing and non-destabilizing spindle poisons. Cells were treated for 16 hr with nocodazole, monastrol, or STLC in the presence or absence of 3-MB-PP1. Mitotic indices were determined by MPM-2 staining and flow cytometry.
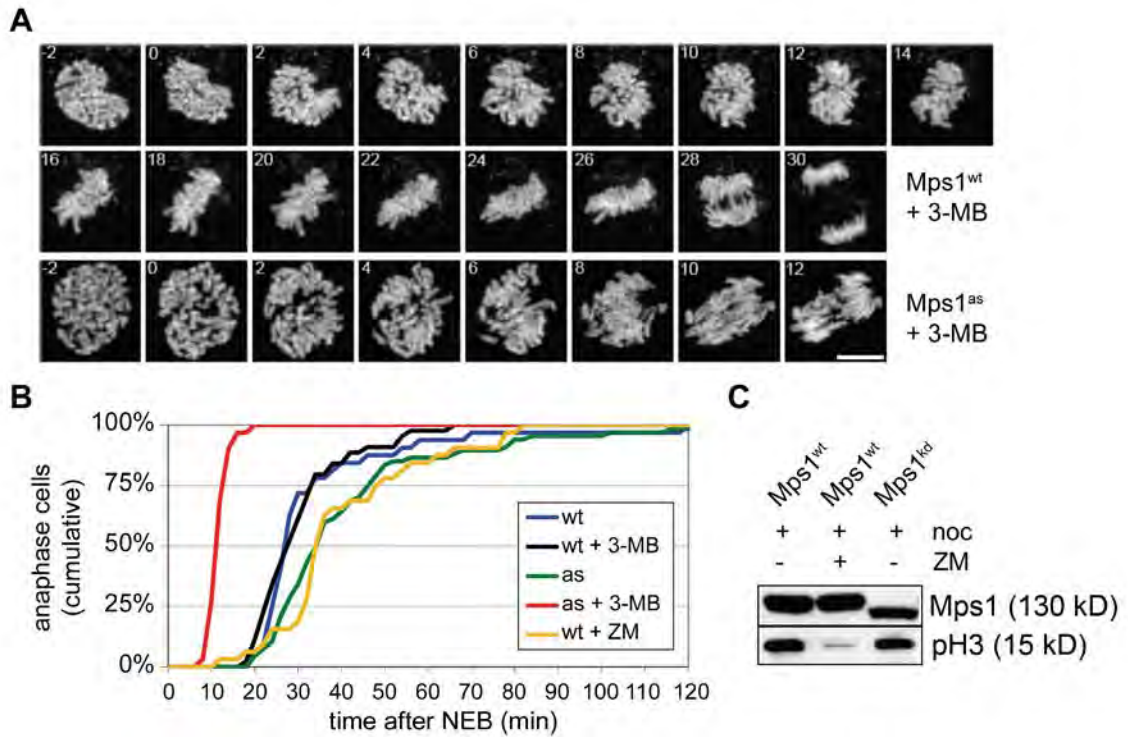
Figure 2.3 Mps1 is a component of the M phase timer.
(A) Mps1^wt and Mps1^as cells stably expressing mCherry-tagged histone H2B were treated with 10 µM 3-MB-PP1 and filmed at 1-minute intervals by spinning-disk confocal microscopy. Maximum intensity projections are shown. Scale bar, 10 µm. (B) Quantification of the mitotic timing defect in Mps1-inhibited cells. Cumulative frequency of anaphase onset is plotted as a function of time after NEB. (C) Strong Aurora B inhibition does not block the autophosphorylation of Mps1. HEK293 cells were transfected with GFP-tagged Mps1 expression plasmids (wt, wildtype; kd, kinase-dead), arrested in M phase with nocodazole, and then treated with or without 1 µM ZM for 2 hours. Cell extracts were resolved by SDS-PAGE and probed with antibodies to serine 10-phosphorylated histone H3 (to confirm suppression of Aurora B kinase activity) and GFP (to assess Mps1's electrophoretic mobility, which becomes retarded by its mitotic activation and autophosphorylation (Stucke et al., 2004)).

Mps1 is continuously required for the assembly of Cdc20-inhibitory complexes during interphase and mitosis

M phase timing is known to depend on Mad2 and BubR1, but not on other SAC components or mediators of kinetochore-MT attachment (Meraldi et al., 2004). Both Mad2 and BubR1 bind to Cdc20 either simultaneously (Herzog et al., 2009; Sudakin et al., 2001) or separately (Kulukian et al., 2009; Nilsson et al., 2008; Tang et al., 2001) and inhibit APC/C^{Cdc20}-mediated ubiquitylation. Notably, Cdc20-inhibitory complexes, composed of Mad2 and/or BubR1 bound to Cdc20, are present during interphase (Malureanu et al., 2009; Sudakin et al., 2001; Tang et al., 2001), before either MT-binding proteins or SAC transducers have been targeted to centromeres (Cheeseman and Desai, 2008). To probe Mps1's role in the formation of such complexes, asynchronous Mps1^{wt} and Mps1^{as} cultures were depleted of mitotic cells by shakeoff and treated with 3-MB-PP1 for 2 hours, after which Cdc20 and associated proteins were immunoprecipitated and analyzed by quantitative immunoblotting. Mps1 inhibition caused Cdc20 to dissociate from Mad2 and BubR1, while its association with the APC/C was only mildly affected (Fig. 2.4A). By contrast, ZM treatment failed to disrupt these interphase complexes (Fig. 2.4B), in keeping with its inability to accelerate mitotic timing (Fig. 2.3B).

Figure 2.4 Mps1 directs the assembly of Cdc20-inhibitory complexes in interphase.

(A) Mps1[wt] and Mps1[as] cells were treated with 3-MB-PP1 for 2 hours. Extracts were immunoprecipitated with antibodies to Cdc20 and resolved by SDS-PAGE. Levels of BubR1, APC8, Mad2, and Cdc20 in each IP were determined by quantitative immunoblotting. The ratio of each protein to Cdc20 was computed and normalized to ratios obtained from untreated Mps1[wt] cells (= 1.0). Error bars denote s.e.m. (B) Mps1[wt] cells were treated with ZM for 2 hours and processed as in panel A. (C) Interphase and mitotic Cdc20 IPs were electrophoresed on 6% gels to resolve mitotically phosphorylated APC8 (left) and BubR1 (right) polypeptides as distinct species.

Importantly, the APC8 and BubR1 polypeptides analyzed in these experiments lacked mitotic phosphorylation-induced mobility shifts ((Elowe et al., 2007; Kraft et al., 2003; Lénárt et al., 2007); Fig. 2.4C), confirming that Mps1 regulates their interaction with Cdc20 specifically during interphase. Recent evidence indicates that BubR1 binding to Cdc20 is required to prevent premature turnover of APC/C^{Cdc20} substrates in early mitotic cells (Malureanu et al., 2009). Consistent with its effect on this interaction, Mps1 inhibition reduced the abundance of two well-characterized APC/C^{Cdc20} substrates, securin and cyclin B, during prophase (Fig. 2.5A). This decrease was attributable to proteasome-mediated turnover, as it was fully suppressed by MG132 treatment (Fig. 2.5B). We conclude that by promoting the formation of Cdc20-inhibitory complexes, Mps1 protects cyclin B and securin from degradation in early mitosis, and thus guards against premature anaphase onset.

To extend these results, we tested whether Mps1 also controls the assembly of Cdc20-inhibitory complexes during mitosis, or if it becomes dispensable as long as these complexes were assembled previously in interphase. Briefly, Mps1^{wt} and Mps1^{as} cells were treated overnight with STLC and collected by shakeoff. Each population of pure (>95%) mitotic cells was transferred to medium containing STLC, 3-MB-PP1, and/or MG132. After 2 hours, cells were analyzed by Cdc20 immunoprecipitation and quantitative immunoblotting. Intramitotic Mps1 inhibition dissociated Mad2 and BubR1 from Cdc20 (Figs. 2.6A and 2.6B).
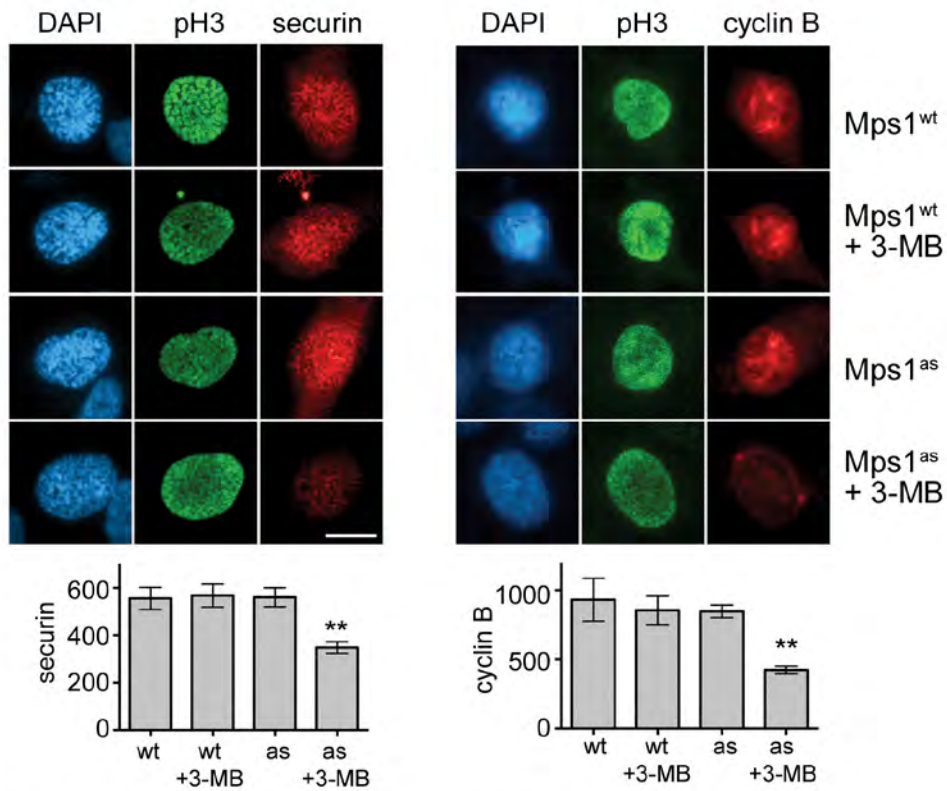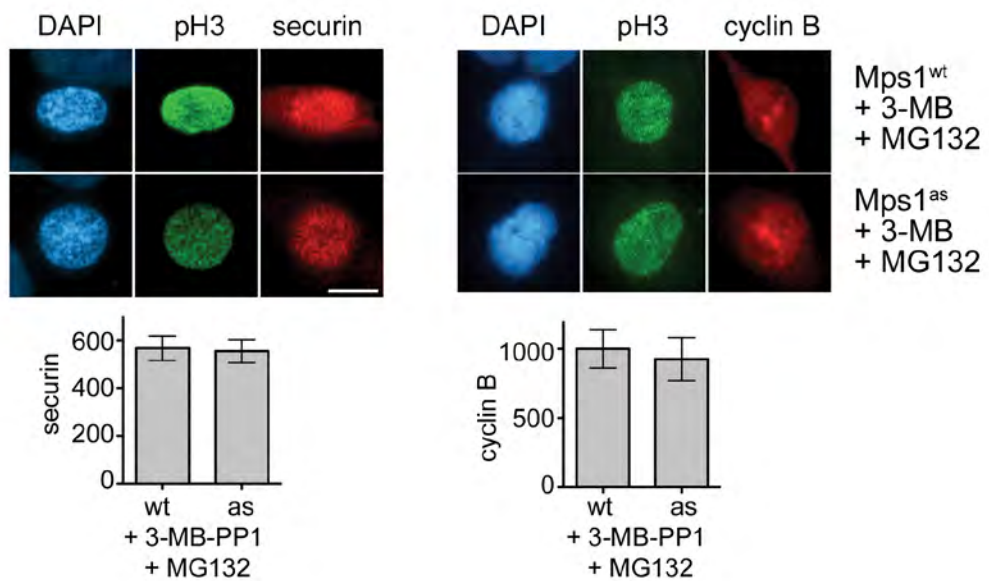
Figure 2.5 Mps1 protects cyclin B and securin from premature destruction.
(A) Cells of the indicated genotypes were treated with or without 3-MB-PP1, then fixed and stained with antibodies to serine 10-phosphorylated histone H3 (pH3) and securin (left panel) or cyclin B (right panel). Nuclei were counterstained with DAPI. Prophase cells were identified by their uniform pH3 staining (Hendzel et al., 1997), partially condensed chromatin (left panel), and nuclear import of cyclin B ((Hagting et al., 1999); right panel). Note that cyclin B staining employed methanol fixation, which preserves chromatin condensation less well than aldehyde fixation. (B) Cells were treated with both 3-MB-PP1 and MG132 for 2 hours, and then analyzed as in panel A. Scale bar, 10 µm. Asterisks indicate statistically significant deviation ($p<0.01$ by one-way ANOVA) from Mps1^{wt} cells treated with 3-MB-PP1.

In contrast, Mad2's interaction with its kinetochore receptor Mad1 was unaffected (Fig. 2.6B). In the absence of MG132, intramitotic Mps1 inhibition resulted in rapid destruction of cyclin B and M phase exit (Fig. 2.6C). We conclude that Mps1 activity is continuously required for the assembly of Cdc20-inhibitory complexes during interphase and mitosis.

Mps1 promotes chromosome alignment independently of Aurora B

In addition to restraining anaphase onset, Mps1 is necessary for alignment of sister chromatids at the metaphase plate, a function that has been attributed to Mps1-dependent activation of Aurora B (Jelluma et al., 2008b). In an attempt to confirm this finding, we treated Mps1^{wt} and Mps1^{as} cells with 3-MB-PP1 and MG132 to analyze chromosome alignment while blocking anaphase onset. Whereas almost all cells with active Mps1 had well-formed metaphase plates, 47% of Mps1-inhibited cells had misaligned chromosomes near one or both spindle poles, as well as broader-than-normal metaphase plates (Fig. 2.7A). In parallel, we measured levels of phosphorylated histone H3 and centromere protein A (CENP-A) via quantitative immunoblotting and fluorescence microscopy with phosphospecific antibodies (Fig. 2.7B-D). Surprisingly, allele-specific Mps1 inhibition failed to suppress the phosphorylation of either Aurora B substrate. To corroborate these results, we examined CENP-A phosphorylation levels in *MPS1*-null cells, and again detected no significant loss of phosphorylation (Fig. 2.7E). These results have two important implications: first, that Mps1 promotes metaphase chromosome alignment independently of Aurora B, and second, that

Mps1 inhibition can be used to interrogate the SAC without collateral suppression of Aurora B-dependent phosphorylation.
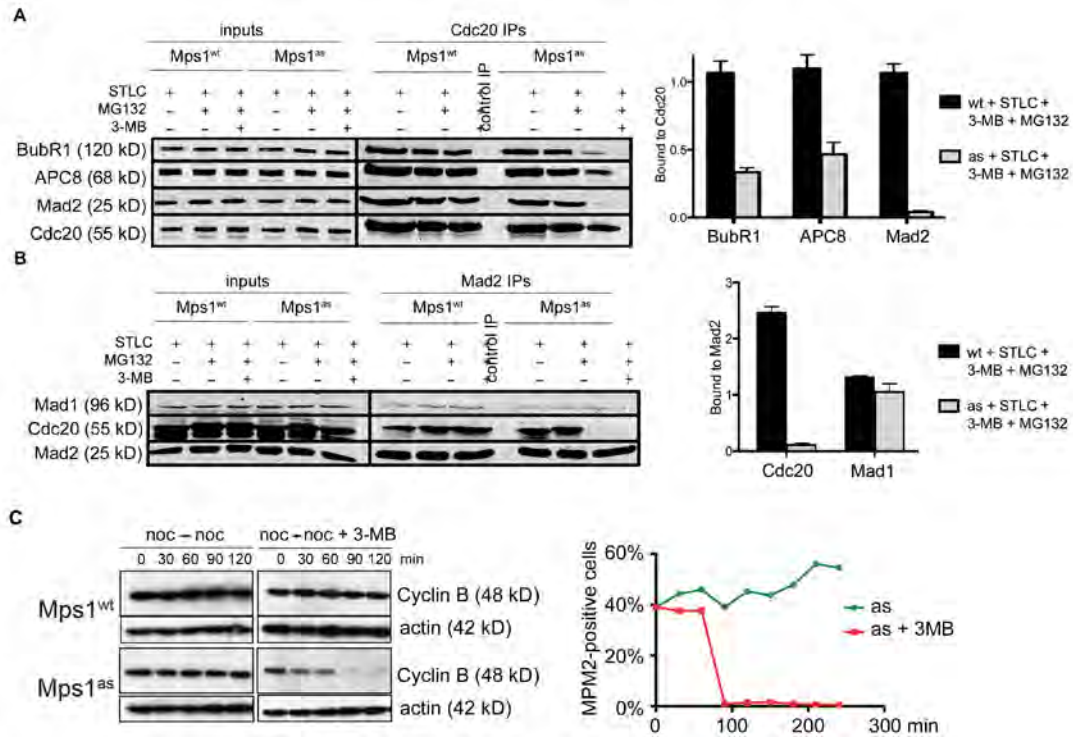
Figure 2.6 Mps1 continuously stabilizes Cdc20-inhibitory complexes in M phase.
(A) Mitotic cells were harvested by STLC treatment and shakeoff, then incubated in medium containing STLC, 3-MB-PP1, and/or MG132 for 2 hours. Extracts were immunoprecipitated with antibodies to Cdc20 and resolved by SDS-PAGE. Levels of BubR1, APC8, Mad2, and Cdc20 in each IP were determined by quantitative immunoblotting. The ratio of each protein to Cdc20 was computed and normalized to ratios obtained from STLC-treated Mps1^{wt} cells (= 1.0). Error bars denote s.e.m. (B) Extracts were analyzed as in panel A, except that Mad2 antbodies were used for immunoprecipitation, and Mad1 antibodies were also used for immunoblotting. (C) Cells were arrested in M phase via overnight treatment with nocodazole. At time 0, cells were either treated with 3-MB-PP1 or left untreated as a control. Samples were collected at 30-min intervals for analysis of cyclin B levels (left) and determination of mitotic indices (right).

46

Mps1 recruits Bub1 and all other SAC transducers to the outer kinetochore and is necessary for centromeric targeting of shugoshin

To investigate why chromosomes misalign despite normal phosphorylation of Aurora B substrates, we examined known regulators of SAC signaling, kinetochore-microtubule attachment, and error correction in Mps1-inhibited cells using quantitative microscopy (Fig. 2.8). Remarkably, all SAC transducers tested, including Bub1, BubR1, Mad1, Mad2, and Zw10, were evicted after Mps1 inhibition (Fig. 2.8 and Fig. 2.9). Also lost were CENP-E and Plk1, which are important stabilizers of kinetochore-MT attachment (Fig. 2.9). In contrast, core MT-binding factors such as Ndc80 and hKNL1 (also called AF15q14, Blinkin, or CASC5) remained tightly bound at the kinetochore, as did Mps1 itself (Fig. 2.8). Similarly, Aurora B and INCENP were properly localized at the inner centromere (Fig. 2.9), consistent with the intact phosphorylation of CENP-A in these cells (Fig. 2.7).

A

Mps1^wt + 3-MB + MG132

3% misaligned

Mps1^as + 3-MB + MG132

47% misaligned

B

	Mps1^wt				Mps1^as			
STLC	−	+	+	+	−	+	+	+
MG132	−	−	+	+	−	−	+	+
3-MB	−	−	−	+	−	−	−	+
pH3									(15 kD)
cyclin B									(48 kD)
tubulin									(55 kD)
pH3/tubulin :	0	1.0	1.5	1.5	0	1.8	2.2	1.9

C

DAPI   CREST   pCENP-A

Mps1^wt

Mps1^wt + 3-MB

Mps1^as

Mps1^as + 3-MB

+ noc and MG132

D

pCENP-A

wt
wt + 3-MB
as
as + 3-MB

+ noc and MG132

E

DAPI   BubR1   pCENP-A

flox/Δ

Δ/Δ

+ STLC and MG132

48
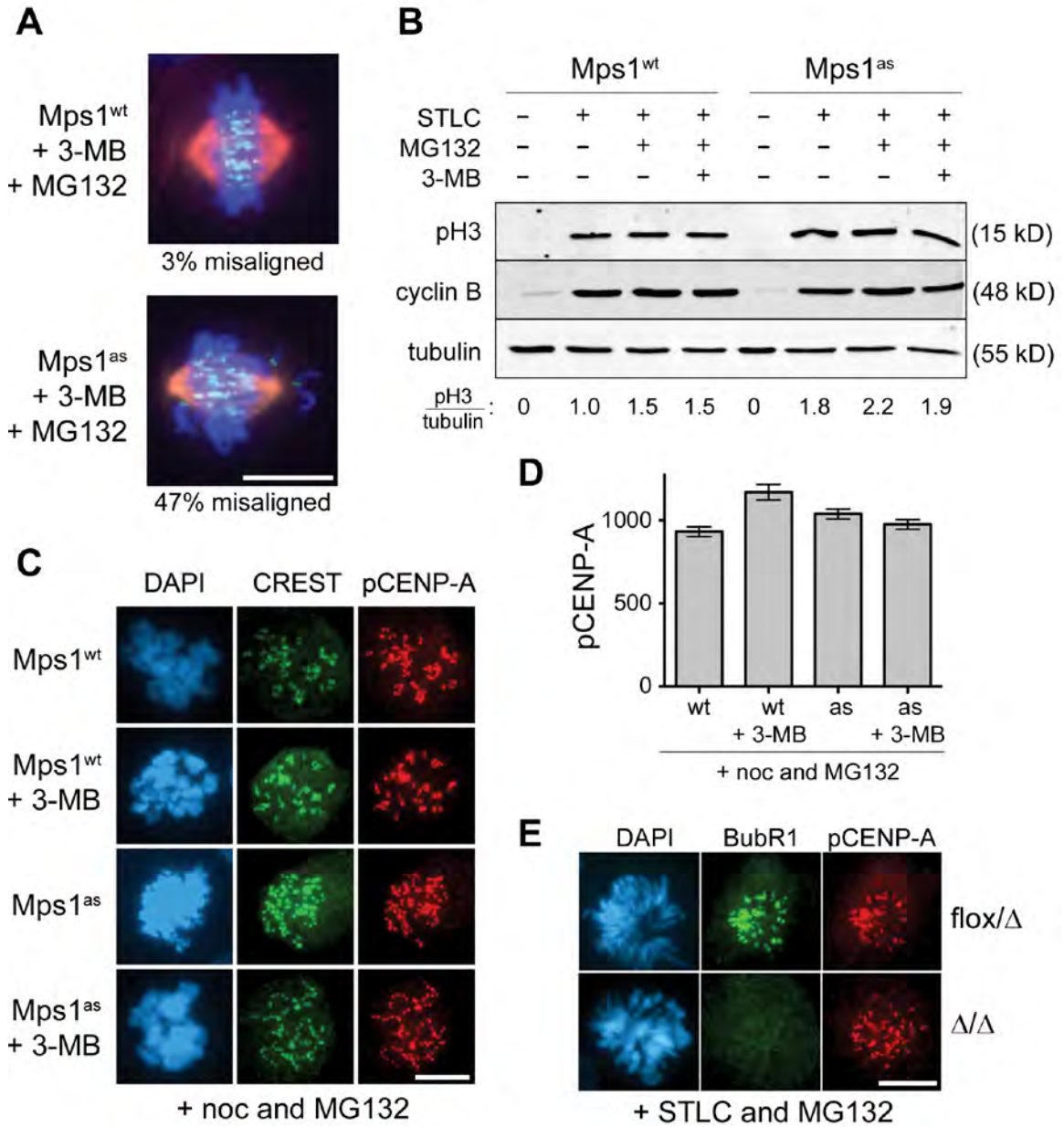
Figure 2.7 Mps1 promotes chromosome bi-orientation independently of Aurora B.

(A) Cells of the indicated genotypes were treated with 3-MB-PP1 and MG132 for 1 hr, then fixed and stained to detect centromeres (CREST, green), spindle MTs (α-tubulin, red), and chromosomes (DAPI, blue). (B) Mitotic Mps1^{wt} and Mps1^{as} cells were collected via STLC treatment and shakeoff, then maintained in the presence of STLC, MG132, and/or 3-MB-PP1 for 2 hours. Lysates were resolved by SDS-PAGE and quantitative immunoblotting. The ratio of phosphorylated histone H3 to tubulin was computed for each lane and normalized to the ratio in STLC-treated Mps1^{wt} cells. (C) Cells were treated with nocodazole for 4 hr to activate the SAC, then treated for an additional 4 hr with nocodazole, MG132, and/or 3-MB-PP1. Centromeres (CREST) and serine 7-phosphorylated CENP-A (pCENP-A) were detected by immunofluorescence microscopy. (D) Quantification of results in (C). At least 100 centromeres in ≥ 5 cells were scored per sample. Error bars denote s.d. (E) *MPS1*$^{flox/Δ}$ cells were infected with Adβgal (top) or AdCre (bottom). Three days later, both populations were treated with STLC and MG132 for 30 minutes, then fixed and stained with the indicated antibodies. BubR1 loss from kinetochores was used as a functional marker of Mps1 inactivation (see Fig. 2.8). Scale bar, 10 μm.

A

Mad1 Mad2 Bub1 BubR1

Mps1wt + 3-MB + MG132

Mps1as + 3-MB + MG132

B

Ndc80 hKNL1 Zwint Mps1

Mps1wt + 3-MB + MG132

Mps1as + 3-MB + MG132

C

relative intensity at KTs

Mad1 Mad2 Bub1 BubR1 CENP-E Plk1 Aurora B hKNL1 Ndc80

wt + 3-MB   as + 3-MB

50
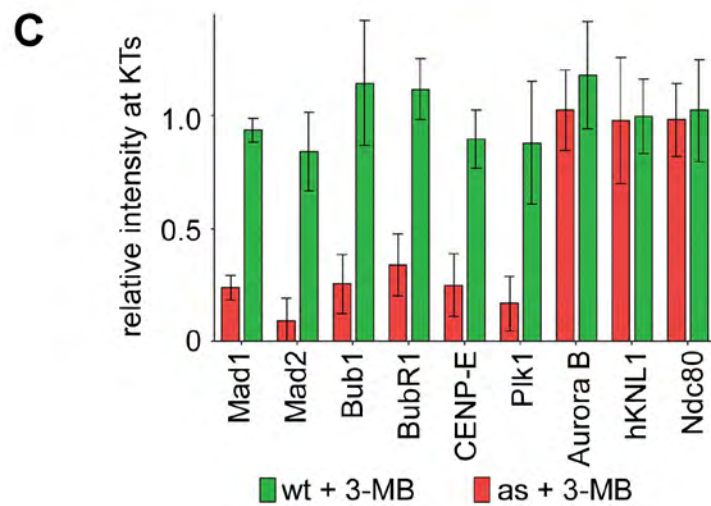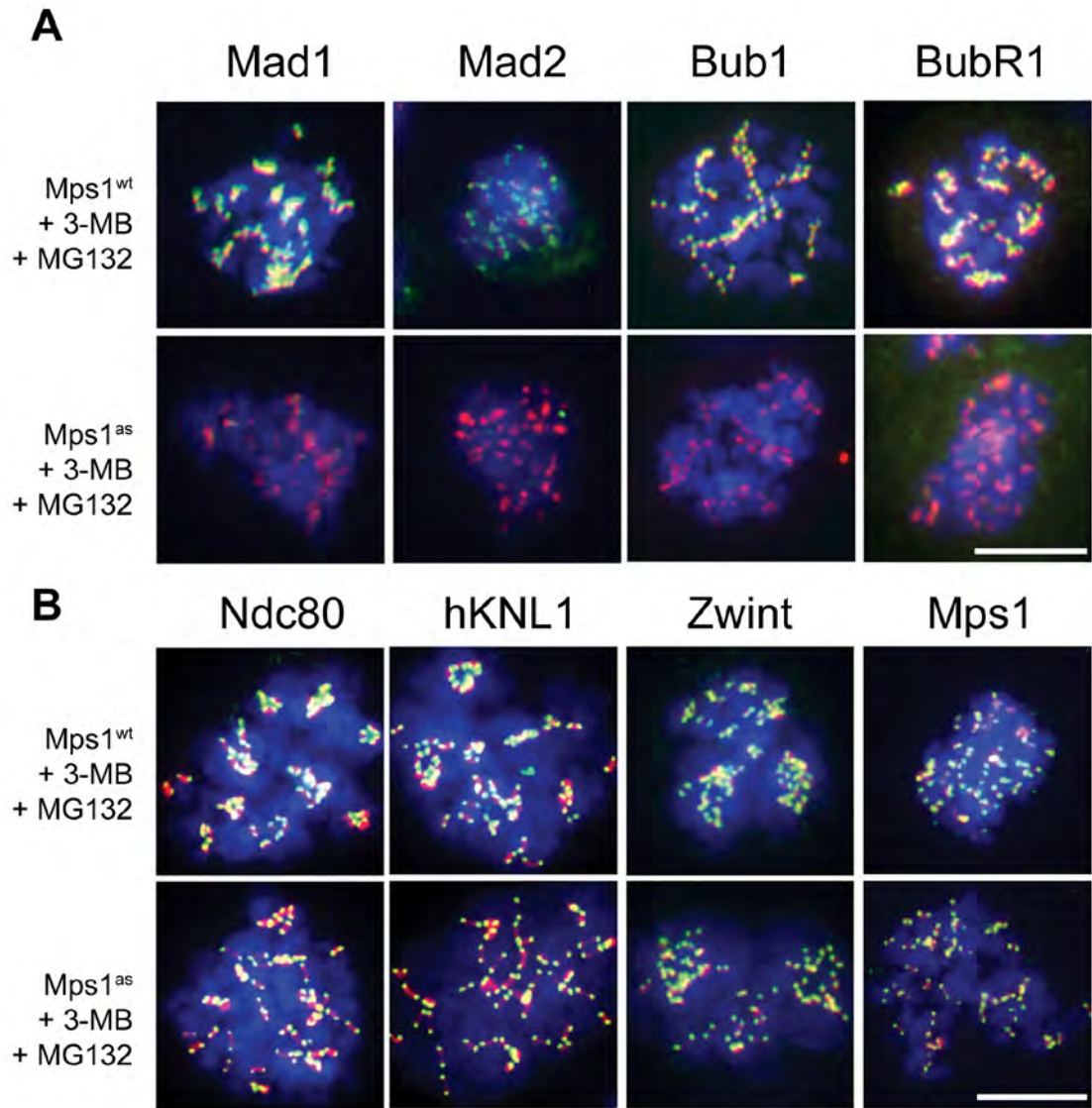
Figure 2.8 Mps1 kinase activity is continuously required to maintain Bub1 and all other SAC effectors at unattached kinetochores.
(A and B) Mps1^{wt} and Mps1^{as} cells were treated with nocodazole for 4 hr to activate the SAC, then treated with nocodazole, MG132, and/or 3-MB-PP1 for an additional 2 hours. Cells were fixed and stained with antibodies against the indicated SAC or kinetochore components (green) and CREST antiserum (red). Note that cells not treated with 3-MB-PP1 retained normal kinetochore localization patterns and thus have been omitted from these montages for clarity. Additional kinetochore/centromere proteins analyzed in this assay are shown in Fig. 2.9. (C) Kinetochore-specific signal intensities were determined in 3-MB-PP1-treated Mps1^{as} and Mps1^{wt} cells (>100 kinetochores in >5 cells per sample) and normalized to the equivalent values in untreated Mps1^{wt} cells. Scale bar, 10 μm.
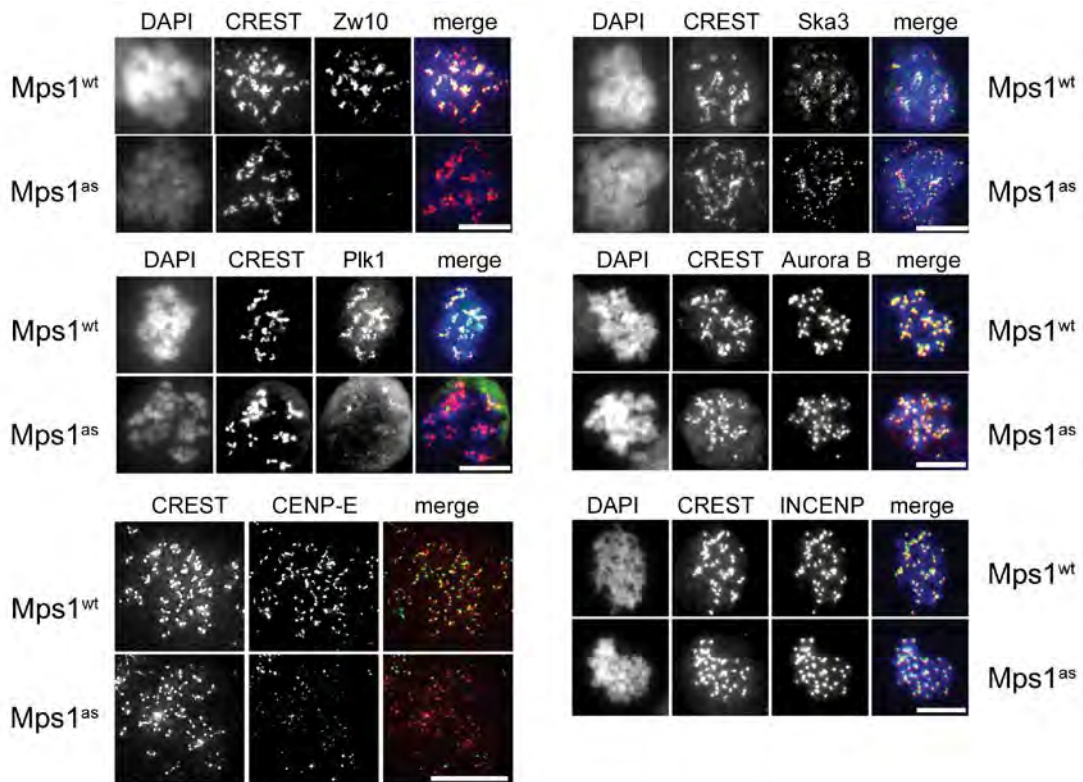
Figure 2.9 Mps1 kinase activity is continuously required to maintain SAC effectors at kinetochores.
Cells treated as in Fig.2.8 were stained with antibodies to the indicated SAC/kinetochore proteins (green), CREST antiserum (red), and DAPI (blue). All images were acquired via widefield microscopy except for CENP-E, which was acquired and deconvolved on a Deltavision Image Restoration microscope. Scale bar, 10 µm.

This spectrum of kinetochore targeting defects parallels the known consequences of Bub1 inactivation in both mammalian cells and frog egg extracts (Johnson et al., 2004; Perera et al., 2007; Sharp-Baker and Chen, 2001). In addition to regulating the SAC, Bub1 facilitates pericentromeric cohesion by phosphorylating histone H2A on threonine 120, which in turn recruits the cohesin protector Sgo1 (Kawashima et al., 2010). Interestingly, inactivating Mps1 hindered T120 phosphorylation at centromeres, causing Sgo1 to spread out onto chromosome arms (Fig. 2.11). Together these findings demonstrate that Mps1 regulates Bub1 spatially and functionally, providing a simple explanation for the chromosome bi-orientation defects of Mps1-inhibited cells, which occurred despite normal levels of Aurora B-catalyzed phosphorylation.

Cytosol-specific rescue of Mps1 inhibition restores mitotic timing and SAC proficiency to human cells

Both Mad2 and BubR1 can inhibit APC/C^{Cdc20} and regulate the timing of anaphase onset independently of kinetochores (Malureanu et al., 2009; Meraldi et al., 2004). To determine if the same is true for Mps1, we exploited the fact that Mps1's association with kinetochores depends on its N-terminus (Liu et al., 2003; Stucke et al., 2004). Briefly, we constructed a mutant allele lacking the first 100 amino acids (henceforth referred to Mps1$^{\Delta N}$) that indeed fails to localize to kinetochores (Fig. 2.10A). Both Mps1$^{\Delta N}$ and Mps1^{wt} were then introduced into Mps1^{as} cells as mCherry fusions, generating Mps1$^{as/\Delta N}$ and Mps1$^{as/wt}$ cells. These cells were then treated with 3-MB-PP1 to inactivate Mps1^{as} and probe the

functionality of the remaining allele. This assay revealed that Mps1 localization is crucial for targeting Bub1 to kinetochores (Fig. 2.10B) but not for assembling Cdc20-Mad2 complexes (Fig. 2.10C). Interestingly, Mps1$^{\Delta N}$ not only rescued the accelerated mitosis seen in Mps1^{as} cells but actually prolonged it in a 3-MB-PP1-dependent manner (Fig. 2.10D), suggesting that this cytosolic kinase can respond to (but not correct) bi-orientation defects caused by inhibition of kinetochore-bound Mps1^{as}. As a direct test of SAC proficiency, we quantified the duration of M phase in each cell line upon treatment with nocodazole (Fig. 2.10E). Whereas Mps1^{as} cells completed mitosis in 23 ± 5 minutes, Mps1$^{as/\Delta N}$ cells remained in M phase for 742 ± 80 minutes, or roughly half as long as Mps1$^{as/wt}$ cells (1419 ± 95 minutes; Fig. 2.10E). These data establish that Mps1 can indeed delay anaphase without being targeted to kinetochores. Nevertheless, its targeting substantially increases the perdurance of this delay. Thus, Mps1 uses both soluble and kinetochore-dependent mechanisms to generate and maintain the "wait anaphase" signal.

A

DAPI CREST Mps1 merge

Mps1^wt

Mps1^ΔN

B

Bub1

as

as/wt

as/ΔN

- as
- as/wt
- as/ΔN

Bub1 intensity at KTs

1.5
1.0
0.5

C

inputs | Cdc20 IPs

as | as | as/wt | as/ΔN | as | as | as/wt | as/ΔN

STLC + + + + | + + + +
MG132 + + + + | + + + +
3-MB - + + + | - + + +

Mad2 (25 kD)

Cdc20 (55 kD)

- as
- as/wt
- as/ΔN

Mad2 bound to Cdc20

0.6
0.4
0.2

D

cells exiting mitosis (cumulative)

100%
75%
50%
25%
0

0 15 30 45 60 75 90 105 ≥120

time after M phase entry (minutes)

— as
— as + 3-MB
— as/wt
— as/wt + 3-MB
— as/ΔN
— as/ΔN + 3-MB

E

duration of nocodazole-
induced mitotic arrest

minutes

2000
1500
1000
500

as
as + 3-MB
as/wt
as/wt + 3-MB
as/ΔN
as/ΔN + 3-MB

Figure 2.10 Cytosolic-specific rescue of Mps1 inhibition restores mitotic timing and SAC proficiency to human cells.
(A) Cells were fixed and stained with antibodies to centromere autoantigens (CREST, red) and transgene-encoded Mps1^{wt} and Mps1$^{\Delta N}$ (green). (B) Mps1^{as}, Mps1$^{as/wt}$, and Mps1$^{as/\Delta N}$ cells were treated with nocodazole for 4 hr to activate the SAC, then treated with nocodazole, MG132, and/or 3-MB-PP1 for an additional 2 hours. Cells were fixed and stained with antibodies against Bub1 (green) and CREST antiserum (red). Kinetochore-specific signal intensities were determined in 3-MB-PP1-treated Mps1^{as}, Mps1$^{as/wt}$, and Mps1$^{as/\Delta N}$ cells (>100 kinetochores in >5 cells per sample) and normalized to values in untreated Mps1^{as} cells. Scale bar, 10 µm. (C) Mitotic cells were harvested by overnight STLC treatment and shakeoff, then incubated in medium containing STLC, 3-MB-PP1, and/or MG132 for 2 hours. Extracts and Cdc20 immunoprecipitates were analyzed as in Fig. 5. Recovery of Mad2 relative to Cdc20 was determined and normalized to its recovery from STLC- and MG132-treated Mps1^{as} cells (= 1.0). Error bars denote s.e.m. (D) Quantification of mitotic timing. Cumulative frequency of anaphase onset is plotted as a function of time after NEB. (E) Mps1$^{\Delta N}$ rescues the SAC. Cells were traced by phase-contrast microscopy during treatment with nocodazole ± 3-MB-PP1 (cf. Fig. 2.1F). Error bars indicate s.e.m.
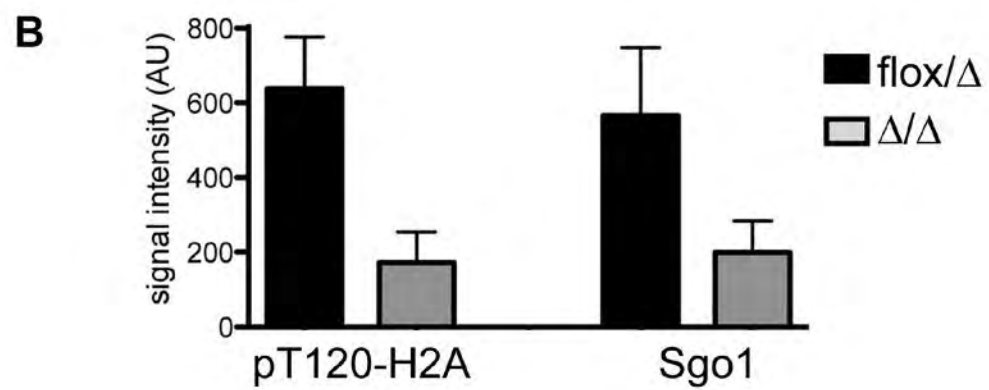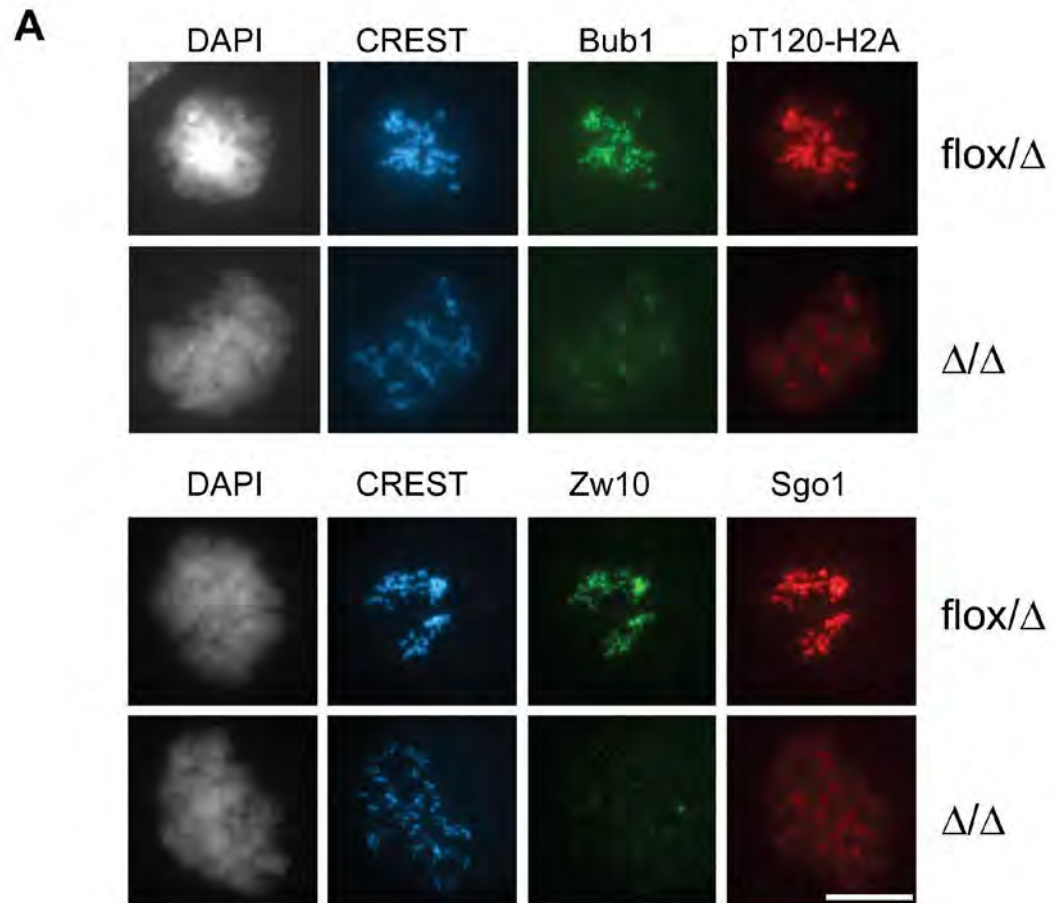
Figure 2.11 Mps1 promotes Bub1-catalyzed histone H2A phosphorylation and targeting of Sgo1 to centromeres.

(A) MPS1$^{flox/\Delta}$ cells were infected with Adβgal (top) or AdCre (bottom). Three days later, both populations were treated with nocodazole and MG132 for 60 minutes, then fixed and stained with the indicated antibodies. Bub1 and Zw10 were used to verify functional inactivation of Mps1 (see Figs. 7 and S2). Scale bar, 10 μm. (B) Quantification of results in (A). At least 100 centromeres in ≥ 5 cells were scored per sample. Error bars denote s.d.

Discussion

Classically the SAC has been conceptualized as a sensor of kinetochore-MT attachment defects. However, recent studies have painted a more complex picture, as the terminal anaphase inhibitors Mad2 and BubR1 (but not other canonical SAC components or kinetochores themselves) are also required to sustain basal M phase timing. These and related observations have led to newer models in which Mad2 and/or BubR1 can be activated away from kinetochores. Indeed, Mad2 and BubR1 can spontaneously form a potent APC/C^{Cdc20} inhibitor *in vitro* from purified proteins (Kulukian et al., 2009), which could in theory account for the cytosolic assembly of Cdc20-inhibitory complexes during interphase (Malureanu et al., 2009; Sudakin et al., 2001). However, our data reveal that such complexes cannot be formed or maintained in the absence of Mps1 kinase activity. Consequently, Mps1-inhibited cells progressed from NEB to anaphase onset in just 12 minutes, a timeframe similar to the delay between Cdk1 and APC/C^{Cdc20} activation in cycling *Xenopus* egg extracts (Pomerening et al., 2005).

How might Mps1 promote the cytosolic formation of Cdc20-inhibitory complexes? Quantitative models of the SAC indicate that the rate at which a single unattached kinetochore generates Mad2-Cdc20 heterodimers is too slow to account for the global suppression of APC/C^{Cdc20} activity under these conditions (Ciliberto and Shah, 2009). Rather, this high degree of sensitivity requires further

rounds of Mad2-Cdc20 complex assembly in the cytoplasm (De Antoni et al., 2005). We speculate that Mps1 activates this cytosolic amplification mechanism, either by phosphorylating soluble Mad2 or Mad2-Cdc20 complexes directly (Wassmann et al., 2003), or by suppressing p31[comet], a structural mimic of Mad2 that competitively destabilizes Mad2-Cdc20 complexes (Vink et al., 2006; Xia et al., 2004; Yang et al., 2007). This would also explain why a cytosolic form of the kinase (Mps1[ΔN]) was able to restore Mad2-Cdc20 binding and inhibit anaphase onset in Mps1[as] cells (Fig. 2.10). Nevertheless, long-term maintenance of this inhibition (for example, during chronic treatment with spindle poisons) depends on Mps1's targeting to kinetochores, which presumably aids Mps1's phosphorylation of docking partners and/or activators of Bub1 and other SAC mediators. In support of this view, cytosolic versions of Bub1 only partially rescue the SAC deficiency and chromosome misalignment phenotypes of Bub1 RNAi cells (Kiyomitsu et al., 2007; Klebig et al., 2009a).

Many of the functions of Mps1 elucidated in this study were inapparent when this kinase was strongly (>90%) depleted from human cells using RNAi (Jelluma et al., 2008b; Liu et al., 2003; 2006; Stucke et al., 2002; Tighe et al., 2008). Two observations argue that this difference reflects more complete inactivation of Mps1 using chemical genetics, rather than an off-target effect on other kinases or ATPases. First and foremost, Mps1[wt] cells were treated in the same manner as Mps1[as] cells and proved to be completely resistant to 3-MB-PP1 in all assays. Second, the epistasis pattern exposed by Mps1 inhibition in human cells mirrors those defined by orthogonal methods in other model systems (i.e.,

immunodepletion in *Xenopus* egg extracts (Vigneron et al., 2004; Wong and Fang, 2005)and strong Mps1 overproduction in budding yeast (Hardwick et al., 1996)). This concurrence suggests that Mps1's proximal targets, and their mode of regulation by phosphorylation, are likely to be conserved among all eukaryotes.

It was recently reported that Mps1 is needed to sustain normal levels of Aurora B kinase activity, and hence required for proper alignment of chromosomes at the metaphase plate (Jelluma et al., 2008b). Although mal-oriented chromosomes were frequently observed in Mps1-inhibited cells, we failed to detect any significant decrease in the phosphorylation of histone H3 or CENP-A, two well-known *in vivo* substrates of Aurora B. One potentially relevant difference is that our analysis utilized human retinal pigment epithelial cells (a non-transformed and chromosomally stable cell type) whereas the earlier study used U2OS cells, a cancer cell line that harbors multiple genetic alterations. Such alterations might have disabled other regulatory networks that normally sustain Aurora B activity independently of Mps1. Alternatively, because the RNAi machinery regulates centromeric heterochromatin (Fukagawa et al., 2004), it is conceivable that high levels of some Mps1-directed shRNAs interfere with the processing of endogenous centromere-derived transcripts, and thus produce subtle anomalies in inner centromere structure and function that manifest as a synthetic defect in Aurora B regulation. Consistent with our findings, an orthogonal Mps1 kinase

inhibitor, reversine, also induces SAC override and chromosome bi-orientation defects without dampening Aurora B activity *in vivo* (Santaguida et al., 2010).

In mammals, the SAC plays an essential role in suppressing aneuploidy, developmental anomalies, and malignancy (Weaver and Cleveland, 2009). Moreover, SAC signaling can either enhance or attenuate the ability of spindle poisons to kill cancer cells (Gascoigne and Taylor, 2008; Janssen et al., 2009; Swanton et al., 2007). Thus, understanding how the SAC operates in molecular terms remains an important objective with broad scientific and medical relevance. Because the SAC itself is required for most methods of synchronizing cells in mitosis, biochemical analyses of SAC signaling require the development of specific and fast-acting inhibitors that can be applied to homogenous populations of mitotic cells. While Aurora B inhibitors can sometimes be used for this purpose, whether these compounds actually inactivate the SAC, or merely lead to its satisfaction via stabilization of kinetochore-MT attachments, remains controversial (Ditchfield et al., 2003; Hauf et al., 2003; Pinsky and Biggins, 2005; Vanoosthuyse and Hardwick, 2009; Yang et al., 2009). In contrast, Mps1 inhibition was effective in overriding the SAC even when MTs were depolymerized, yet did not perturb phosphorylation of endogenous Aurora B substrates. By enabling more surgical manipulation of the SAC, the tools developed here should clarify how this pathway and others interact to achieve high-fidelity chromosome segregation in human cells.

CHAPTER THREE: The Mps1-regulated phosphoproteome identifies Ska3 as an Mps1 substrate required for accurate chromosome segregation during mitosis

Summary

Accurate segregation of chromosomes during mitosis depends on the successful collaboration of a large set of mitotic kinases. Untangling the linear relationships between these kinases and their substrates are key problems in understanding mitotic progression. The evolutionarily conserved kinase Mps1 protects genome stability by promoting chromosome bi-orientation and by enforcing the spindle assembly checkpoint, a surveillance pathway that restrains anaphase until all chromatids properly attach to the mitotic spindle (Lan and Cleveland, 2010; Musacchio and Salmon, 2007). Despite a central role for Mps1 in these processes few of its substrates have been identified in higher eukaryotes. Here, we couple quantitative proteomics and chemical genetics to identify Mps1-dependent phosphorylation sites *in vivo.* Quantitation of over 20,000 phosphorylation sites revealed Mps1-regulated modifications on numerous kinetochore proteins including Mps1 itself, Histone H2A, the spindle checkpoint proteins Bub1, BubR1, and Mad1, and the outer kinetochore proteins Hec1,KNL1 and Ska3 (Santaguida and Musacchio, 2009). Analysis of the spatial and temporal distribution of Mps1-regulated phosphorylations with modification-specific antibodies demonstrates that Mps1 targets its substrates within the outer kinetochore primarily when microtubule occupancy is weak to non-existent and

does so under the regulation of the B56-PP2A phosphatase(Foley et al., 2011). Finally, we identify Ska3 as a direct Mps1 substrate that mediates efficient chromosome bi-orientation and K-fiber stability (Daum et al., 2009; Gaitanos et al., 2009; Hanisch et al., 2006; Ohta et al., 2010; Raaijmakers et al., 2009; Schmidt et al., 2012). Total internal reflection microscopy (TIRF-M) experiments indicate that this phosphorylation event increases the number of short-lived Ska complex particles on microtubules and reduces the size of tracking complexes on dynamic microtubules. Our study has identified and functionally validated the first Mps1 substrate in higher eukaryotes and shows how this kinase monitors and regulates kinetochore activity to achieve high fidelity chromosome segregation. This partnership of chemical genetics and quantitative proteomics promises to be a potent tool in making confident, accurate, and direct links from kinases to their substrates.

Introduction

Dynamic protein phosphorylation is central to nearly every aspect of cell biology. This is especially true during mitosis, when a large number of protein kinases, led by Cdk1, are activated in order to ensure orderly mitotic progression by building the mitotic spindle, promoting chromosome bi-orientation and accurate segregation, and coordinating cytokinesis (Funabiki and Wynne, 2013). The mitotic kinase Mps1 plays integral roles in both high fidelity chromosome segregation, through regulation of the spindle assembly checkpoint (SAC) and chromosome bi-orientation, yet few, if any, of its substrates have been identified

in higher eukaryotes (Liu and Winey, 2012) (Fig. 3.1A). These critical functions have made Mps1 an attractive anti-cancer drug target as Mps1 inhibition leads to rapid aneuploidy and cell death (Janssen et al., 2009; 2011; Kops et al., 2004).

The SAC maintains genome stability during mitosis by delaying anaphase until all chromosomes are properly bi-oriented on the mitotic spindle (Foley and Kapoor, 2013; Musacchio and Salmon, 2007; Santaguida and Musacchio, 2009). This delay stems from checkpoint-mediated inhibition of the anaphase promoting complex/cyclosome (APC/C), a ubiquitin ligase that triggers mitotic exit by targeting Cyclin B and securin for degradation (Buschhorn and Peters, 2006; Peters, 2006). Unattached kinetochores are a major source of this "wait anaphase" signal (Kulukian et al., 2009; Sudakin et al., 2001). As chromosomes bi-orient on the mitotic spindle, incorrect attachments are made and must be corrected. In addition to priming checkpoint signaling, kinetochores also serve as the chromosome attachment site to the mitotic spindle and regulate these attachments to ensure efficient bi-orientation (Santaguida and Musacchio, 2009). Spindle microtubule capture is mainly accomplished by the large, outer kinetochore complex known as the KMN network, an assembly of the KNL1, Mis12, and Ndc80 complexes (Cheeseman et al., 2006). Efficient kinetochore-MT interaction also requires the Ska1 complex, which is thought to help couple kinetochores with depolymerizing MT ends (Hanisch et al., 2006; Gaitanos et al., 2009; Raaijmakers et al., 2009). Not surprisingly, these complexes have

emerged as prime targets of the mitotic kinases that monitor proper kinetochore-microtubule attachment (Chan et al., 2012; Welburn et al., 2010).

The conserved Mps1, Bub1, Plk1, and Aurora kinases ensure accurate chromosome segregation by mediating SAC signaling and promoting chromosome bi-orientation, but few of their corresponding substrates have been identified (Zich and Hardwick, 2010). However, recent progress has been made in both budding and fission yeast, where Mps1 was shown to stimulate SAC signaling by phosphorylating the outer kinetochore proteins Ndc80 and KNL1 (Kemmler et al., 2009; London et al., 2012; Shepperd et al., 2012) and to promote efficient coupling of kinetochores to MT plus ends by phosphorylating Dam1, a component of the DASH complex, which is thought to be the functional ortholog of the Ska1 complex (Chan et al., 2012; Shimogawa et al., 2006; Welburn et al., 2009). Mps1 substrate identification in higher eukaryotes has proven particularly difficult. Indeed, progress in this area has been hampered by Mps1's promiscuity *in vitro*, low affinity for kinetochores *in vivo*, and, until very recently, a lack of a well defined consensus motif (Dou et al., 2011; Hennrich et al., 2013). Mps1 has been proposed to promote chromosome bi-orientation by stimulating Aurora B activity through phosphorylation of borealin, a component of the chromosomal passenger complex (Jelluma et al., 2008a). However, this proposal has proven to be controversial as several studies, using structurally unrelated small molecule inhibitors, found no defects in Aurora B activity after

Mps1 inhibition. (Hewitt et al., 2010; Maciejowski et al., 2010; Santaguida et al., 2010).

We identified Mps1-dependent phosphorylations *in vivo* in human cells in a global and unbiased manner via large-scale quantitative phosphoproteomics, taking advantage of a chemical genetic system for monospecific Mps1 inhibition. We find that Mps1 targets many proteins of the centromere and outer kinetochore. Furthermore, through the use of modification-specific antibodies, we find that Mps1 primarily targets its substrates when MT attachments are weak to non-existent. Finally, we find that Mps1 regulates Ska complex function to ensure efficient chromosome bi-orientation and accurate chromosome segregation.

Results

Quantitative Phosphoproteomic Profiling of the Mps1 Signaling Network

To identify direct substrates of Mps1 *in vivo*, we coupled quantitative phospho-proteomics with our previously described system for chemical genetic inhibition of Mps1, where a point mutant of Mps1,Mps1[as], was shown to be sensitive to inhibition by the bulky ATP analog 3-MB-PP1. (Maciejowski et al., 2010). To enable quantitative proteomics, we performed stable isotope labeling by amino acids in cell culture (SILAC) of RPE cells expressing either Mps1[as] or Mps1[wt] (Fig. 3.1B). These SILAC-encoded cell lines were then mitotically arrested in nocodazole prior to treatment with the proteasome inhibitor, MG132, and 3-MB-PP1. Over four biological replicate experiments, we identified nearly 23,000

distinct phosphopeptides in either cell line (Fig 3.1, 3.2). Twenty four phospho-peptides were determined to contain Mps1-dependent phosphorylation sites, defined as phosphorylated peptides in control cells (Mps1^{as}-3MB, Mps1^{wt}+/-3MB) whose abundance were more than twice that in samples from Mps1 inhibited cells (Mps1^{as}+3MB) (Fig. 3.1,3.2,3.3). Many known proteins of the centromere and outer kinetochore were identified in this down-regulated population including Mps1 itself, Histone H2A, BubR1, CENP-E, Spindly, KNL1, and Ska3 (Fig. 3.1D). Comparison of Mps1-dependent phosphorylation sites suggests that Mps1 prefers to target phospho-acceptor residues that are preceded by an acidic residue in the -2 position (Fig. 3.4). In order to study the phosphorylation of Mps1 T33,S37 (pMps1-N); T360,S363 (pMps1-C), H2A T120 (pH2A), KNL1 S1831,S1834 (pKNL1-C),Rod T13,S15 (pRod-N) and Ska3 S34 (pSka3) *in vivo*, rabbit polyclonal antibodies were generated against phosphopeptides containing these identified phosphorylation sites (Fig. 3.4). The affinity purified anti-pT33,pS37 and pT360,pS363 antibodies recognized recombinant human Mps1 only in the presence of active kinase (Fig 3.5) and recognition of anti-pT33,pS37 was abolished by T33A,S37A mutation of Mps1.(Fig. 3.5). The anti-pT33,pS37 and pT360,pS363 antibodies also recognized wild-type Mps1 that had been immunoprecipitated from nocodazole-arrested human (HeLa) cells, but anti-pT33,pS37 could not recognize a T33A,S37A mutant (Fig 3.5C, 3.5). Rod exhibited a similar profile (Fig. 3.11). Together, these results demonstrate that the Mps1 anti-pT33,pS37 and pT360,pS363 and anti-Rod pT13,pS15 antibodies specifically recognize their phosphorylated epitopes.

a

Mps1 → Mps1

b

Mps1^{wt} or Mps1^{as} cells

R^{0}K^0 R^{10}K^8

(−) 3MB-PP1 (+)

SCX/IMAC

LC-MS/MS

MaxQuant

statistical analysis
& bioinformatics

Mps1-regulated
phosphosites

c

Mps1^{wt} Mps1^{as}

19,201

4,214   3,620

27,035 phosphopeptides

d

$\log_2(\text{Mps1}^{as} \pm \text{3MB-PP1})$

$\log_2(\text{Mps1}^{wt} \pm \text{3MB-PP1})$

Histone H2A
Spindly
Hec1
CENP-F
BubR1
Bub1
KNL1
Ska3
CENP-E
Mps1
Rod

69
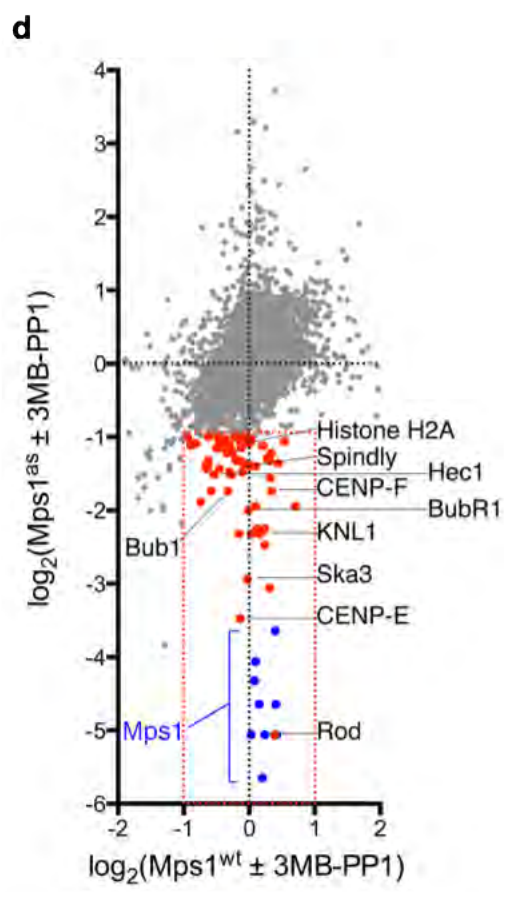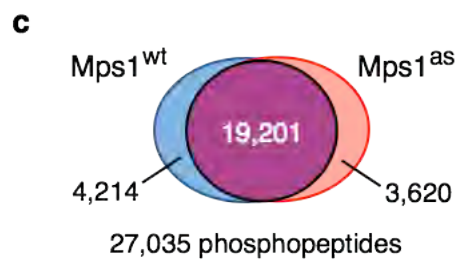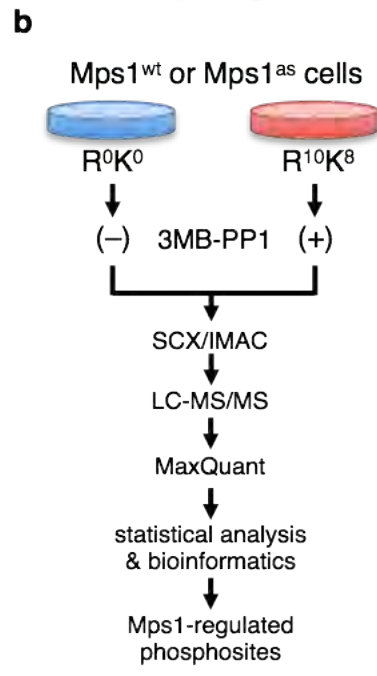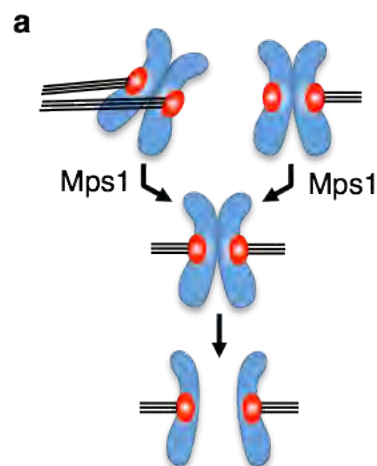
Figure 3.1 The Mps1 Phosphoproteome.
(A) Mps1 ensures accurate sister chromatid segregation at anaphase. Mps1 participates in both a signaling role, by inhibiting mitotic progression in the presence of unattached kinetochores, and in a kinetochore-microtubule attachment regulatory role, by monitoring the quality of attachments. (B) Scheme illustrating the experimental design and workflow. Four biological replicate experiments were performed in Mps1[as] and Mps1[wt] cells upon SILAC encoding as indicated. In each experiment, Mps1[as] inhibitor 3-MB-PP1 was added to one mitotically arrested cell population before lysis and protein digestion. Phosphopeptides were enriched by SCX chromatography combined with IMAC prior to LC-MS/MS analysis and data processing. (C) SILAC analysis mapped and quantitated nearly 30,000 phosphorylation sites with a high degree of overlap in Mps1[wt] and Mps1[as] cell lines. (D) Phosphopeptides identified in the SILAC screen. Mps1 autophosphorylation sites are labeled in blue. Other phosphopeptides showing significant regulation (greater than 2-fold down-regulated in Mps1[as] cells and not regulated in Mps1[w]t cells) are labeled in red. (All work in this figure performed by Kathrin Grundner-Culemann and Henrik Daub).
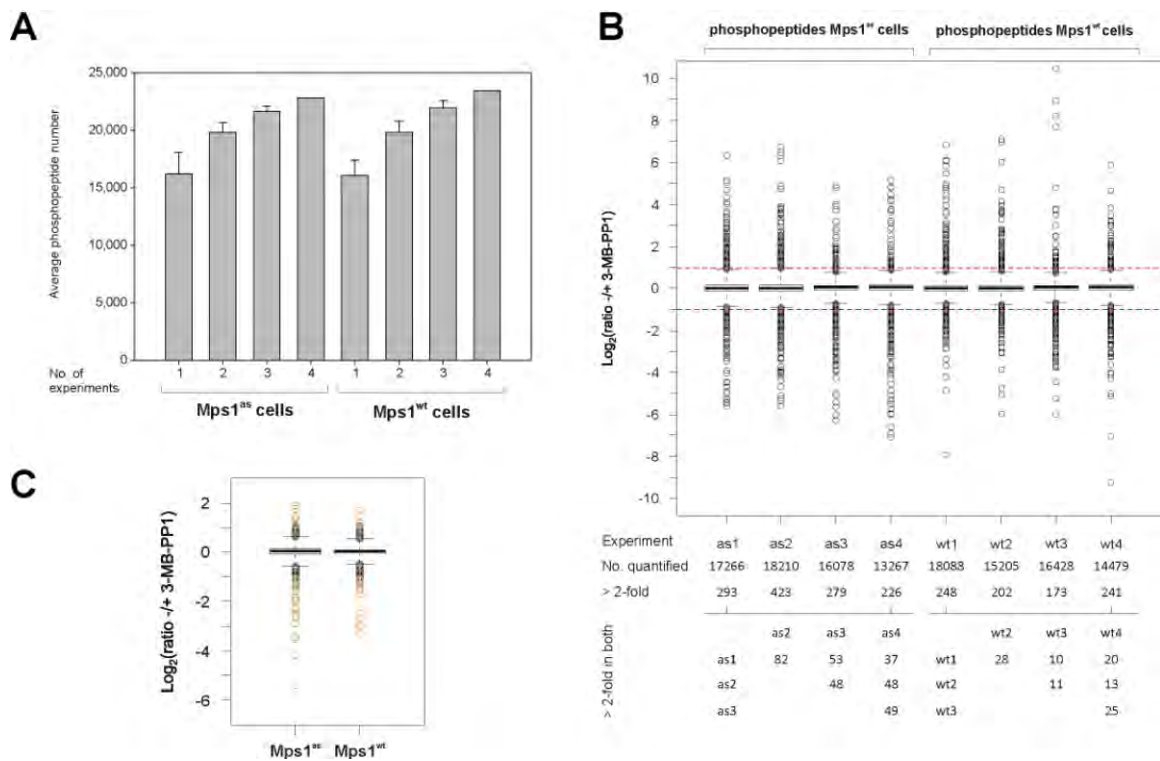
Figure 3.2 The Mps1 Phosphoproteome.
(A) Effect of biological replicate analyses on overall phosphoproteome coverage. The average numbers of phosphopeptide quantifications from one, two or three replicates and the total numbers based on all four experiments are shown for Mps1^{as} and Mps1^{wt} phosphoproteome analyses. (B)Ratio distribution and reproducibility across replicate experiments. The distribution of phosphopeptide ratios is shown as box plot for all individual MPS1^{as} and MPS1^{wt} experiments. For each SILAC analysis, the numbers of all quantified phosphopeptides and those measured with more than two-fold changes upon 3-MB-PP1 wash-out are shown. In the lower part, numbers of consistently more than two-fold regulated phosphopeptides are shown for all pair-wise comparisons of either MPS1^{as} or MPS1^{wt} experiments. The dashed red lines indicate thresholds for two-fold up- and downregulation. (C) Ratio distributions of consistently quantified phosphopeptides (coefficient of variation < 0.3) from Mps1^{as} or Mps1^{wt} cells are shown as box plots. The green dots represent a more than two-fold up- or downregulation of the Mps1^{as} ratio with respect to the corresponding ratio of Mps1^{wt} cells. The orange dots indicate a unidirectional, more than two-fold up- or downregulation of corresponding ratios in both cell lines. (All work in this figure performed by Kathrin Grundner-Culemann and Henrik Daub).

71
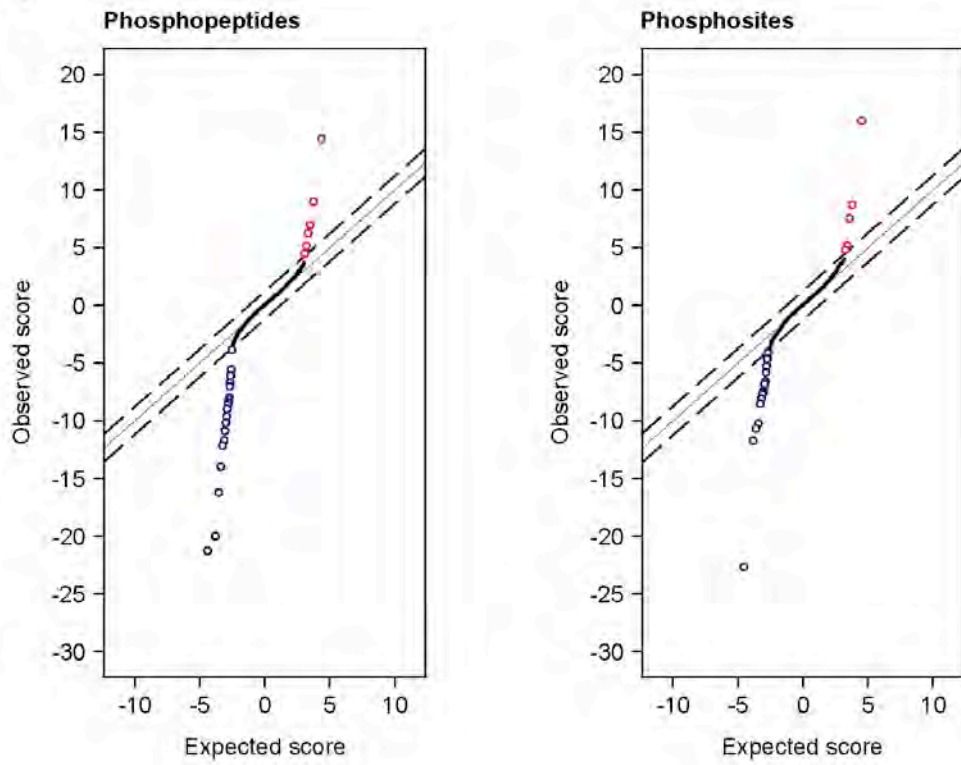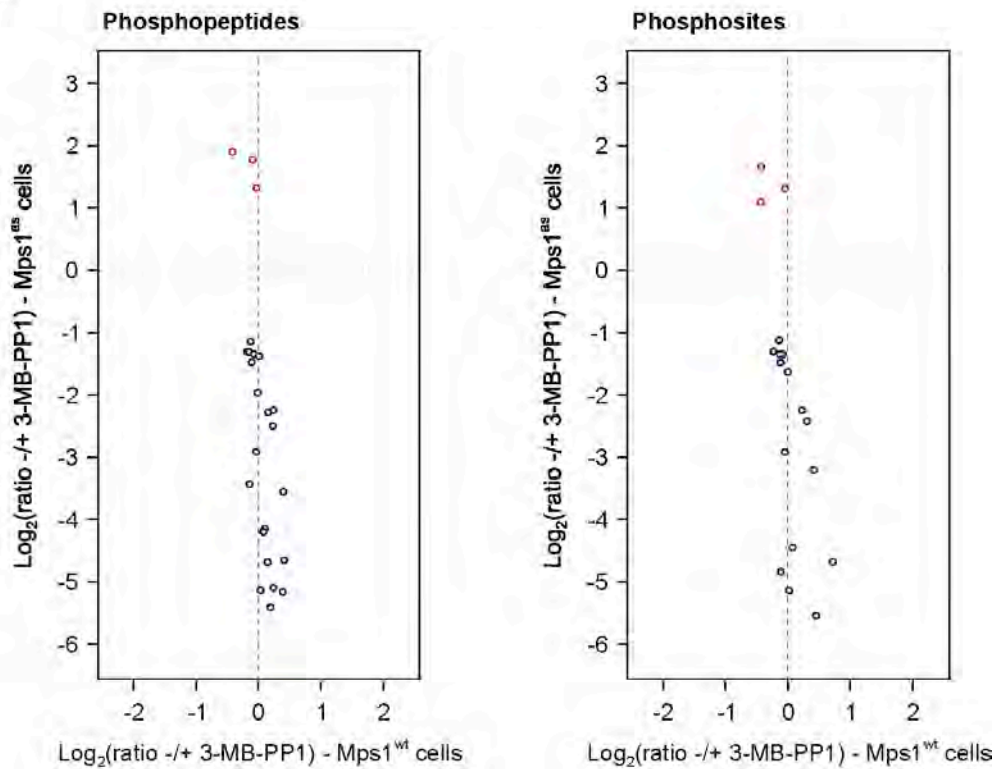
Figure 3.3 Identification of Mps1-dependent phosphorylation changes by statistical analysis of microarrays (SAM).
(a) Scatter plots of the observed score versus the expected score showing the results of differential SAM analysis of Mps1[as] or Mps1[wt] ratios of phosphopeptides (left panel) and phosphosites (right panel). The solid line indicates identity of observed and expected scores whereas the dashed lines depict the threshold of $\Delta = 1.189$ and $\Delta = 1.268$ respectively, beyond which phosphopeptides or phosphosites were identified as significantly up- and downregulated (red and blue circles) according to a false discovery rate (FDR) of 0%. (b) Regulated phosphopeptides (left panel, FDR of 0% for $\Delta = 1.189$) and phosphosites (right panel, FDR of 0% for $\Delta = 1.268$) with significantly different -/+ 3-MB-PP1 ratios in Mps1[as] compared to Mps1[wt] cells. Average ratios from Mps1[as] cell SILAC analyses were plotted against the respective ratios from Mps1[wt] experiments. All more than two-fold regulated phosphopeptides and phosphosites according to SAM analysis were either selectively upregulated (red circles) or downregulated (blue circles) in Mps1[as] versus Mps1[wt] cells. (All work in this figure performed by Kathrin Grundner-Culemann and Henrik Daub).
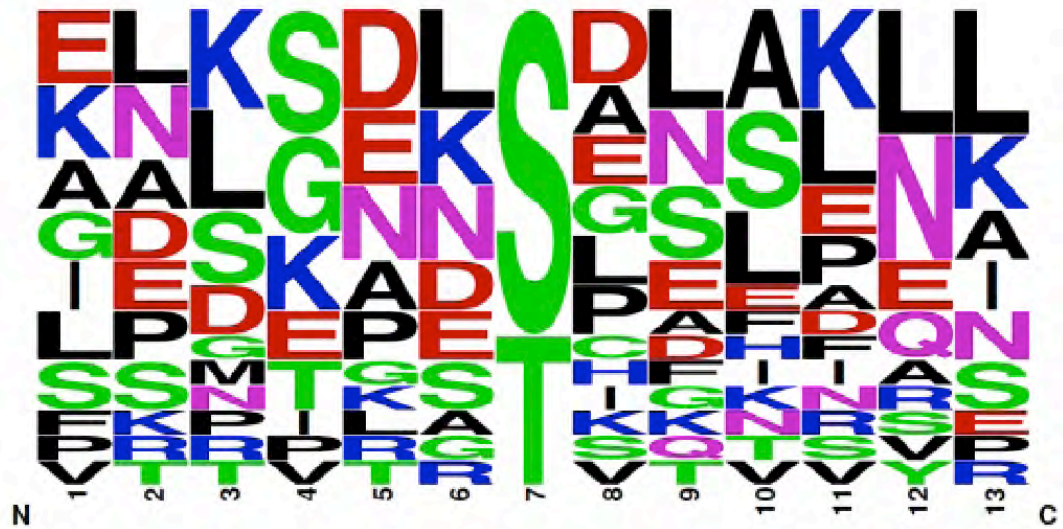
Figure 3.4 Bioinformatics analysis of Mps1-mediated phosphoregulation.
(a) Sequence logo plot visualizing the relative abundances of amino acids at
positions around Mps1-induced phosphorylation sites. (All work in this figure
performed by Kathrin Grundner-Culemann and Henrik Daub).

Protein	IPI	Sequence	Number of p(S/T)	Ratio +/- 3MB-PP1 Mps1^as	Ratio +/- 3MB-PP1 Mps1^wt
Centromere protein F	IPI00855998	LALSPLSLGK	2	0.45	0.92
Centromere-associated protein E	IPI00296365	SLPSPHPVR	2	0.09	0.91
Coiled-coil domain-containing protein 99	IPI00030845	LIGVPADAEALSERSGNTPNSPRLAAESK	2	0.38	1.01
Coiled-coil domain-containing protein 99	IPI00030845	SGNTPNSPRLAAESK	2	0.40	0.88
Coiled-coil domain-containing protein 99	IPI00030845	LIGVPADAEALSERSGNTPNSPR	2	0.40	0.90
Dual specificity protein kinase TTK	IPI00151170	NSVPLSDALLNK	1	0.03	1.02
Dual specificity protein kinase TTK	IPI00151170	DLVVPGSKPSGNDSCELR	1	0.04	1.33
Dual specificity protein kinase TTK	IPI00151170	NEDLTDELSLNK	1	0.05	1.06
Dual specificity protein kinase TTK	IPI00151170	FKNEDLTDELSLNK	1	0.06	1.07
Dual specificity protein kinase TTK	IPI00151170	NKTESSLLAK	1	0.08	1.32
Dual specificity protein kinase TTK	IPI00151170	NEDLTDELSLNK	2	0.02	1.15
Dual specificity protein kinase TTK	IPI00151170	NKTESSLLAK	2	0.03	1.31
Dual specificity protein kinase TTK	IPI00151170	FKNEDLTDELSLNK	2	0.03	1.18
Dual specificity protein kinase TTK	IPI00151170	ISADTTDNSGTVNQIMMMANNPEDWLSLLLK	2	0.04	1.11
E3 ubiquitin-protein ligase HUWE1	IPI00456919	GNDTPLALESTNTEK	1	2.47	0.98
E3 ubiquitin-protein ligase HUWE1	IPI00456919	LGSSGLGSASSIQAAVR	1	3.38	0.94
E3 ubiquitin-protein ligase HUWE1	IPI00456919	LGSSGLGSASSIQAAVR	2	3.69	0.75
Histone H2A type 2-C	IPI00339274	VTIAQGGVLPNIQAVLLPKKTESHK	2	0.39	0.95
Microtubule-associated protein 1B	IPI00008868	SLMSSPEDLTK	3	0.18	1.18
Mitotic checkpoint S/T-protein kinase BUB1 beta	IPI00141933	LELTNETSENPTQSPWCSQYRR	1	0.25	0.99
Nexilin	IPI00180404	EMLASDDEEDVSSKVEK	2	0.20	1.12
Protein CASC5	IPI00220694	SANSVLIK	1	0.36	0.93
Protein CASC5	IPI00220694	SANSVLIK	2	0.21	1.18
Spindle and kinetochore-associated protein 3	IPI00333014	ALDGEESDFEDYPMR	1	0.13	0.98

Table 3.1 List of Mps1-regulated phosphopeptides.
Included in this list are phosphopeptides what were more than two-fold downregulated specifically in Mps1^as cells and seen in at least two independent experiments. CASC5 is also known as KNL1 or Blinkin. (All work in this table performed by Kathrin Grundner-Culemann and Henrik Daub).

75

Protein	IPI	Position	Sequence Window	Ratio +/- 3MB-PP1 Mps1ᵃˢ	Ratio +/- 3MB-PP1 Mps1ʷᵗ
Centromere protein F	IPI00855998	3122	LALSPL **S** LGKENL	0.46	0.92
Coiled-coil domain-containing protein 99	IPI00030845	450	EALSER **S** GNTPNS	0.39	0.92
Coiled-coil domain-containing protein 99	IPI00030845	453	SERSGN **T** PNSPRL	0.40	0.86
Dual specificity protein kinase TTK	IPI00151170	33	FKNEDL **T** DELSLN	0.05	1.07
Dual specificity protein kinase TTK	IPI00151170	49	ADTTDN **S** GTVNQI	0.03	0.93
Dual specificity protein kinase TTK	IPI00151170	80	KNSVPL **S** DALLNK	0.03	1.02
Dual specificity protein kinase TTK	IPI00151170	321	KPSGND **S** CELRNL	0.04	1.66
Dual specificity protein kinase TTK	IPI00151170	360	ITLKNK **T** ESSLLA	0.02	1.38
Dual specificity protein kinase TTK	IPI00151170	363	KNKTES **S** LLAKLE	0.11	1.34
E3 ubiquitin-protein ligase HUWE1	IPI00456919	1722	ENKGND **T** PLALES	2.47	0.98
E3 ubiquitin-protein ligase HUWE1	IPI00456919	3757	GSSGLG **S** ASSIQA	3.12	0.75
E3 ubiquitin-protein ligase HUWE1	IPI00456919	3760	GLGSAS **S** IQAAVR	2.11	0.75
Histone H2A type 2-C	IPI00339274	121	VLLPKK **T** ESHKAK	0.39	0.96
Histone H2A type 2-C	IPI00339274	123	LPKKTE **S** HKAKSK	0.39	0.96
Kinesin light chain 2	IPI00021634	581	PRMKRA **S** SLNFLN	0.32	1.01
Microtubule-associated protein 1B	IPI00008868	837	SSPEDL **T** KDFEEL	0.19	1.25
Protein CASC5	IPI00220694	1831	EEDIDK **S** ANSVLI	0.36	0.93
Protein CASC5	IPI00220694	1834	IDKSAN **S** VLIKNL	0.21	1.18
Spindle and kinetochore-associated protein 3	IPI00333014	34	ALDGEE **S** DFEDYP	0.13	0.98

Table 3.2 List of Mps1-regulated phosphorylation sites.
Included in this list are phosphorylation sites what were more than two-fold downregulated specifically in Mps1ᵃˢ cells and seen in at least two independent experiments. (All work in this table performed by Kathrin Grundner-Culemann and Henrik Daub).
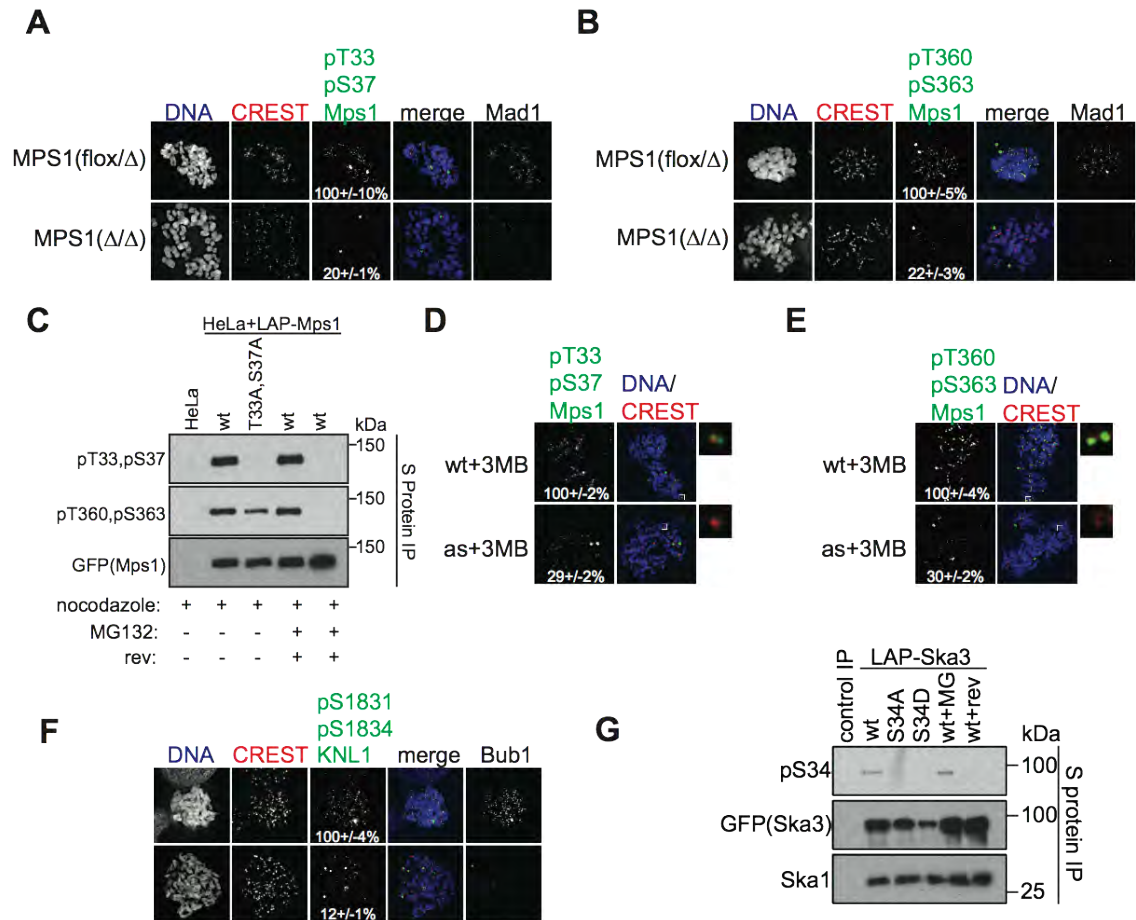
Figure 3.5 Specificity controls for affinity purified polyclonal phosphorylation-specific antibodies.
(A,B) nocodazole-arrested MPS1 (flox/Δ) and MPS1 (Δ/Δ) cells were stained with affinity purified polyclonal phosphorylation-specific antibodies as indicated. Mad1 staining was used as a control to mark effective MPS1 deletion. Mad1 depends on Mps1 for kinetochore recruitment (see chapter 2). (C) anti-pT33,pS37 Mps1 and anti-pT360,pS363 Mps1 recognize Mps1 purified from nocodazole arrested cells. This signal is completely diminished after Mps1 inhibition with the small molecule inhibitor reversine (Santaguida et al., 2010). (D,E) Mps1as inhibition by 3MB diminishese anti-pT33,pS37 Mps1 and anti-pT360,pS363 Mps1 levels at kinetochores in nocodazole-arrested mitotic cells. (F) anti-pS1831, pS1834 KNL1 levels at kinetochores are diminished after KNL1 depletion by siRNA. Bub1 was used as a marker for effective KNL1 depletion. Bub1 depends on KNL1 for kinetochore recruitment (Kiyomitsu et al., 2007). (G) anti-pS34 Ska3 recognizes Ska3 purified from nocodazole-arrested HeLa cells, but not S34A, S34D Ska3 mutants, or wild type Ska3 purified from Mps1-inhibited cells.

To determine whether Mps1 can directly phosphorylate Histone H2A, KNL1, Rod and Ska3 we incubated recombinant, human, full-length, or truncated, proteins with active kinase. In all cases, Mps1 was able to efficiently phosphorylate these proteins on the phosphorylation sites we identified in our SILAC screen (Fig. 3.1D).

Mps1 was also directly able to phosphorylate Spindly, another protein identified in the SILAC screen, *in vitro.* However, mutation of both of our identified phosphorylation sites on Spindly did not diminish the level of trans-phosphorylation by Mps1 (Fig. 3.7) suggesting that Mps1 may phosphorylate Spindly on many other sites in vitro or that an intervening kinase exists. In addition, we found that Spindly is mislocalized after Mps1 inhibition (Fig. 3.7).

In addition to direct phosphorylation of histone H2A by Mps1 *in vitro*, Mps1 inhibition diminished, but did not completely abolish, H2A pT120 staining at centromeres (Fig. 3.8). This incomplete effect may reflect a lingering contribution from Bub1 kinase, a known regulator of this phosphorylation site (Kawashima et al., 2010).
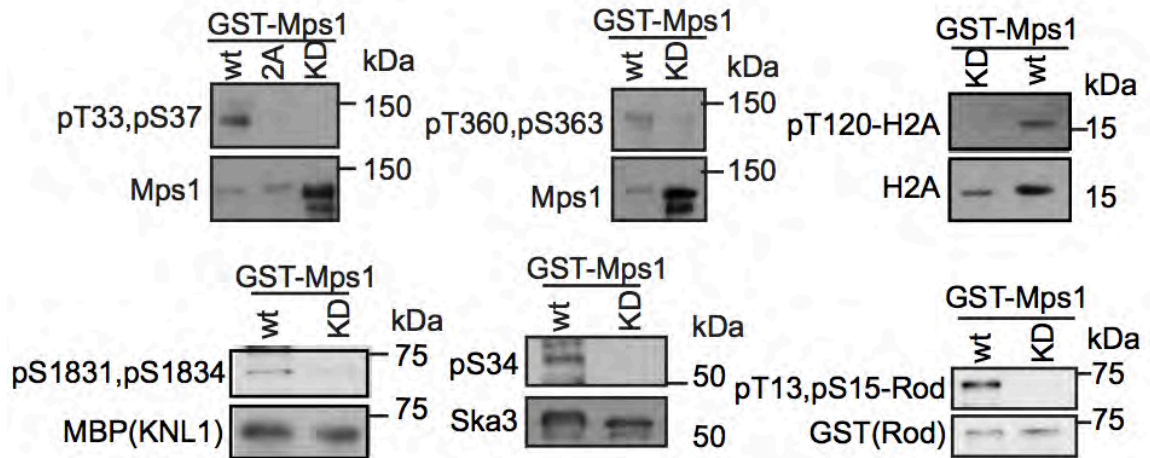
Figure 3.6 Mps1 directly phosphorylates several proteins identified in the SILAC screen.
GST-Mps1 wt, 2A(T33A,S37A), and kinase dead (KD), purified from insect cells, was incubated with purified Histone H2A, KNL1 fragment, Ska3, or an N-terminal fragment of Rod, and ATP. Phosphorylation was detected using affinity purified rabbit polyclonal phosphoantibodies identified in the screen including anti-pT33,pS37 Mps1, anti-pT360, pS363 Mps1, anti-pT120 H2A, anti-pS1831,pS1834 KNL1, anti-pS34 Ska3, and anti-pT13,pS15 Rod.
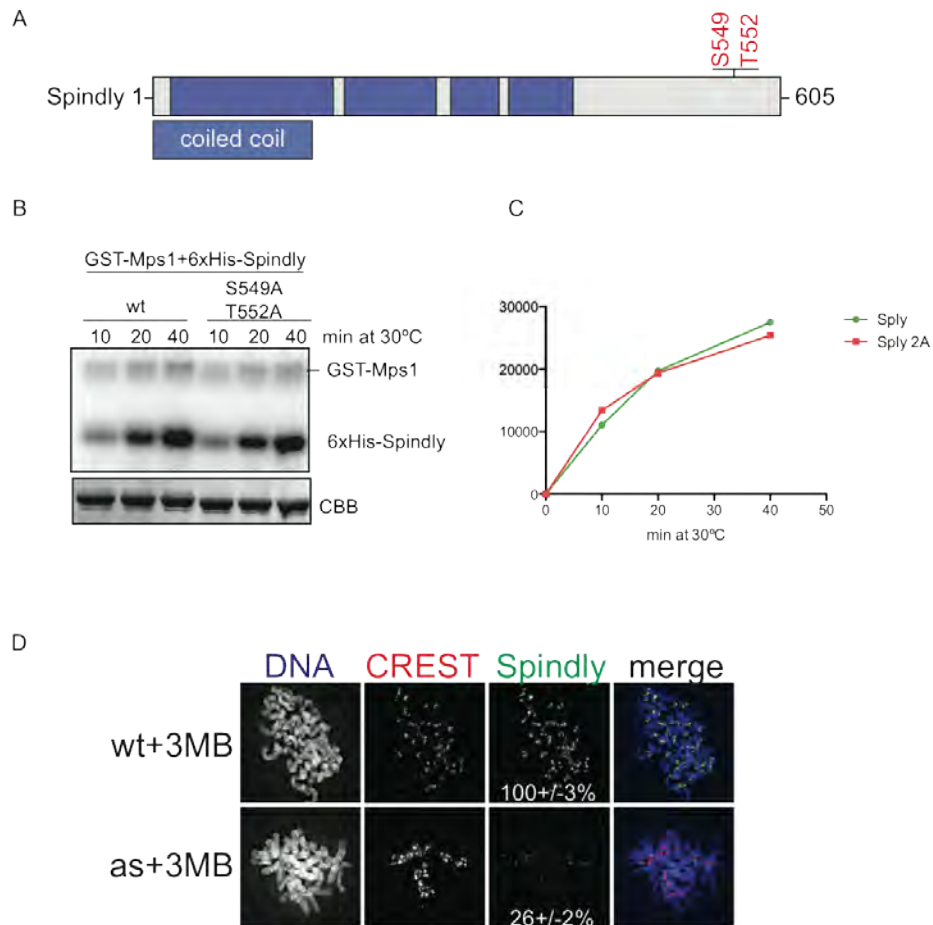
Figure 3.7 Mps1 directly phosphorylates Spindly *in vitro.*
(A) Schematic of Spindly protein domain organization including identified Mps1-dependent phosphorylation sites. (B) Mps1 was incubated with purified Spindly, wild type or a S549A, T552A mutant, and gamma 32P ATP. (C) Quantitation of transphosphorylation of Spindly by Mps1. (D) Immunofluorescent staining of Spindly localization to kinetochores in nocodazole arrested mitotic cells. Spindly is mislocalized from kinetochores, as marked by CREST, after Mps1 inhibition.
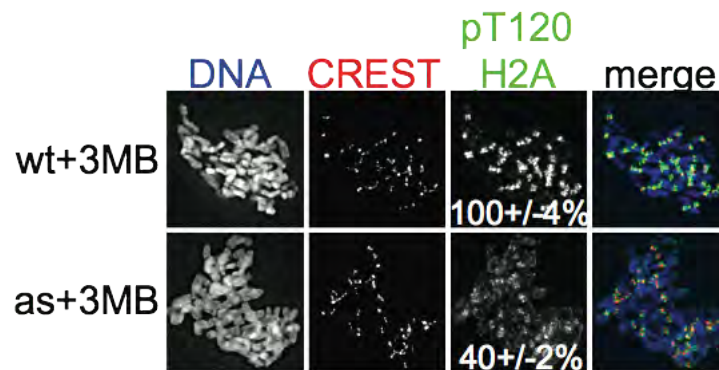
Figure 3.8 pT120 Histone H2A phosphorylation depends on Mps1 in cells.
Nocodazole-arrested, Mps1-inhibited cells were stained for DNA, CREST, and
anti-pT120 H2A.

Occupancy-sensitive Phosphorylation of the Outer Kinetochore by Mps1

Mps1 is thought to be activated at kinetochores early in mitosis. To test this, we stained asynchronous cells with our anti-Mps1 pT360, pS363 antibody. Mps1 activation was initiated at prophase kinetochores, and peaked in early prometaphase cells, before being largely extinguished at metaphase (Fig. 3.9A,C). This pattern of activity tracks well temporally with Mps1 and Mad2 localization dynamics, confirming that Mad2 kinetochore localization is a good surrogate marker of Mps1 activity, and suggesting that Mps1 is sensitive to occupancy and tension across sister kinetochores (Howell et al., 2004; Saurin et al., 2011).

To better understand Mps1's response to different kinetochore-microtubule attachment states we used anti-Mps1 and anti-KNL1 phosphospecific antibodies to stain RPE cells treated with different spindle poisons (Fig. 3.10B,C). Cells arrested at metaphase with the proteasome inhibitor, MG132, showed little to no phospho-Mps1 or phospho-KNL1 staining at all kinetochores (Fig. 3.10B,C). After nocodazole treatment, Mps1 was strongly autophosphorylated and trans-phosphorylated KNL1 (Fig. 3.10B,C). MG132 treatment had no effect on nocodazole-arrested cells, but addition of the small molecule Mps1 inhibitors, reversine and IN-1, strongly diminished pMps1 and pKNL1 signals at kinetochores. Inhibition of Eg5 with monastrol also stimulated Mps1 autophosphorylation and phosphorylation of KNL1. Interestingly, taxol-induced microtubule stabilizationonly modestly stimulated Mps1 activity, indicating that Mps1 primarily responds to occupancy status at kinetochores. Aurora B targets a

similar network of outer kinetochore proteins with similar timing and sensitivity to MT occupancy (Welburn et al., 2010). Aurora B was recently found to be regulated by the B56-PP2A phosphatase (Foley et al., 2011). Since Mps1 exhibits similar behaviors we hypothesized that Mps1 could also be subject to regulation by the B56-PP2A phosphatase. Indeed B56 depletion by an siRNA pool increased phosphorylation levels of Mps1, Rod, and KNL1, while also increasing the levels of Plk1 at the kinetochore, a marker for effective B56 depletion (Foley et al., 2011) (Fig. 3.10D,E). This suggests that B56-PP2A regulates the level of phosphorylation of these Mps1 substrates in prometaphase cells.

The B56-PP2A phosphatase was recently found to be required for the generation of stable KT-MT attachments (Foley et al., 2011). This defect, demonstrated by siRNA depletion, could be suppressed, in part, by Aurora B inhibition (Foley et al., 2011). To determine if Mps1 regulation by B56-PP2A was also a critical target in the formation of stable KT-MT attachments, Mps1 was inhibited in B56-depleted cells. Stable KT-MT attachments were monitored by a brief cold treatment prior to fixation. Cold treatment depolymerizes spindle MTs that have not made productive attachments to KTs (Rieder, 1981; Rieder and Borisy, 1981). Indeed, Mps1 inhibition, with the small molecule inhibitor reversine (Santaguida et al., 2010), decreased the number of mitotic cells with few or no cold-stable MT attachments after B56 depletion (Fig. 3.10F,G).
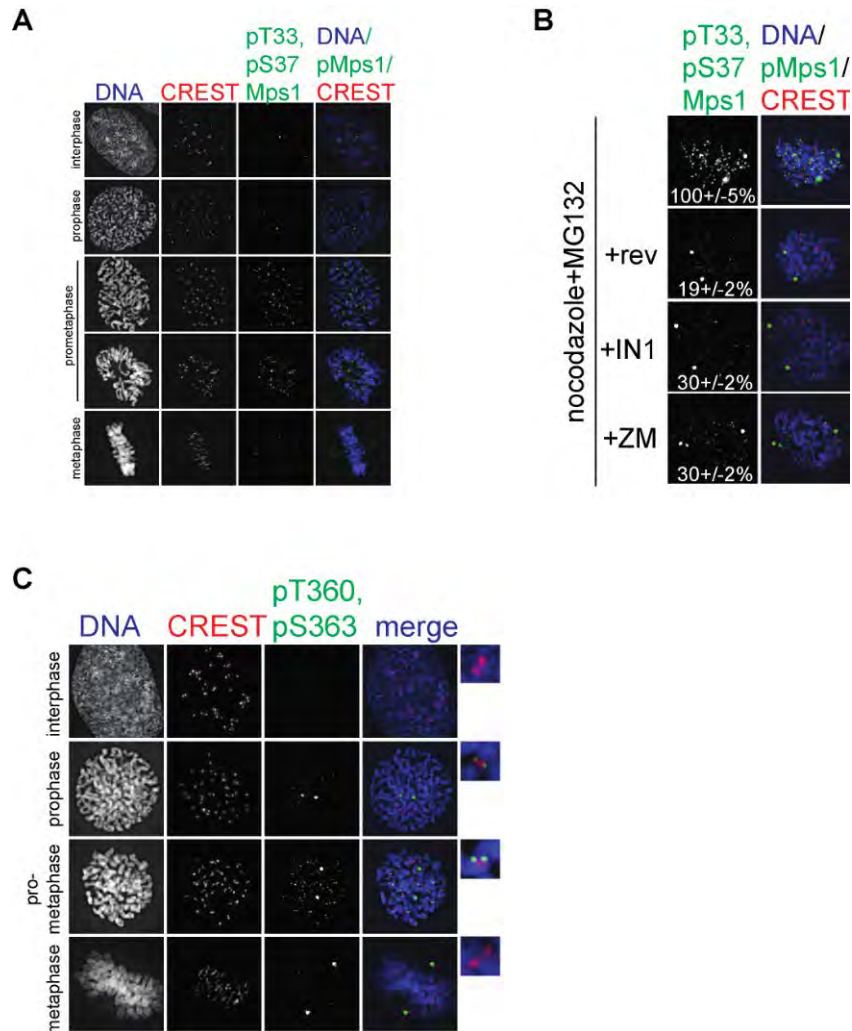
Figure 3.9 Mps1 activity peaks in prometaphase and depends on Aurora B kinase activity for efficient activation in mitosis.
(A,C) anti-pT33,pS37 Mps1 and anti-pT360,pS363 antibodies were used to assess Mps1 activity in different stages of mitosis. (C) Cells were treated with nocodazole, MG132, and DMSO, reversine, IN1, or ZM for 40 minutes prior to fixation and staining. Aurora B inhibition at mitotic entry strongly suppresses Mps1 activation.
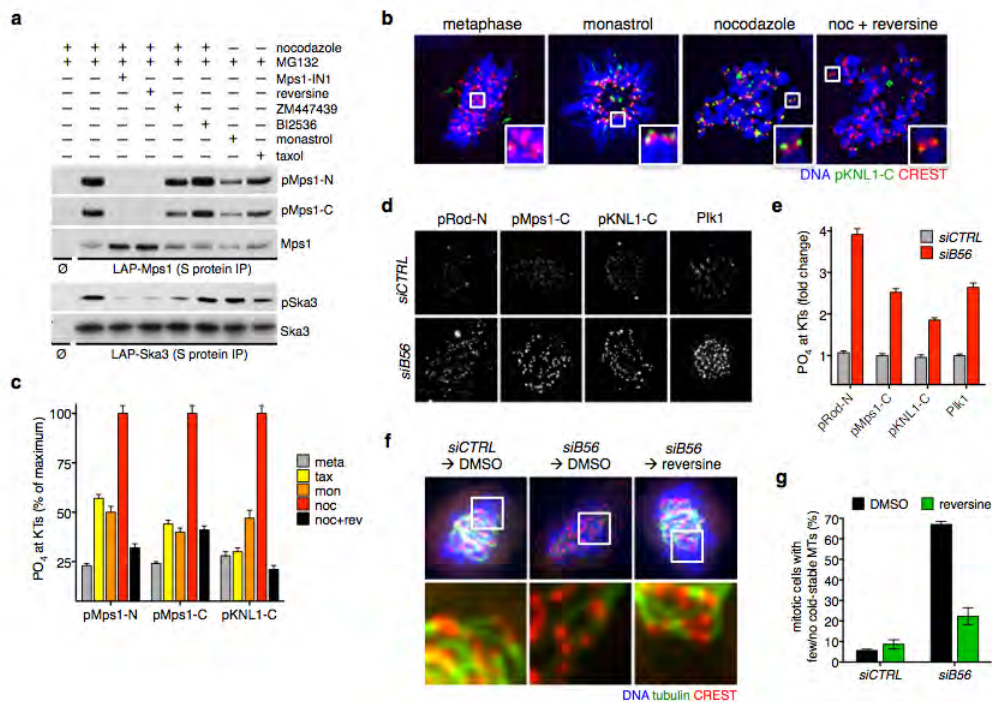
Figure 3.10 Mps1 responds to unattached kinetochores and is regulated by the B56-PP2A phosphatase.

(A) Mps1 and Ska3 phosphorylation depend on Mps1 *in* vivo*.* anti-pMps1-N, anti-pMps1-C and anti-pSka3 Western Blots on immunoprecipitated Mps1 and Ska3 purified from cells treated with the indicated drug combinations. (B) Occupancy sensitive phosphorylation by Mps1. Cells were treated with the indicated drugs prior to fixation and staining with Hoechst (blue) to mark DNA, CREST (red) serum to mark the inner centromere, and pKNL1 (green). (C) Quantitation of results presented in B. Images for pMps1-N and pMps1-C are not shown. (D) B56-PP2A phosphatase regulates Mps1 activity in mitosis. Cells were transfected with control or B56 specific siRNAs prior to fixation and staining with pRod-N, pMps1-C, pKNL1-C, and Plk1 antibodies. Only prometaphase cells were imaged and analyzed. (E) Quantitation of D. (F) Mps1 inhibition restores K-fiber stability in B56-PP2A depleted cells. Cells were transfected with control or B56 specific siRNAs and treated with 10 µM MG132 and 0.5 µM reversine or DMSO for 1.5 hours prior to incubation on ice and fixation. Cells were stained with anti-tubulin to image K-fibers. (G) Quantitation of F. (B56-PP2A depletions performed by Emily Foley in some experiments).

85
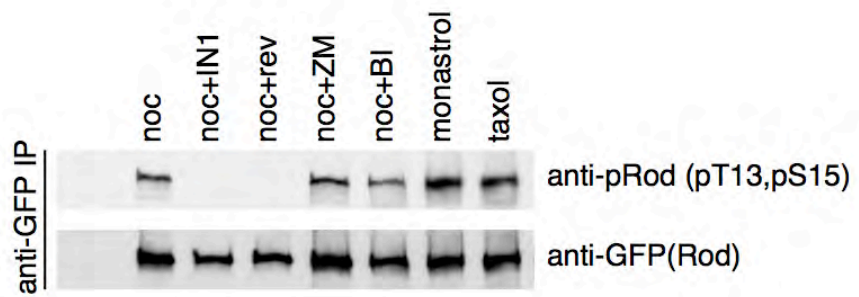
Figure 3.11 Rod phosphorylation depends on Mps1 *in vivo.*
Anti-pRod and anti-GFP (Rod) Western blot on Rod immunoprecipitates. Rod
was immunoprecipitated from cells treated with the indicated drugs.

In addition, we confirmed the recent proposals that Aurora B activity was required for efficient Mps1 activation, as Aurora B inhibition significantly diminished anti-pT33,pS37 staining at kinetochores, to a level similar to direct Mps1 inhibition with the small molecules IN-1 and reversine, in early mitotic cells (Figure 3.9B) (Santaguida et al., 2011; Saurin et al., 2011). Thus, our analysis of the spatial and temporal distribution of phosphorylation with modification-specific antibodies reveals that Mps1 targets its substrates within the outer kinetochore primarily when microtubule occupancy is weak to non-existent, in keeping with its proposed roles in checkpoint signaling and error correction.

Mps1 phosphorylation of Ska3 S34 is required for Ska complex function

We identified 10 phosphorylation sites on Ska3 in our unbiased, whole phospho-proteome screen, however, only phospho-S34 showed significant down-regulation following Mps1 inhibition (Fig. 3.1D, Fig. 3.11). Immunopurification of LAP-Ska3 from HeLa cells, followed by mass spectrometry and phosphorylation site mapping confirmed that Ska3 was a heavily phosphorylated protein (Fig. 3.11). Importantly, we were able to confirm that S34 is phosphorylated in multiple cell lines and found that S110, a proposed Aurora B phosphorylation site, is phosphorylated *in vivo* (Chan et al., 2012).
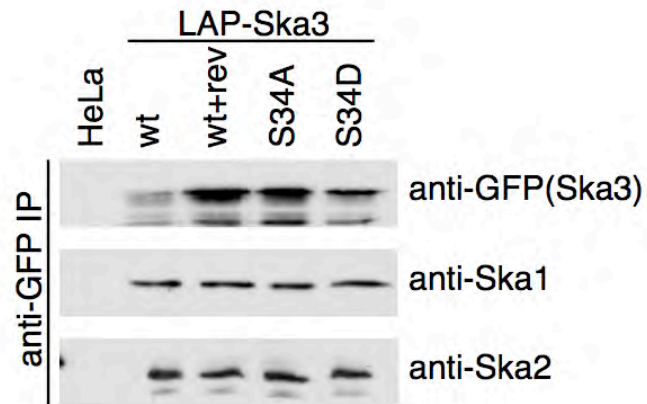
Figure 3.12 Ska complex stability does not depend on Mps1.
Extracts were made from shaken off, nocodazole-arrested mitotic cells. LAP-Ska3 was immunoprecipitated by anti-GFP resin.

We chose Ska3 S34 for further study because Mps1 was able to directly phosphorylate this site *in vitro* and inhibition of Mps1, but not the mitotic kinases Plk1 or Aurora B, strongly reduced this phosphorylation event in vivo (Fig. 3.10). To determine the *in vivo* functional significance of Ska3 S34 phosphorylation, we adapted a strategy to replace endogenous Ska3 with phosphorylation defective and phosphorylation mimicking transgenes (Kim et al., 2010b). Full length LAP-tagged Ska3 was integrated into the genome of HeLa cells using FRT/FLP-mediated recombination and expression was induced by doxycycline (Fig. 3.12). LAP-Ska3 wt, S34A, and S34D all localized correctly to kinetochores in nocodazole-treated cells, in agreement with our previous finding that Mps1 inhibition did not affect Ska3 kinetochore localization (Fig. 3.12B) (Maciejowski et al., 2010). In addition, LAP-Ska3 wt maintained its interaction with Ska1 and Ska2 even after Mps1 inhibition, demonstrating that Mps1 does not regulate Ska complex formation, consistent with the ability of this complex to form in vitro (Gaitanos et al., 2009; Welburn et al., 2009).

Transfection of an siRNA targeting the 3' untranslated region of Ska3 mRNA depleted endogenous Ska1, which was used as a surrogate marker for Ska3 stability as the components of the Ska complex depend on one another for their stability (Gaitanos et al., 2009). Knockdown of endogenous Ska3 induced a mitotic arrest, a high rate of mitotic cell death, and frequent lagging chromosomes (Fig. 3.12). These phenotypes could be rescued by LAP-Ska3wt,

but not the alanine or aspartic acid phosphorylation site mutants, demonstrating that timely Ska3 S34 phosphorylation is crucial for orderly, error-free mitotic progression.

To understand the nature of this defect we determined the ability of Ska3 S34 phosphorylation site mutants to rescue K-fiber formation in cells that had been depleted of endogenous Ska3. K-fibers are preferentially stable during a brief incubation at 4° C. Protein depletions or expression of mutants that interfere with efficient kinetochore-microtubule interaction display severe K-fiber defects after a brief treatment on ice. Consistent with this Ska3 depletion generated a strong K-fiber defect (Fig. 3.13I) that could be rescued by LAP-Ska3wt and S34A, but not the S34D transgene. This demonstrates that Mps1 phosphorylates Ska3 S34 to sever kinetochore-microtubule interactions.
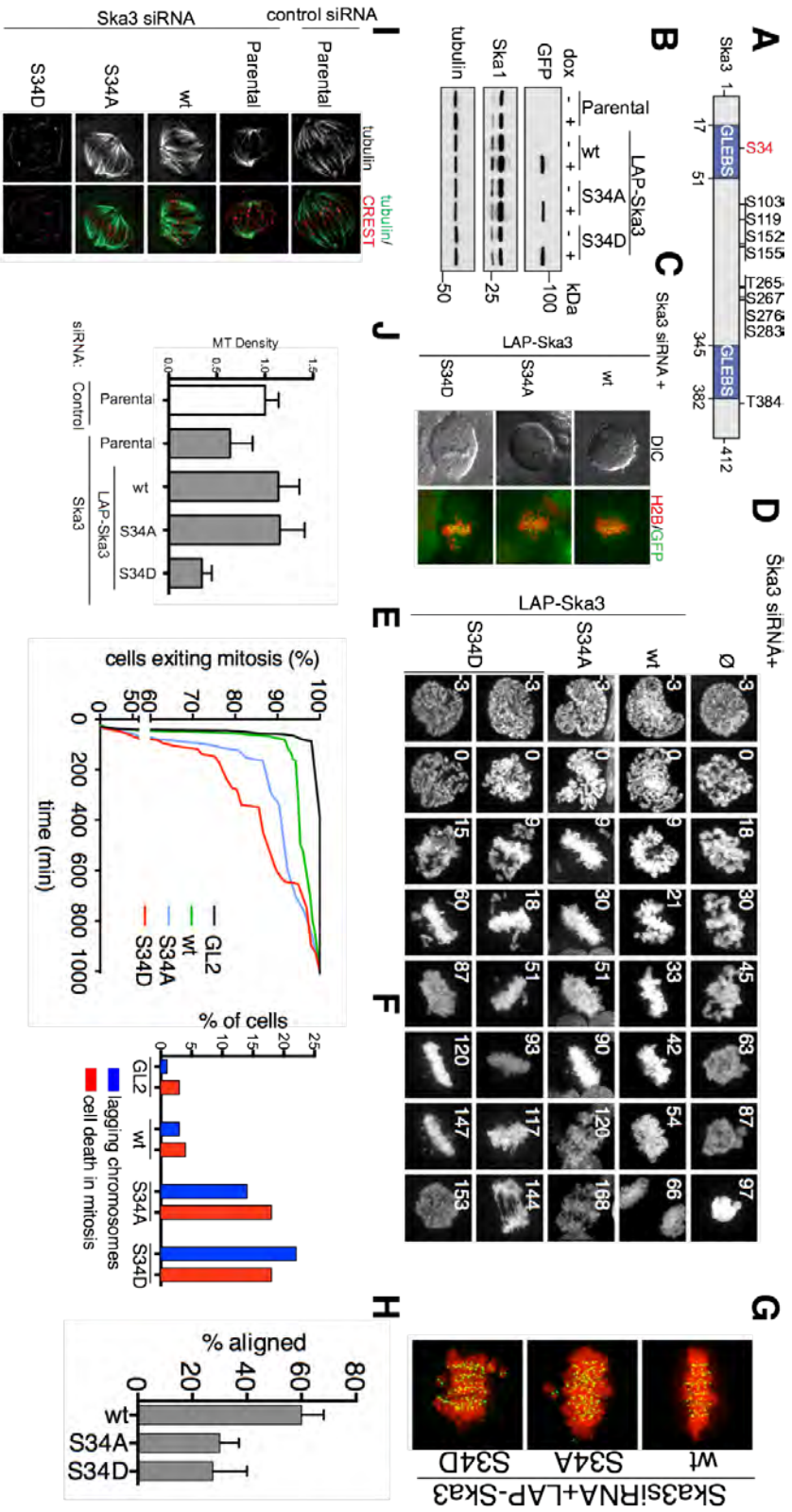
Figure 3.13 Ska3 S34 phosphorylation is required for mitotic progression.
(A) LAP Ska3 was immunopurified from nocodazole arrested HeLa cells and phosphorylation sites were mapped by mass spectrometry. Only S34 showed Mps1 dependency. (B) anti-GFP(Ska3) Western Blot with extracts generated from HeLa cells expressing RNAi resistant LAP-Ska3 wt or S34A, S34D mutants. (C) GFP-Ska3 localization after endogenous Ska3 knockdown in live cells. (D) Spinning disk confocal imaging of cells expressing RNAi resistant LAP-Ska3 wt, or S34A,S34D mutants. Endogenous Ska3 is depleted by siRNA. DNA imaged with a Histone H2B RFP marker. (E) Cumulative percentage of cells exiting mitosis as in D. (F) Quantitation of percent of cells in D showing lagging chromosomes at anaphase or cell death during mitosis. (G,H) Chromosome alignment during 1.5 hour MG132 arrest. DNA is stained with Hoechst and kinetochores were marked using CREST serum. Endogenous Ska3 depleted by siRNA (I) Maximum intensity projection of tubulin (green) and CREST (red) in Ska3 depleted cells. Cells were treated with nocodazole for 40 minutes, followed by nocodazole washout and 1.5 hour MG132 arrest. MG132 arrested cells were incubated on ice for 15 minutes prior to fixation and staining. (J) Quantitation of results in I. MT density was quantitated as a percentage of pixels in a cell area stained twice as bright as background in the tubulin channel.

Ska3 S34 phosphorylation could affect Ska1 complex activity by altering the localization of the Ska1 complex to kinetochores, the affinity of the Ska1 complex for microtubules, or the structure of the Ska1 complex. However, S34 mutation or Mps1 inhibition do not alter the localization of the complex (above, Fig. 3.13C) (Maciejowski et al., 2010). Mps1 inhibition also does not seem to alter the stability of the Ska1 complex in cells (above, Fig. 3.12). However, although S34 phosphorylation does not affect the affinity of Ska3 for Ska1 and Ska2, it may affect complex dimerization (Gaitanos et al., 2009; Jeyaprakash et al., 2012; Welburn et al., 2009). To look at this directly we purified wt and S34D mutant Ska1 complexes from bacterial cells and analyzed complex dimerization by gel filtration chromatography and sucrose gradient fractionation (Fig. 3.14, 3.15C). In both cases the elution profiles of wt and S34D mutant complexes were identical. We conclude that the Ska1 holocomplex is assembled normally despite S34 mutation.

The majority of the Ska1 complex's binding affinity depends on Ska1, with minor contributions from Ska1 and Ska2 (Welburn et al., 2009). Nevertheless, we reasoned that Mps1 phosphorylation of Ska3 S34 could affect the Ska1 complex's affinity for MTs. To test this we incubated purified Ska1 complex, wt, or S34D, with rhodamine labeled microtubules (Fig. 3.15 C). Both complexes were able to efficiently bundle MTs *in vitro.* In addition, both complexes were also able to associate with MTs as gauged by a MT pelleting assay (Fig. 3.15 D).

Although informative, these assays can be highly artificial as they depend on μM concentrations of Ska1 complex and MTs. In addition, they require the use of static MTs, and can provide no information on the affinity of a complex for depolymerizing or dynamic MTs. To determine the relative binding affinities of the wt and S34D Ska1 complexes for MTs, we used single molecule total internal reflection microscopy (TIRF-M) to image the one-dimensional diffusion of complex particles on MT lattices. To visualize the Ska1 complex we purified Ska1 complex, with a GFP tag incorporated into the Ska1 protein. Inclusion of the GFP tag did not affect complex stability or dimerization (data not shown).
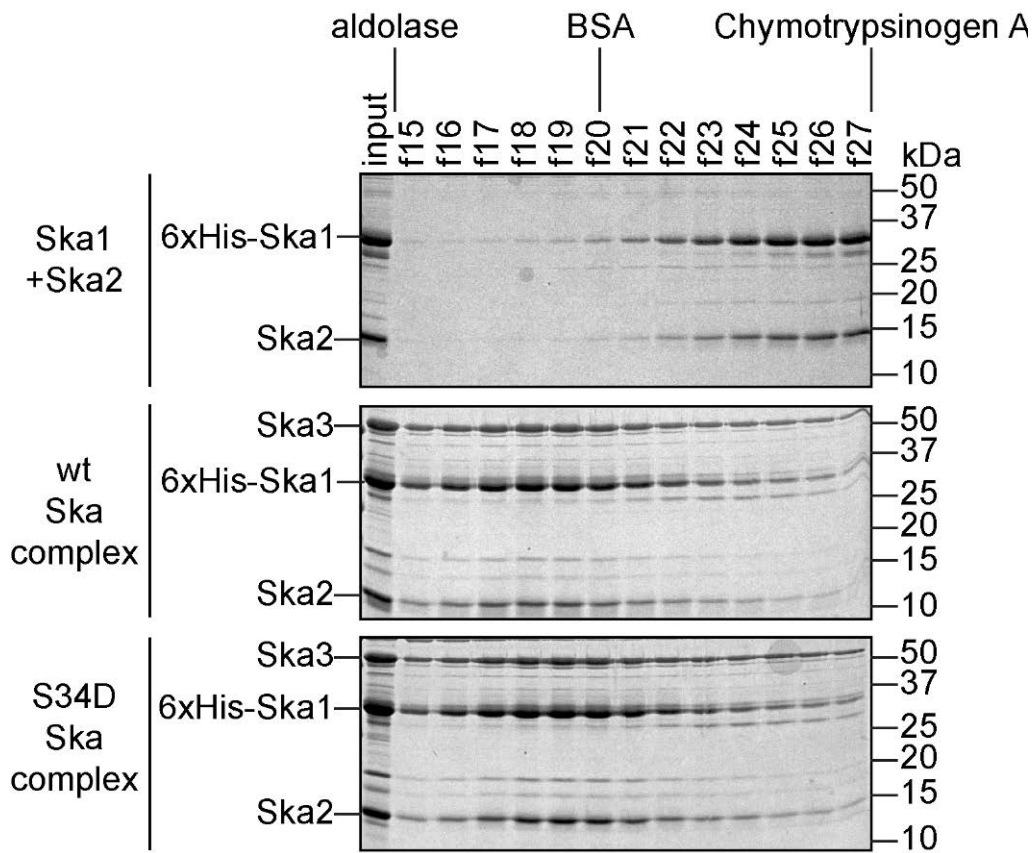
Figure 3.14 The Ska1 complex assembles normally in vitro, despite S34 mutation.
Coomassie stained gels showing migration of purified Ska1 complex on a 5-20% sucrose gradient. Aldolase (6.5), BSA (4.3 S), and chymotrypsinogen A (2.58 S) were used as markers.
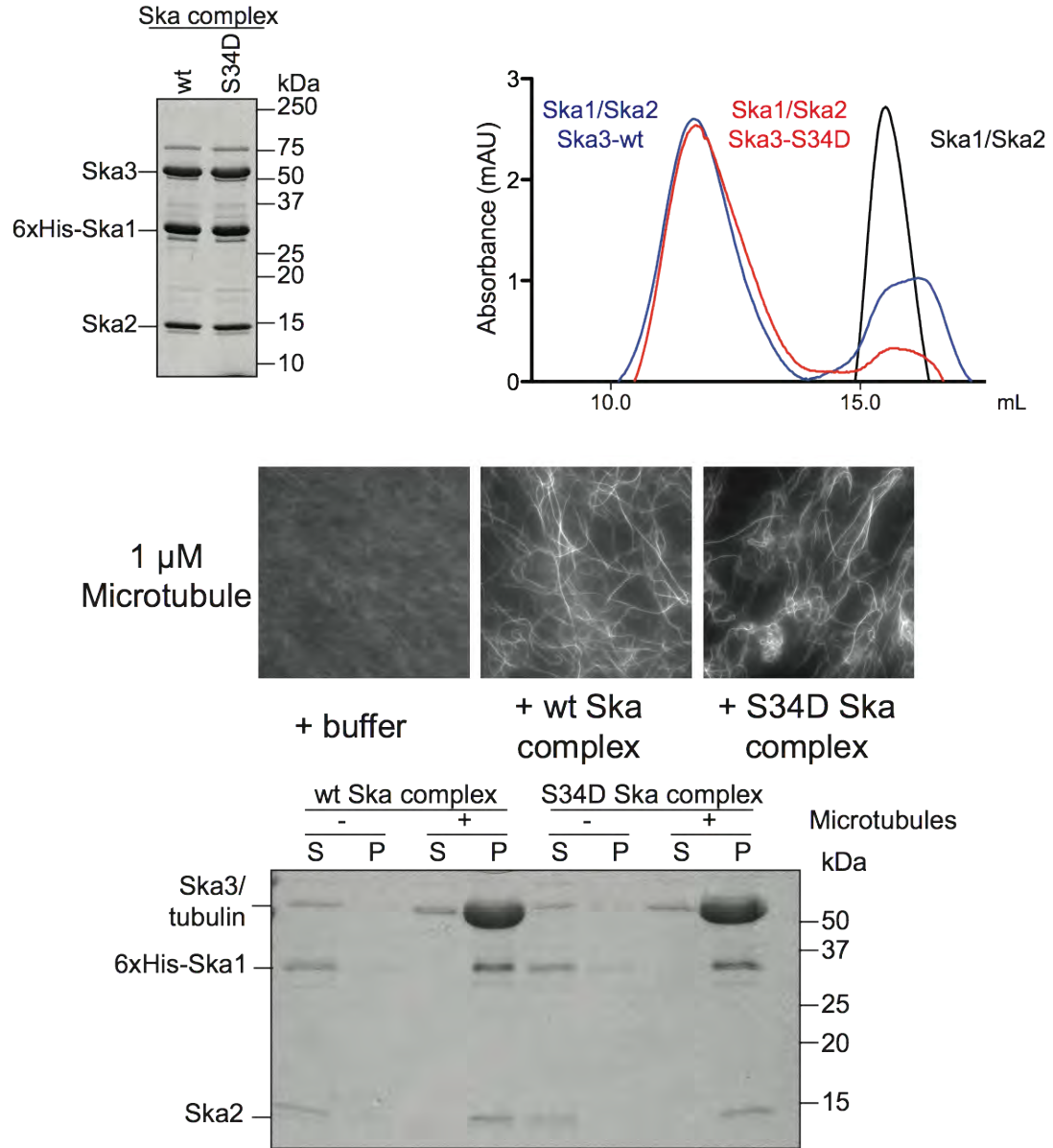
Figure 3.15 S34D mutation does not obviously diminish the affinity of the Ska1 complex for microtubules.
(A) Coomassie-stained gel showing purified 6xHis-Ska1, Ska2, and Ska3, isolated as a GST-Ska3 fusion and cleaved with PreScission protease. (B) Graph showing the elution profile of the full Ska1 complex, wt or S34D, on a Superose 6 size-exclusion column. (C) Fluorescent light microscopy images of 1 µM rhodamine-labeled microtubules incubated with equivalent amounts of wt or S34D Ska1 complex. (D) Microtubule co-sedimentation assays with wt or S34D Ska1 complex.

As expected, wt GFP-Ska1 complex readily diffused along MTs, as has been previously shown (Fig. 3.16A) (Schmidt et al., 2012). Similarly, the S34D complex could also bind to MTs and undergo one-dimensional diffusion along the lattice (Fig. 3.16A). Consistent with the gel filtration elution profiles (Fig. 3.15B) of the wt and S34D complexes and their sedimentation in sucrose gradients (Fig. 3.14) and with previous reports (Jeyaprakash et al., 2012; Schmidt et al., 2012; Welburn et al., 2009), both the wt and S34D complexes bound to MTs as dimers (Fig. 3.16B,C). This data confirms that the Ska1 complex dimerizes to generate a complex with two MT-binding sites. However, an elevated portion of the S34D complex undergoes extremely short-lived MT associations (Fig. 3.16D).

We next investigated how the Ska1 complex behaves on dynamic MTs polymerized from a GMPCPP-stabilized seed. Again confirming results from the Cheeseman lab (Schmidt et al., 2012), we see that the Ska1 complex tracks the shrinking plus-end of MTs that are undergoing dynamic instability. Once the Ska1 complex attaches to the shrinking end, it remains associated until the next rescue (or longer, but in lattice diffusion mode) (Fig. 3.16E). The S34D complex can also track shrinking MT plus-ends. However, the wt complexes that are tracking shrinking ends have a broader intensity distribution, compared to the S34D complex (Fig. 3.16F). This is not due to differences in protein concentration because the number MT-bound particles was identical (Fig. 3.16E). In addition, these experiments were performed with 10 nM Ska1 complex so the free pool of protein in the chamber is in large excess.
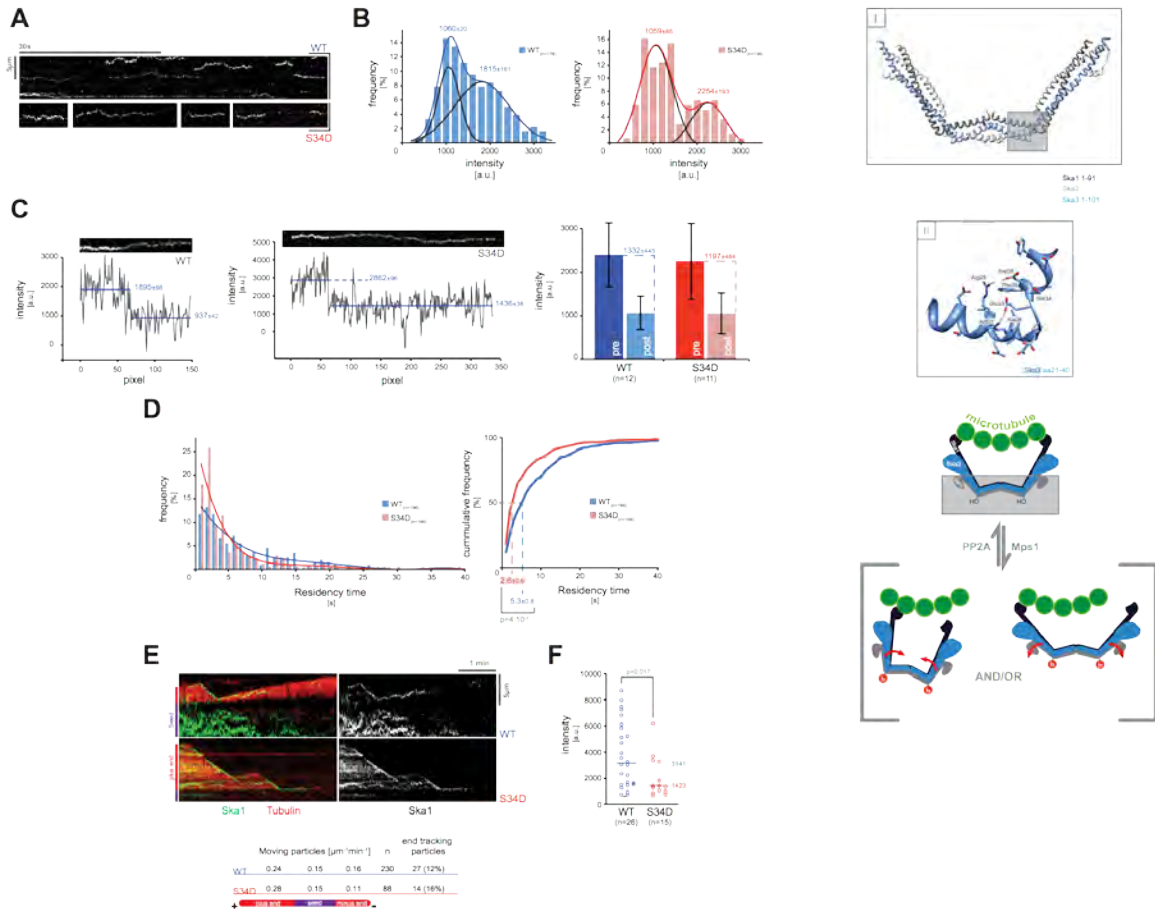
Figure 3.16 S34D mutation increases the number of short-lived particles and reduces the size of complexes diffusing along microtubules.
(A) Representative kymographs with time along the horizontal axis showing one-dimensional diffusion of GFP-Ska1 wt or S34D complex on taxol-stabilized microtubules. (B) Intensity distribution of the binding events. (C) Photobleaching analysis of wt and S34D Ska1 complex particles. Left, kymograph and corresponding fluorescent intensity for one photobleaching event Right, graph showing the average intensity before and after photobleaching events. (D) Distribution of the residence time of wt and S34D complexes on microtubules. (E) Representative kymographs showing wt and S34D complexes binding to depolymerizing microtubules. (F) Quantitation of the intensity of tracking complexes in E. Right panel, model for the consequences of Ska3 S34 phosphorylation on Ska1 complex activity. I, Ska3 S34 is located in the hinge region of the Ska1 complex (Jeyaprakash et al., 2012). II, Ska3 S34 is immediately surrounded by charged residues. Mps1 phosphorylation may alter the Ska1 complex's structure to lower its affinity for microtubules. (All work in this figure, except for GFP-Ska complex purification, performed by Hauke Drechsler and Andrew McAinsh).

Making confident, functional links from kinases to substrates is a key problem in understanding mitotic progression. Here, we have identified and validated some of the first Mps1 substrates in human cells. Our unbiased, whole phosphoproteome screen suggests that Mps1 activity in mitosis is primarily restricted to the outer kinetochore (Fig. 3.1, 3.2). We have validated six different sets of phosphorylation sites with phosphorylation-specific antibodies: anti-pMps1(T33,S37), anti-pMps1(T360,S363), anti-pKNL1(S1831,S1834), anti-pRod(T13,S15), anti-pSka3(S34), and anti-pH2A(T120).

In addition, our work demonstrates that Mps1 targets these substrates at the outer kinetochore under the regulation of the B56-PP2A phosphatase (Fig. 3.10).The B56-PP2A phosphatase was recently shown to promote K-fiber stability, in part by regulating Aurora B and Plk1 activity during mitosis (Foley et al., 2011). Mps1 inactivation, and presumably dephosphorylation of Mps1 targets, is required for timely anaphase (Hardwick et al., 1996; Jelluma et al., 2010; Palframan et al., 2006). Here, we show that the B56-PP2A phosphatase regulates Mps1 activity during mitosis.

Mps1 kinase activity is required for efficient chromosome bi-orientation (Jelluma et al., 2008b; Maciejowski et al., 2010; Santaguida et al., 2010). Mps1 was originally proposed to contribute to this process by enabling Aurora B activity through phosphorylation of borealin, a subunit of the chromosome passenger complex (Jelluma et al., 2008b). However, several studies have not seen any

defects in Aurora B after Mps1 inhibition, or in RPE cells lacking MPS1 (Lan and Cleveland, 2010; Maciejowski et al., 2010; Santaguida et al., 2010). These results suggested that, instead, Mps1 phosphorylates other targets to enable efficient chromosome bi-orientation. Likely candidates can be found at the outer kinetochore, especially the proteins that mediate interaction with the spindle such as the KMN network components and members of the Ska1 complex. Ska3 is a notable candidate because Dam1, a proposed functional analog of the Ska1 complex, is a target of Mps1 in budding yeast (Shimogawa et al., 2006). In addition, S34's position in the Ska1 complex core structure suggests that this phosphorylation event could alter the shape of the W-shaped dimer, in such a way as to disrupt efficient MT-binding (Fig. 3.16 right panel) (Jeyaprakash et al., 2012).

S34D Ska complex is insufficient to support stable K-fiber formation and GFP-tagged S34D complex exhibited a higher dissociation rate and lower oligomerization ability on taxol-stabilized and dynamic microtubules respectively (Fig. 3.13I, Fig. 3.16). Therefore, the interpretation is clear: Mps1-mediated phosphorylation of Ska3 S34 negatively and allosterically regulates Ska1's microtubule binding function leading to defects in K-fiber formation and mitotic progression. However, the non-phosphorylatable S34A Ska complex also exhibits defects in mitotic progression despite supporting K-fiber formation and presumably microtubule-binding. Instead, this mutation is predicted to lead to hyper-stable kinetochore-microtubule attachments, consistent with its

requirement in monastrol washout error correction assays (Fig. 3.13 G,H). Future experiments will determine whether S34A Ska complex mutants inappropriately support K-fibers of incorrectly attached kinetochores. It is also possible that Aurora B mediated removal of the Ska complex is complicating our analysis of S34A and S34D mutant complexes (Chan et al., 2012). To remove this variable future experiments will employ intra-mitotic Aurora B inhibition to "hyper-load" mutant Ska complexes onto kinetochores (Kim et al., 2010). S34A complex mediated stabilization of incorrect attachments will be analyzed in this context of Aurora B inhibition.

One other unexplored possibility is that S34 phosphorylation initiates or disrupts a protein-protein interaction motif. S34 is located in the middle of a Bub binding motif, however our unpublished data and that of others has not been able to detect any interactions with Bub family members (Jeyaprakash et al., 2012). Nevertheless, it is possible that this motif does support binding to an unidentified protein, such as a component of the Ndc80 complex, and its mutation disrupts effective, the synthetic ability of these complexes to bind and track with depolymerizing microtubule plus ends.

CHAPTER FOUR: Discussion & Future Directions

The partnership of chemical genetics and quantitative phosphoproteomics promises profoundly enhance our ability to identify meaningful kinase and substrate relationships. This approach was first used to identify a large set of Plk1-dependent phosphorylation events (Oppermann et al., 2012) and we have now used this approach to study Mps1. Although this partnership makes great promises, validation of identified targets through the use of phosphorylation-specific antibodies and characterization of identified sites is crucial to enhance our understanding of the underlying biology.

Our chemical genetic analysis of Mps1 has revealed a previously unappreciated role for this kinase away from the kinetochore (Chapter Two). This observation placed Mps1 in the same company as SAC components that are thought to have a more intimate relationship with the APC/C (Meraldi et al., 2004). Since our publication, another study has shown that Mps1 kinase activity is also required to maintain SAC arrest in response to a kinetochore-tethered allele of Mad1 (Maldonado and Kapoor, 2011). Since chromosomes efficiently bi-orient in this cell line, Mps1 recruitment to the kinetochore, although not quantitated in this study, is presumably at a minimum. Nevertheless, small molecule inhibition of Mps1 in this line immediately triggers anaphase, suggesting that Mps1 activity, in addition to being required apart from the hierarchical building of the kinetochore,

at least in terms of Mad1 recruitment and localization, is also required away from the kinetochore.

The outstanding question, of course, is what does Mps1 target away from the kinetochore? Upcoming work from the lab suggests that Mad1 is also required for the production of mitotic checkpoint complexes in interphase cells (Veronica Rodriguez-Bravo, unpublished results), suggesting that the core framework operating at unattached kinetochores is also present in interphase cells. The conspicuous, and often ignored, localization of Mad1 and Mad2 to the nuclear envelope suggests that the Mad1/Mad2 heterodimer may also use a scaffold to aid in the catalytic production of a "wait anaphase" inhibitor in interphase. Although Mps1 shares kinetochore localization with Mad1 and Mad2 in mitosis, Mps1 does not localize to the nuclear envelope in interphase cells (Liu et al., 2003). In addition, Mps1 activity does not localize Mad1 and Mad2 to the nuclear envelope, nor does it affect shuttling of the heterodimer from the cytosol to the nucleus (Veronica Rodriguez-Bravo, unpublished results). Mps1 may be required to prime the interaction between Mad2 and Cdc20 downstream of this nuclear envelope recruitment event. One intriguing possibility is that this priming event operates in mitosis as well as interphase. Since Mps1 is required for Mad1 and Mad2 recruitment to unattached kinetochores in mitosis, it has been difficult to identify a role for Mps1 in Mad1 and Mad2 function downstream of this localization event, as localization to unattached kinetochores has long been recognized to be crucial for Mad2 function. However, the observation that Mps1 activity continues to be required for SAC arrest in a kinetochore-tethered Mad1

cell line suggests that Mps1 could be operationally required downstream of Mad1 and Mad2 kinetochore recruitment. This same requirement may extend to interphase cells.

The production of mitotic checkpoint complexes by Mps1, Mad1, and Mad2 in interphase presents a simplified system for SAC study. The elimination of tangentially required proteins, such as those at the outer kinetochore, promises a system stripped down to its core elements. This should allow for conceptually simple experiments to study the interaction of these core elements. The conserved nature of the participants suggests that the same mechanisms are likely to be in place in mitotic cells, only modified in order to be primed to respond to unattached kinetochores. The most likely targets for Mps1 modification in this system are Mad1, Mad2, and Cdc20. We have identified Mps1-dependent phosphorylation sites in the Mad2-binding region of Mad1 (John Maciejowski and Veronica Rodriguez-Bravo, unpublished results). One exciting possibility is that Mps1 phosphorylates Mad1, as has been observed in yeast (Hardwick et al., 1996), to prime the generation of the closed conformer of Mad2. Replacement of endogenous Mad1 with a non-phosphorylateable mutant will facilitate our understanding of any possible functions of these phosphorylation events.

One other possibility is that Mps1 directly targets Mad2 or Cdc20 for phosphorylation. Our *in vitro* kinase assays have demonstrated that Mps1 can specifically target the closed conformer of Mad2 S195 for phosphorylation (John Maciejowski, unpublished results). This phosphorylation event has been shown

to regulate the conformational stability of Mad2 and its association with the APC/C. (Kim et al., 2010a; Wassmann et al., 2003). Our identification of phosphorylation sites on the structurally similar N terminus of p31 suggests that Mps1 could also regulate the conformational stability of this Mad2 mimicking protein (John Maciejowski, unpublished results).

Our phoshpo-proteome screen undoubtedly missed more substrates than it found. Subsequent versions of this experiment will include complex-enrichment steps prior to phosphorylation site identification and quantitation. Good candidates for affinity purification of endogenously tagged potential substrates include, but are not limited to, Dsn1, Mad1, KNL1, Cdc20, and APC16. This enrichment step should enable a more comprehensive analysis of likely Mps1 targets. In addition, our whole phosphoproteome screen for Mps1-dependent phosphorylation sites was performed in mitotically arrested cells. It would be interesting to repeat this analysis in G2 cells to identify Mps1-dependent phosphorylation events on kinetochore-free substrates.

What are the SAC-relevant Mps1 substrates we did find in our screen? One of the most compelling candidates is Rod, which is phosphorylated on its N terminal residues, T13 and S15. Rod belongs to the RZZ complex, which plays important roles in kinetochore function during mitosis and the SAC (Karess, 2005). The RZZ complex is required for Mad1/Mad2 and dynein recruitment to unattached kinetochores (Buffin et al., 2005; Chan et al., 2000; Foley and Kapoor, 2013; Lu

et al., 2009; Wainman et al., 2012; Williams et al., 2003). Unlike most metazoan kinetochore components, RZZ has no identifiable counterpart in yeast (Menant and Karess, 2010).

Our identified phosphorylation sites reside in an N terminal motif recognized to be required for protein-protein interactions (Çivril et al., 2010). However, our unpublished results demonstrate that Mps1 is not required for RZZ stability (John Maciejowski, unpublished results). However, Mps1 inhibition does mis-localize components of the RZZ and its downstream effectors (Fig. 4.2). One possibility is that Mps1 phosphorylation of the N-terminus of Rod contributes to the formation of a docking site for proteins involved in SAC signaling, such as dynein or Spindly (Barisic and Geley, 2011; Griffis et al., 2007). Inactivation of endogenous Rod followed by rescue with a non-phosphorylatable mutant should provide valuable information.

One other interesting target identified in our screen is Bub1. As detailed in the introduction Bub1 is a conserved kinase and is required for SAC signaling (Morrow et al., 2005; Rischitor et al., 2007; Yu and Tang, 2005). Our phosphorylation site is particularly interesting because it lies in a highly conserved domain in Bub1 (Fig. 4.2) (Klebig et al., 2009b). Moreover, this conserved domain is absolutely required for SAC signaling and our identified phospho-acceptor threonine is invariant from yeast to humans (Fig. 4.2) (Klebig et al., 2009b). Mutation of this phosphorylation site has the potential to shut down the SAC in human cells.
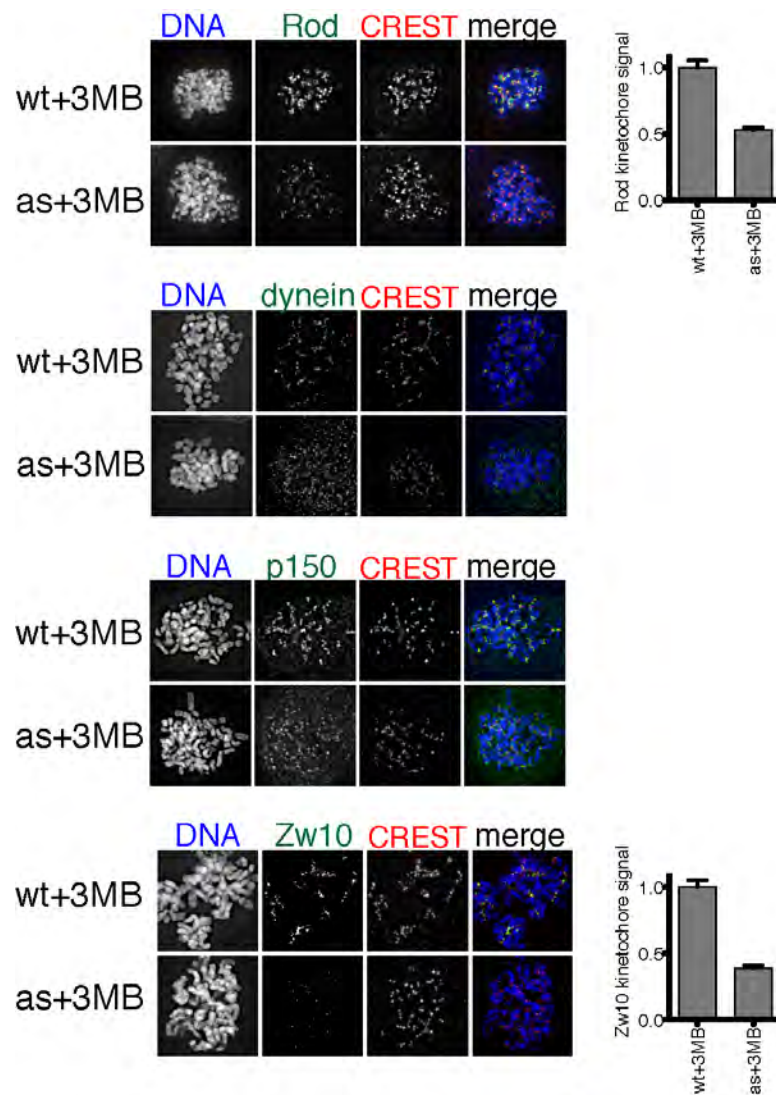
Figure 4.1 Mps1 targets Rod, dynein, p150, and Zw10 to kinetochores.
Mps1^{wt} and Mps1^{as} cells were arrested in mitosis with nocodazole and treated with 3-MB-PP1 and MG132. Cells were processed for immunofluorescence and stained for Rod, dynein, p150, and Zw10.
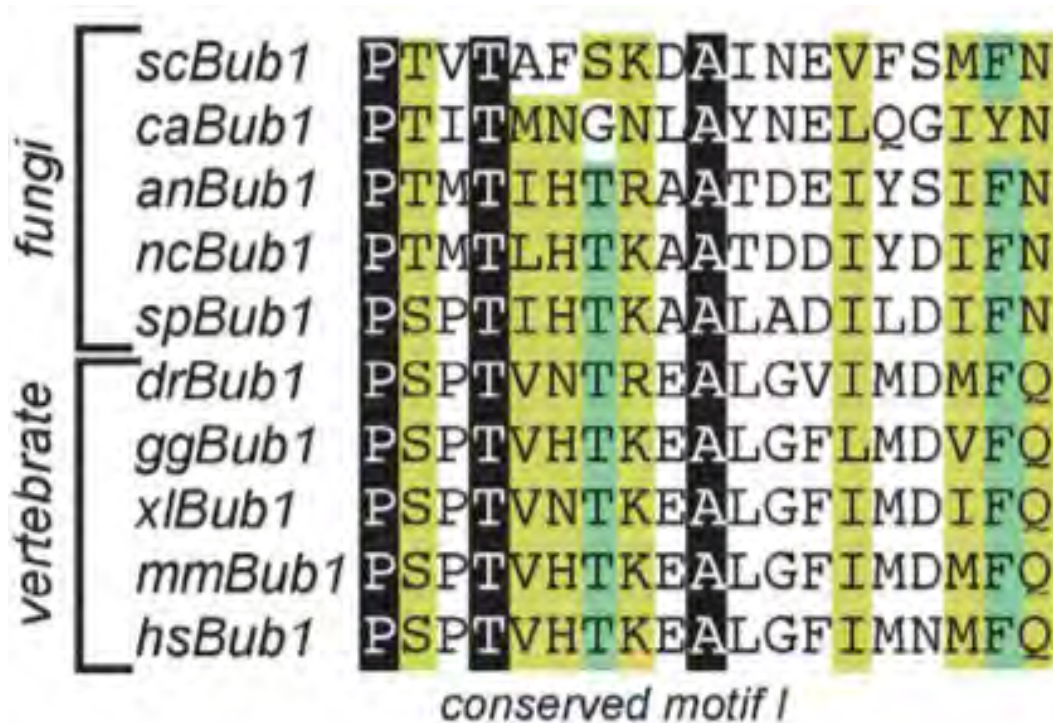
Figure 4.2 Multiple sequence alignment of conserved motif I of Bub1.
Identical residues are in a black, residues conserved in ≥80% of the species are in a dark green, and similar residues in ≥80% of the species are in a light green background. Sc, S. cerevisiae; ca, Candida albicans; an, Aspergillus nidulans; nc, Neurospora crassa; sp, S. pombe; dr, Danio rerio; gg, Gallus gallus; xl, X. laevis; mm, Mus musculus; hs, Homo sapiens. Reprinted with permission (Klebig et al. 2009).

108

CHAPTER FIVE: Materials and Methods

Cell Culture, Transfection and Chemicals

All cell lines were maintained at 37ºC and 5% CO_2 in the following media supplemented with 10% tetracycline free fetal bovine serum and 100 U/ml penicillin, 100 U/ml streptomycin: HeLa, Dulbecco's modified eagle medium (DMEM), hTERT-RPE1, 1:1 mixture of DMEM and Ham's F-12 medium supplemented with 2.5 mM L-glutamine. Where indicated, 200 ng/ml nocodazole (Sigma-Aldrich), 100 µM monastrol (EMD), 10 µM 3MB-PP1 (Burkard et al., 2007), 10 µM MG132 (Cayman Chemicals), 0.5 µM reversine (Cayman Chemicals), 10 µM Mps1 IN-1 a gift of Nathanael S. Gray (Harvard), 0.2 µg/ml doxycycline, 200 nM BI2536, 10 µM taxol (Sigma-Aldrich), and 2 µM ZM (Tocris Bioscience) were added.

For siRNA treatment, $1.5x10^5$ cells were plated in a 6-well plate and duplexed siRNAs were transfected using Oligofectamine (Invitrogen) (Kim et al., 2010b). siRNA directed against Ska3 3'UTR (5'-AGACAAACAUGAACAUUAA-3') was purchased from Sigma-Aldrich.

Stable HeLa, H2B-RFP cell lines expressing Mps1 or Ska3 were generated using FRT/Flp-mediated recombination as described previously in cells provided by S. Taylor (The Universtiy of Manchester, Manchester, England, UK) (Holland et al., 2010).

Molecular biology and retroviral transgenesis

To generate the *MPS1^flox* targeting construct, PfuTurbo polymerase (Stratagene) was used to amplify left and right homology arms from BAC clone RP11-472L12. Both homology arms were cloned into pNY (Berdougo et al., 2009; Burkard et al., 2007; Terret et al., 2009), and a BglII-marked *loxP* site was added via linker ligation. The entire targeting construct was then transferred to pAAV as a NotI fragment. All manipulated regions were checked by sequencing to ensure their integrity. A similar strategy was employed to create the pAAV-*MPS1^Δ* construct used to delete the second allele in *MPS1^flox/+* cells. Procedures for preparation of infectious AAV particles, transduction of hTERT-RPE1 cells, and isolation of properly targeted clones have been described (Berdougo et al., 2009).

For retroviral transduction, inserts were cloned into pQCXIN and pQCXIB (Clontech), and the resulting plasmids were cotransfected with a vesicular stomatitis virus glycoprotein envelope expression construct into Phoenix cells. Infectious supernatants were collected, diluted 1:1 with complete medium containing 20 µg/ml polybrene, and applied to target cells for 12 hr. Selection with 0.4 mg/ml G418 or 5 µg/ml blasticidin was initiated 48 hr later.

Antibodies, flow cytometry, and timelapse imaging

For flow cytometry, cells were fixed in 70% ethanol at -20º C for 24 hours. Afterwards, cells were rehydrated, blocked in 1% fetal calf serum in 0.1% Triton and PBS, and stained with a mouse anti-MPM-2 antibody and an Alexa 633-conjugated anti-mouse secondary antibody. For timelapse studies, cells were grown on 6-well plates (for phase-contrast imaging) or 35 mm glass-bottomed dishes (for confocal imaging).

Widefield and phase-contrast images were acquired on a Nikon TE2000 inverted microscope equipped with 10x and 40x long working distance and 100x oil objectives, single bandpass excitation and emission filters, Hamamatsu ORCA ER camera, a temperature-controlled stage enclosure with CO_2 support (Solent Scientific), and NIS Elements software (Nikon). Spinning-disk microscopy (Fig. 2.3) was carried out on a Zeiss Axiovert 200 microscope fitted with an UltraView confocal head (Perkin-Elmer), iXon 512x512 EMCCD camera (Andor), XYZ piezo stage (Prior), and temperature-controlled enclosure with CO_2 support (Solent Scientific). Imaging was performed in normal growth media at 37º C. Acquisition was performed with MetaMorph (Molecular Devices). For deconvolution microscopy (Fig. 2.11), a DeltaVision Image Restoration System (Applied Precision) based on an Olympus IX-70 microscope with a 100x oil objective and a CoolSnap QE cooled CCD camera (Photometrics) was used. Calculations were performed using measured point spread functions. Individual images were cropped and assembled into figures using Photoshop CS4 (Adobe).

Extract preparation and immunoprecipitation

For analysis of mitotic Cdc20-inhibitory complexes, cells were arrested in STLC for 16 hrs, isolated by shakeoff, and plated in medium containing STLC, 3-MB-PP1, and/or MG132 for 2 hr. Cells were then harvested, washed twice in ice cold PBS, and snap frozen in a dry ice-methanol bath. For analysis of interphase complexes, unsynchronized cells were treated with 3-MB-PP1 or ZM447493 for 2 hr and then collected by trypsin-EDTA treatment prior to snap freezing. Cell pellets were thawed on ice prior to resuspension in Buffer B (140 mM NaCl, 30 mM Hepes, pH 7.8, 5% glycerol, 1 mM DTT, 0.2 µM microcystin, and 1x protease inhibitor cocktail [Sigma]) and disruption by nitrogen cavitation (1250 psi, 45 min; Parr Instruments). Extracts were clarified by centrifugation at 20,000 g for 30 min and quantified by Bio-Rad assay. 2 mg of mitotic extracts or 1 mg of interphase extracts were used for each IP. Briefly, extracts were incubated with mouse monoclonal antibody to Cdc20 crosslinked to Dynabeads using BS3 (Pierce). After 2 hr, beads were washed four times in Buffer B, resuspended in 1x Laemmli buffer, and boiled for 5 min to elute Cdc20 and any associated proteins.

Quantitative immunoblotting

SDS-PAGE resolved proteins were transferred to PVDF membranes and incubated with primary antibodies. Secondary antibodies (goat anti-rabbit IRDye 680 and goat anti-mouse IRDye 800CW) were used at 1:5000. Fluorescence was measured using the Odyssey Infrared Imaging System (Li-Cor Biosciences) according to the manufacturer's instructions.

Stable Isotope Labeling by Amino Acids in Cell Culture

For differential SILAC encoding cells were grown in DMEM:F12 supplemented with 10% dialyzed fetal bovine serum (Invitrogen), and either 175 µM unlabeled L-arginine (Arg^0) and 250 µM unlabelled L-lysine (Lys^0) or the same concentrations of L-[U-^{13}C$_6$,^{14}N$_4$]-arginine (Arg^{10}) and L-[U-^{13}C$_6$,^{15}N$_2$]-lysine (Lys^8) (Sigma). After six cell doublings to ensure complete proteome labeling 1.6 x 10^6 cells were seeded per 15-cm dish (in total 6 dishes per experiment). 18 h later, 1 µg/ml aphidicoline (Sigma) was added for a further 12 h to synchronize cells in early S phase. Cells were then washed with PBS and cultured for another 13 h in fresh SILAC medium containing 50 ng/ml nocodazole (Sigma) to arrest cells in M phase. (For the subsequent 2 h inhibitor treatment) To inhibit mutant kinase activity in Mps1^{as} cells, 10 µM MG132 (Sigma) was added to Arg^0/Lys^0-labeled cells with 5 µg/ml 3-MB-PP1 (Priaxon, Germany) or Arg^{10}/Lys^8-encoded cells without inhibitor added and cells were incubated for further 2 h. This labeling scheme was used in two biological replicate experiments with Mps1^{as} (referred to as as1, as2) and Mps1^{wt} cells (wt1, wt2), whereas in two further

replicate experiments with either cell line reciprocal labelling conditions were used (as3, as4 and wt3, wt4).

Cells were lysed in 500 µl 8 M urea, 50 mM Tris-HCl pH 8.2, 75 mM NaCl, 1 mM EDTA, 1 mM EGTA, 1 mM PMSF, 10 mM NaF, 2.5 mM Na_3VO_4, 50 ng/ml calyculin A (Alexis Biochemicals), 10 µg/ml aprotinin, 10 µg/ml leupeptin and 1% phosphatase inhibitor cocktail 1 and 2 (v/v) (Sigma) per two 15-cm dishes for 5 min on ice. Cell extracts were sonicated three times for 1 minute on ice. Cell debris was then removed by centrifugation and equal protein amounts from differentially SILAC-encoded cells were pooled for subsequent MS sample preparation.

MS Sample Preparation (performed by Kathrin Grundner-Culemann and Henrik Daub)

Pooled lysates were adjusted to 6 M urea/1.5 M thiourea and reduced, alkylated and digested in-solution with endoproteinase Lys-C and trypsin as detailed before (Daub et al., 2008). Tryptic peptides were then filtered through a 0.22 µm polyvinylidene fluoride membrane (Millipore) and desalted using reversed-phase C_{18} SepPak cartridges (500 mg maximum capacity, Waters) as described previously (Villén and Gygi, 2008). Desalted peptide samples were snap-frozen in liquid nitrogen, lyophilized, and stored at -20°C. Lyophilized peptides were dissolved in 600 µl 7 mM KH_2PO_4 pH 2.65, 30% acetonitrile (ACN) and loaded onto a 250 x 9.4 mm polySULFOETHYL A column (200 Å pore size, 5 µm

particle size, from PolyLC) operated with an ÄKTA explorer system (GE Healthcare) at 3 ml/min. The flow-through was collected and bound peptides were fractionated by a 30 min gradient ranging from 0% to 30% elution buffer (7 mM KH_2PO_4 pH of 2.65, 30% ACN, 350 mM KCl) (Villén and Gygi, 2008). 3 ml fractions were collected throughout SCX separation and pooled based on the measured UV absorption at 215 nm to twelve samples with rather even peptide amounts. The pooled fractions were snap-frozen in liquid nitrogen and lyophilized to remove ACN. Samples were then desalted using reversed-phase C_{18} SepPak cartridges (100 mg maximum capacity, Waters) prior to a second lyophilisation step.

For phosphopeptide enrichment, lyophilized peptide samples were re-suspended in 200 µl 25 mM formic acid, 40% acetonitrile, and incubated with 2.5 µl PHOS-Select Iron Affinity Gel (Sigma) for 1 h at 25 °C under continuous agitation. Phosphopeptide elution and subsequent desalting with C_{18} StageTips were performed as described (Rappsilber et al., 2007; Villén and Gygi, 2008). StageTip-purified peptide samples were concentrated to 4 µl and mixed with an equal volume of 0.2% trifluoroacetic acid (TFA), 4% ACN prior to MS analysis of technical replicates of each sample.

Mass Spectrometry and Data Processing (performed by Kathrin Grundner-Culemann and Henrik Daub)

All LC-MS/MS analyses were performed on an LTQ-Orbitrap (Thermo Fisher Scientific) connected to a nanoflow HPLC system (Agilent 1100) via a nanoelectrospray ion source (Proxeon Biosystems) as described (Daub et al., 2008; Olsen et al., 2005). Briefly, phosphopeptide-enriched samples were resolved by 15 cm analytical column (75 µm inner diameter) packed with 3 µm C18 beads (Reprosil-AQ Pur, Dr. Maisch GmbH, Germany) in 140 min runs by a gradient from 5% to 40% acetonitrile in 0.5% acetic acid and at a flow rate of 250 nl per minute. Eluting peptides were directly electrosprayed into the mass spectrometer. The LTQ-Orbitrap was operated with Xcalibur 2.0 in the data-dependent mode to automatically switch between full scan MS acquisition in the orbitrap analyser (resolution R=60,000 at m/z=400) and the acquisition of tandem mass spectra of ten multiply charged ions by in the LTQ part of the instrument (Olsen et al., 2006). Multi-stage activation was enabled in the linear ion trap to activate neutral loss species of phosphopeptides at 97.97, 48.99, or 32.66 m/z below the precursor ion for 30 ms during fragmentation (Schroeder et al., 2004). For all full scans in the orbitrap detector a lock-mass ion from ambient air (m/z 429.08875) was used for internal calibration as described (Olsen et al., 2005). Typical mass spectrometric conditions were: spray voltage, 2.4 kV; no sheath and auxiliary gas flow; heated capillary temperature, 175°C; normalized collision

energy 35% for MSA in LTQ. The ion selection threshold was 500 counts for MS^2. An activation q = 0.25 was used.

All 192 raw files (except for raw files 10 and 11 of experiment as4b due to unsuccessful MS runs) acquired in this study were collectively processed with the MaxQuant software suite (version 1.0.13.13), which performs peak list generation, SILAC-based quantification, estimation of false discovery rates, peptide to protein group assembly, and phosphorylation site localization as described previously (Cox and Mann, 2008; Olsen et al., 2010). Peak lists were searched against concatenated forward and reversed version of the human International Protein Index (IPI) database version 3.37 (containing 69141 protein entries and 175 frequently detected contaminants such as porcine trypsin, human keratins and Lys-C) using the Mascot search engine (Matrix Science; version 2.2.04). Carbamidomethylation of cysteine was set as a fixed modification and oxidation of methionine, N-terminal acetylation, losses of ammonia from N-terminal glutamine and cysteine, and phosphorylation on serine, threonine and tyrosine were set as variable modifications. SILAC spectra detected by pre-search MaxQuant analysis were searched with the additional fixed modifications Arg^{10} and/or Lys^8, whereas spectra for which a SILAC state was not assignable prior database searching were searched with Arg^{10} and Lys^8 as variable modifications. Accepted mass tolerances were 7 ppm for the MS and to 0.5 Da for MS/MS peaks. The minimum required peptide length was six amino acids and up to 3 missed cleavages and three labeled amino acids were allowed.

The accepted estimated FDR determined on the basis peptide-spectral matches in the reversed database version was set to 1% for both peptide and protein identifications. Phosphorylation sites were assigned by the PTM scoring algorithm implemented in MaxQuant as described (Olsen et al., 2006; 2010).

Prior to further processing all phosphopeptide evidences were filtered for a Mascot score of at least 7 and a mass error of less than 5 ppm. Phosphopeptides were specified by their amino acid sequence and number of phosphorylation sites. In each technical replicate experiment, the median SILAC ratio was calculated for repeatedly quantified phosphopeptides. These ratios were averaged for each biological replicate experiment in case of SILAC-based phosphopeptide quantification in both technical replicate analyses. The resulting quantified phosphopeptide ratios from biological Mps1^{as} and Mps1^{wt} replicate experiments were considered for all further comparative and statistical analyses. The pair-wise overlap of quantified phosphopeptides for all biological replicate analysis was calculated as described (Choudhary et al., 2009). The distribution of phosphopeptide ratios was visualized by box plots with whiskers indicating 2.5 times the interquartile range. Box plots were computed in the R statistical environment and were either generated for individual biological replicate experiments or average ratios from either all Mps1^{as} or all Mps1^{wt} cell analyses. For the latter box plots, only phosphopeptide ratios were included which were quantified in at least two biological Mps1^{as} as well Mps1^{wt} replicate experiments and exhibited a coefficient of variation of less than 0.3 in both cell lines. For

phosphorylation site analysis, only those with a localization probability of at least 0.75 (class I sites) were considered for further analysis. SILAC ratios determined for localized phosphorylation events were also averaged for each biological replicate experiment in case such ratios were available for both technical replicates.

To identify differential 3-MB-PP1 phosphoregulation in Mps1^{as} *versus* Mps1^{wt} cells, all phosphopeptide or –site ratios measured in at least two biological replicates in both cell lines were log$_2$-transformed and subjected to two-class, unpaired SAM analysis (Tusher et al., 2001). SAM computes a statistics d_i for each ratio to identify significantly different -/+ 3-MB-PP1 ratios in Mps1^{as} *versus* Mps1^{wt} cells and uses permutations of the repeated measurements to calculate false-discovery rates (q values) for different values of a threshold parameter Δ. Missing ratio values were imputed by SAM via a K-Nearest Neighbor algorithm normalization (number of neighbours set to 10).

For all Mps1^{as} / Mps1^{wt} cell ratios reported by SAM (up to an FDR of 60%) we further analyzed whether either the Mps1^{as} or the Mps1^{wt} ratio deviated more strongly from one for different Δ parameters. For further analysis, phosphopeptides and -sites of the SAM output with a false discovery rate (FDR or q value) of 0% obtained for $\Delta \geq 1.189$ and $\Delta \geq 1.268$, respectively, were considered as regulated.

Bioinformatics analysis. (performed by Kathrin Grundner-Culemann and Henrik Daub)

WebLogo was used to display the normalized amino acid frequencies for ± 6 residues surrounding all induced phosphorylation sites upon 3-MB-PP1 wash-out in Mps1[as] cells (Crooks et al., 2004).

Immunological methods

For immunofluorescence microscopy cells were pre-extracted and fixed in formaldehyde as described previously (Maldonado and Kapoor, 2011). In brief, cells were pre-extracted at 37ºC in PEM buffer (100 mM PIPES, 10 mM EGTA, 1 mM $MgCl_2$, pH 6.9) with 0.5% Triton X-100 and 4 M glycerol and then fixed for 10 minutes at 37ºC in form fix (3.7% formaldehyde and 0.2% Triton X-100 in PEM buffer). For analysis of cold-stable microtuble K-fibers, cells were incubated on ice in L-15 medium (Invitrogen) for 10 minutes before 10 minute room temperature fixation in form fix. All subsequent incubations for immunofluorescence microscopy were done at room temperature. Cells were blocked in either 2% BSA (anti-tubulin, anti-GFP) or 10% goat serum (pMps1, pKNL1, pSka3). The following antibodies were used for immunofluorescence FITC-conjugated anti-tubulin monoclonal antibody (Sigma F2168), 1:3000, anti-GFP monoclonal antibody (Invitrogen A-11120), 1:1000, human anti-centromere antibodies (Immunovision, HCT-0100), 1:5000, anti-H2A, pT120 (Active Motif, 39391) 1:2000, anti-Spindly (Bethyl, A301-355A), anti-Bub1 (Santa Cruz, sc-47743) 1:500, and anti-Mad1 (kind gift from Andrea Musacchio) 1:1000. The

phospho-specific antibodies against Mps1 pT33,pS37, Mps1 pT360,pS363, KNL1 pS1831,pS1834, and Ska3 pS34 were generated in rabbits (Pocono Rabbit Farm and Laboratory) through immunization of keyhole limpet hemocyanin (KLH)-conjugated phosphopeptides (EZBiolab). Sera were screened for phospho-selectivity by enzyme-linked immunosorbent assay (ELISA). For positive and negative affinity purification, phosphopeptides and their corresponding unphosphorylated peptides were coupled to a solid-phase support via maleimide chemistry. anti-Mps1 pT33,pS37 was used at 1:1000, anti-Mps1 pT360,pS363 was used at 1:2000, anti-KNL1 pS1831,pS1834 was used at 1:2000, anti-Ska3 pS34 was used at 1:500.

Widefield and phase-contrast images were acquired on an inverted microscope (TE2000; Nikon) equipped with 10x and 40x long-working distance and 100x oil objectives, single-bandpass excitation and emission filters, a camera (ORCA ER; Hamamatsu Photonics), a temperature controlled stage enclosure with CO_2 support (Solent Scientific), and NIS Elements software (Nikon). Imaging was performed in normal growth media at 37ºC. For deconvolution microscopy, an image restoration system (DeltaVision; Applied Precision) based on a microscope (IX-70;Olympus) with a 100x oil objective and a cooled charge-coupled device camera (CoolSnap QE; Photometrics) was used. Calculations were performed using measured point-spread functions. All image analysis was performed in ImageJ. Individual images were cropped and assembled into figures using PhotoShop (CS5; Adobe).

Antibodies used for Western blot include anti-Mps1, pT33,pS37, 1:1000, anti-Mps1 pT360,pS363, 1:2000, anti-KNL1 pS1831,pS1834, 1:1000, anti-Ska3 pS34, 1:500, anti-Ska1 (GeneTex, 119803) 1:1000, anti-Ska3 (Abcam, ab91559) 1:1000, anti-Mps1 (Santa Cruz, sc-56968), anti-GFP (Santa Cruz, sc-9996) 1:1000, anti-H2A (Abcam, Ab18255), 1:2000, anti-H2A, pT120 (Active Motif, 39391) 1:1000, anti-polyHistidine-HRP (Sigma, A7058) 1:5000, anti-MBP-HRP (NEB, E8038), anti-tubulin (Santa Cruz, sc-5286) 1:2000.

Protein Purification and Biochemical Assays (with some help from Rohit Prakash and Paul Smith)

Human Mps1 was expressed as a GST-tagged polypeptide in Sf9 cells in the pDEST15 vector (Invitrogen). Cells were lysed by sonicating in insect cell breakage buffer (100 mM Tris, pH7.5, 20% sucrose, 4 mM EDTA, 0.01% NP-40) and purified on immobilized glutathione. Ska1 complex was purified from BL21 (DE3) *Escherichia coli* strain (Novagen) as previously described (Cheeseman et al., 2006; Welburn et al., 2009). Mps1 N and C terminal fragments were also purified from BL21 (DE3) cells as hexahistidine fusions by nickel affinity chromatography.

Kinase assays were performed at 30ºC with 10 nM GST-Mps1 in kinase buffer (50 mM Tris-HCl, pH 7.5, 1 mM dithiothreitol, 10 mM $MgCl_2$, 10 mM ß-glycerophosphate, 100 µM $NaVO_3$). Reactions were carried out for 5, 10, 20 or

40 minutes and stopped by the addition of sample buffer, followed by heating at 100ºC for 5 minutes. For radiolabeling [γ-^{32}P] ATP was diluted with 100 μM cold ATP. For non-radioactive reactions, 1 mM cold ATP was used.

Microtubule pelleting and bundling assays were performed as described (Cheeseman et al., 2006; Welburn et al., 2009).

Analytical size exclusion chromatography of Ska complexes were performed on a Superose 6 column (GE Healthcare) in gel filtration buffer (50 mM Tris, pH 7.4, 150 mM NaCl, 1 mM EDTA, 1 mM dithiothreitol). Glyercol and sucrose gradients were performed in 25 mM Tris-HCl, pH7.5, 1 mM EDTA, 0.01% NP-40, 400 mM NaCl, 1 mM dithiothreitol.

TIRF Microscopy (performed by Hauke Drechsler and Andrew McAinsh)

Stabilized microtubule experiments were imaged with a exposure time was 50 ms, time-lapse for 1 minute and 30 seconds at 100 ms/frame, 25º C, similar to (Schmidt et al., 2012).

Dynamic microtubule experiments were imaged with a 150 ms exposure time, time-lapse for 5 minutes at 1s/frame, 35º C.

BIBLIOGRAPHY

Abrieu, A., Magnaghi-Jaulin, L., Kahana, J.A., Peter, M., Castro, A., Vigneron, S., Lorca, T., Cleveland, D.W., and Labbé, J.C. (2001). Mps1 is a kinetochore-associated kinase essential for the vertebrate mitotic checkpoint. Cell *106*, 83–93.

Akiyoshi, B., Nelson, C.R., Ranish, J.A., and Biggins, S. (2009). Analysis of Ipl1-mediated phosphorylation of the Ndc80 kinetochore protein in Saccharomyces cerevisiae. Genetics *183*, 1591–1595.

Alushin, G.M., Musinipally, V., Matson, D., Tooley, J., Stukenberg, P.T., and Nogales, E. (2012). Multimodal microtubule binding by the Ndc80 kinetochore complex. Nature Structural & Molecular Biology *19*, 1161–1167.

Alushin, G.M., Ramey, V.H., Pasqualato, S., Ball, D.A., Grigorieff, N., Musacchio, A., and Nogales, E. (2010). The Ndc80 kinetochore complex forms oligomeric arrays along microtubules. Nature *467*, 805–810.

Asbury, C.L., Gestaut, D.R., Powers, A.F., Franck, A.D., and Davis, T.N. (2006). The Dam1 kinetochore complex harnesses microtubule dynamics to produce force and movement. Proc. Natl. Acad. Sci. U.S.a. *103*, 9873–9878.

Barisic, M., and Geley, S. (2011). Spindly switch controls anaphase: Spindly and RZZ functions in chromosome attachment and mitotic checkpoint control. Cc *10*, 449–456.

Berdougo, E., Terret, M.-E., and Jallepalli, P.V. (2009). Functional dissection of mitotic regulators through gene targeting in human somatic cells. Methods Mol. Biol. *545*, 21–37.

Bishop, A.C., Ubersax, J.A., Petsch, D.T., Matheos, D.P., Gray, N.S., Blethrow, J., Shimizu, E., Tsien, J.Z., Schultz, P.G., Rose, M.D., et al. (2000). A chemical switch for inhibitor-sensitive alleles of any protein kinase. Nature *407*, 395–401.

Buffin, E., Lefebvre, C., Huang, J., Gagou, M.E., and Karess, R.E. (2005). Recruitment of Mad2 to the kinetochore requires the Rod/Zw10 complex. Current Biology *15*, 856–861.

Burkard, M.E., Randall, C.L., Larochelle, S., Zhang, C., Shokat, K.M., Fisher, R.P., and Jallepalli, P.V. (2007). Chemical genetics reveals the requirement for Polo-like kinase 1 activity in positioning RhoA and triggering cytokinesis in human cells. Proc. Natl. Acad. Sci. U.S.a. *104*, 4383–4388.

Buschhorn, B.A., and Peters, J.-M. (2006). How APC/C orders destruction. Nature Cell Biology *8*, 209–211.

Castillo, A.R., Meehl, J.B., Morgan, G., Schutz-Geschwender, A., and Winey, M. (2002). The yeast protein kinase Mps1p is required for assembly of the integral spindle pole body component Spc42p. J. Cell Biol. *156*, 453–465.

Chan, G.K., Jablonski, S.A., Starr, D.A., Goldberg, M.L., and Yen, T.J. (2000). Human

Zw10 and ROD are mitotic checkpoint proteins that bind to kinetochores. Nature Cell Biology *2*, 944–947.

Chan, G.K., Jablonski, S.A., Sudakin, V., Hittle, J.C., and Yen, T.J. (1999). Human BUBR1 is a mitotic checkpoint kinase that monitors CENP-E functions at kinetochores and binds the cyclosome/APC. J. Cell Biol. *146*, 941–954.

Chan, Y.W., Jeyaprakash, A.A., Nigg, E.A., and Santamaria, A. (2012). Aurora B controls kinetochore-microtubule attachments by inhibiting Ska complex-KMN network interaction. J. Cell Biol. *196*, 563–571.

Chao, W.C.H., Kulkarni, K., Zhang, Z., Kong, E.H., and Barford, D. (2013). Structure of the mitotic checkpointcomplex. Nature *484*, 208–213.

Cheeseman, I.M., Enquist-Newman, M., Müller-Reichert, T., Drubin, D.G., and Barnes, G. (2001). Mitotic spindle integrity and kinetochore function linked by the Duo1p/Dam1p complex. J. Cell Biol. *152*, 197–212.

Cheeseman, I.M., and Desai, A. (2005). A combined approach for the localization and tandem affinity purification of protein complexes from metazoans. Sci. STKE *2005*, pl1.

Cheeseman, I.M., and Desai, A. (2008). Molecular architecture of the kinetochore-microtubule interface. Nature Reviews Molecular Cell Biology *9*, 33–46.

Cheeseman, I.M., Chappie, J.S., Wilson-Kubalek, E.M., and Desai, A. (2006). The conserved KMN network constitutes the core microtubule-binding site of the kinetochore. Cell *127*, 983–997.

Cheeseman, I.M., Hori, T., Fukagawa, T., and Desai, A. (2008). KNL1 and the CENP-H/I/K complex coordinately direct kinetochore assembly in vertebrates. Mol Biol Cell *19*, 587–594.

Chen, R.-H. (2002). BubR1 is essential for kinetochore localization of other spindle checkpoint proteins and its phosphorylation requires Mad1. J. Cell Biol. *158*, 487–496.

Ciferri, C., Pasqualato, S., Screpanti, E., Varetti, G., Santaguida, S., Reis, Dos, G., Maiolica, A., Polka, J., De Luca, J.G., De Wulf, P., et al. (2008). Implications for Kinetochore-Microtubule Attachment from the Structure of an Engineered Ndc80 Complex. Cell *133*, 427–439.

Ciliberto, A., and Shah, J.V. (2009). A quantitative systems view of the spindle assembly checkpoint. The EMBO Journal *28*, 2162–2173.

Cox, J., and Mann, M. (2008). MaxQuant enables high peptide identification rates, individualized p.p.b.-range mass accuracies and proteome-wide protein quantification. Nat. Biotechnol. *26*, 1367–1372.

Crooks, G.E., Hon, G., Chandonia, J.-M., and Brenner, S.E. (2004). WebLogo: a sequence logo generator. Genome Res. *14*, 1188–1190.

Çivril, F., Wehenkel, A., Giorgi, F.M., Santaguida, S., Di Fonzo, A., Grigorean, G.,

Ciccarelli, F.D., and Musacchio, A. (2010). Structural Analysis of the RZZ Complex Reveals Common Ancestry with Multisubunit Vesicle Tethering Machinery. Structure/Folding and Design *18*, 616–626.

Daub, H., Olsen, J.V., Bairlein, M., Gnad, F., Oppermann, F.S., Körner, R., Greff, Z., Kéri, G., Stemmann, O., and Mann, M. (2008). Kinase-selective enrichment enables quantitative phosphoproteomics of the kinome across the cell cycle. Molecular Cell *31*, 438–448.

Daum, J.R., Wren, J.D., Daniel, J.J., Sivakumar, S., McAvoy, J.N., Potapova, T.A., and Gorbsky, G.J. (2009). Ska3 is required for spindle checkpoint silencing and the maintenance of chromosome cohesion in mitosis. Curr. Biol. *19*, 1467–1472.

De Antoni, A., Pearson, C.G., Cimini, D., Canman, J.C., Sala, V., Nezi, L., Mapelli, M., Sironi, L., Faretta, M., Salmon, E.D., et al. (2005). The Mad1/Mad2 Complex as a Template for Mad2 Activation in the Spindle Assembly Checkpoint. Current Biology *15*, 214–225.

DeLuca, J.G., Dong, Y., Hergert, P., Strauss, J., Hickey, J.M., Salmon, E.D., and McEwen, B.F. (2005). Hec1 and nuf2 are core components of the kinetochore outer plate essential for organizing microtubule attachment sites. Mol Biol Cell *16*, 519–531.

Desai, A., Rybina, S., Müller-Reichert, T., Shevchenko, A., Shevchenko, A., Hyman, A., and Oegema, K. (2003). KNL-1 directs assembly of the microtubule-binding interface of the kinetochore in C. elegans. Genes & Development *17*, 2421–2435.

Ditchfield, C., Johnson, V.L., Tighe, A., Ellston, R., Haworth, C., Johnson, T., Mortlock, A., Keen, N., and Taylor, S.S. (2003). Aurora B couples chromosome alignment with anaphase by targeting BubR1, Mad2, and Cenp-E to kinetochores. J. Cell Biol. *161*, 267–280.

Dou, Z., Schubert, von, C., Körner, R., Santamaria, A., Elowe, S., and Nigg, E.A. (2011). Quantitative mass spectrometry analysis reveals similar substrate consensus motif for human Mps1 kinase and Plk1. PLoS ONE *6*, e18793.

Elowe, S., Hümmer, S., Uldschmid, A., Li, X., and Nigg, E.A. (2007). Tension-sensitive Plk1 phosphorylation on BubR1 regulates the stability of kinetochore microtubule interactions. Genes & Development *21*, 2205–2219.

Emanuele, M.J., Lan, W., Jwa, M., Miller, S.A., Chan, C.S.M., and Stukenberg, P.T. (2008). Aurora B kinase and protein phosphatase 1 have opposing roles in modulating kinetochore assembly. J. Cell Biol. *181*, 241–254.

Foley, E.A., and Kapoor, T.M. (2013). Microtubule attachment and spindle assembly checkpoint signalling at the kinetochore. Nature Reviews Molecular Cell Biology *14*, 25–37.

Foley, E.A., Maldonado, M., and Kapoor, T.M. (2011). Formation of stable attachments between kinetochores and microtubules depends on the B56-PP2A phosphatase. Nature Cell Biology *13*, 1265–1271.

Francisco, L., and Chan, C.S. (1994). Regulation of yeast chromosome segregation by Ipl1 protein kinase and type 1 protein phosphatase. Cell. Mol. Biol. Res. *40*, 207–213.

Fraschini, R., Beretta, A., Sironi, L., Musacchio, A., Lucchini, G., and Piatti, S. (2001). Bub3 interaction with Mad2, Mad3 and Cdc20 is mediated by WD40 repeats and does not require intact kinetochores. The EMBO Journal *20*, 6648–6659.

Fukagawa, T., Nogami, M., Yoshikawa, M., Ikeno, M., Okazaki, T., Takami, Y., Nakayama, T., and Oshimura, M. (2004). Dicer is essential for formation of the heterochromatin structure in vertebrate cells. Nature Cell Biology *6*, 784–791.

Funabiki, H., and Wynne, D.J. (2013). Making an effective switch at the kinetochore by phosphorylation and dephosphorylation. Chromosoma.

Gaitanos, T.N., Santamaria, A., Jeyaprakash, A.A., Bin Wang, Conti, E., and Nigg, E.A. (2009). Stable kinetochore–microtubule interactions depend on the Ska complex and its new component Ska3/C13Orf3. The EMBO Journal *28*, 1442–1452.

Gascoigne, K.E., and Taylor, S.S. (2008). Cancer cells display profound intra- and interline variation following prolonged exposure to antimitotic drugs. Cancer Cell *14*, 111–122.

Griffis, E.R., Stuurman, N., and Vale, R.D. (2007). Spindly, a novel protein essential for silencing the spindle assembly checkpoint, recruits dynein to the kinetochore. J. Cell Biol. *177*, 1005–1015.

Grishchuk, E.L., Efremov, A.K., Volkov, V.A., Spiridonov, I.S., Gudimchuk, N., Westermann, S., Drubin, D., Barnes, G., McIntosh, J.R., and Ataullakhanov, F.I. (2008). The Dam1 ring binds microtubules strongly enough to be a processive as well as energy-efficient coupler for chromosome motion. Proc. Natl. Acad. Sci. U.S.a. *105*, 15423–15428.

Guimaraes, G.J., and DeLuca, J.G. (2009). Connecting with Ska, a key complex at the kinetochore-microtubule interface. The EMBO Journal *28*, 1375–1377.

Hagting, A., Jackman, M., Simpson, K., and Pines, J. (1999). Translocation of cyclin B1 to the nucleus at prophase requires a phosphorylation-dependent nuclear import signal. Current Biology *9*, 680–689.

Han, J.S., Holland, A.J., Fachinetti, D., Kulukian, A., Cetin, B., and Cleveland, D.W. (2013). Catalytic Assembly of the MitoticCheckpoint Inhibitor BubR1-Cdc20by a Mad2-Induced Functional Switch in Cdc20. Molecular Cell 1–13.

Hanisch, A., Silljé, H.H.W., and Nigg, E.A. (2006). Timely anaphase onset requires a novel spindle and kinetochore complex comprising Ska1 and Ska2. The EMBO Journal *25*, 5504–5515.

Hardwick, K.G., Johnston, R.C., Smith, D.L., and Murray, A.W. (2000). MAD3 encodes a novel component of the spindle checkpoint which interacts with Bub3p, Cdc20p, and Mad2p. J. Cell Biol. *148*, 871–882.

Hardwick, K.G., Weiss, E., Luca, F.C., Winey, M., and Murray, A.W. (1996). Activation of the budding yeast spindle assembly checkpoint without mitotic spindle disruption. Science *273*, 953–956.

Hauf, S. (2008). Mps1 Checks Up on Chromosome Attachment. Cell *132*, 181–182.

Hauf, S., Cole, R.W., LaTerra, S., Zimmer, C., Schnapp, G., Walter, R., Heckel, A., van Meel, J., Rieder, C.L., and Peters, J.-M. (2003). The small molecule Hesperadin reveals a role for Aurora B in correcting kinetochore-microtubule attachment and in maintaining the spindle assembly checkpoint. J. Cell Biol. *161*, 281–294.

Hendzel, M.J., Wei, Y., Mancini, M.A., Van Hooser, A., Ranalli, T., Brinkley, B.R., Bazett-Jones, D.P., and Allis, C.D. (1997). Mitosis-specific phosphorylation of histone H3 initiates primarily within pericentromeric heterochromatin during G2 and spreads in an ordered fashion coincident with mitotic chromosome condensation. Chromosoma *106*, 348–360.

Hennrich, M.L., Marino, F., Groenewold, V., Kops, G.J.P.L., Mohammed, S., and Heck, A.J.R. (2013). Universal Quantitative Kinase Assay Based on Diagonal SCX Chromatography and Stable Isotope Dimethyl Labeling Provides High-definition Kinase Consensus Motifs for PKA and Human Mps1. J. Proteome Res. 130403153859009.

Herzog, F., Primorac, I., Dube, P., Lénárt, P., Sander, B., Mechtler, K., Stark, H., and Peters, J.-M. (2009). Structure of the anaphase-promoting complex/cyclosome interacting with a mitotic checkpoint complex. Science *323*, 1477–1481.

Hewitt, L., Tighe, A., Santaguida, S., White, A.M., Jones, C.D., Musacchio, A., Green, S., and Taylor, S.S. (2010). Sustained Mps1 activity is required in mitosis to recruit O-Mad2 to the Mad1-C-Mad2 core complex. J. Cell Biol. *190*, 25–34.

Holland, A.J., Lan, W., Niessen, S., Hoover, H., and Cleveland, D.W. (2010). Polo-like kinase 4 kinase activity limits centrosome overduplication by autoregulating its own stability. J. Cell Biol. *188*, 191–198.

Howell, B.J., Moree, B., Farrar, E.M., Stewart, S., Fang, G., and Salmon, E.D. (2004). Spindle checkpoint protein dynamics at kinetochores in living cells. Current Biology *14*, 953–964.

Hoyt, M.A., Totis, L., and Roberts, B.T. (1991). S. cerevisiae genes required for cell cycle arrest in response to loss of microtubule function. Cell *66*, 507–517.

Janssen, A., Kops, G.J.P.L., and Medema, R.H. (2009). Elevating the frequency of chromosome mis-segregation as a strategy to kill tumor cells. Proc. Natl. Acad. Sci. U.S.a. *106*, 19108–19113.

Janssen, A., Kops, G.J., and Medema, R.H. (2011). Targeting the mitotic checkpoint to kill tumor cells. Horm Cancer *2*, 113–116.

Jelluma, N., Brenkman, A.B., McLeod, I., Yates, J.R., Cleveland, D.W., Medema, R.H., and Kops, G.J.P.L. (2008a). Chromosomal instability by inefficient Mps1 auto-activation due to a weakened mitotic checkpoint and lagging chromosomes. PLoS ONE *3*, e2415.

Jelluma, N., Brenkman, A.B., van den Broek, N.J.F., Cruijsen, C.W.A., van Osch, M.H.J., Lens, S.M.A., Medema, R.H., and Kops, G.J.P.L. (2008b). Mps1 phosphorylates Borealin to control Aurora B activity and chromosome alignment. Cell *132*, 233–246.

Jelluma, N., Dansen, T.B., Sliedrecht, T., Kwiatkowski, N.P., and Kops, G.J.P.L. (2010). Release of Mps1 from kinetochores is crucial for timely anaphase onset. J. Cell Biol. *191*, 281–290.

Jemaà, M., Vitale, I., Kepp, O., Berardinelli, F., Galluzzi, L., Senovilla, L., Mariño, G., Malik, S.A., Rello-Varona, S., Lissa, D., et al. (2012). Selective killing of p53-deficient cancer cells by SP600125. EMBO Mol Med *4*, 500–514.

Jeyaprakash, A.A., Santamaria, A., Jayachandran, U., Chan, Y.W., Benda, C., Nigg, E.A., and Conti, E. (2012). Structural and Functional Organization of the Ska Complex, a Key Component of the Kinetochore-Microtubule Interface. Molecular Cell *46*, 274–286.

Joglekar, A.P., Bloom, K.S., and Salmon, E.D. (2010). Mechanisms of force generation by end-on kinetochore-microtubule attachments. Curr. Opin. Cell Biol. *22*, 57–67.

Johnson, V.L., Scott, M.I.F., Holt, S.V., Hussein, D., and Taylor, S.S. (2004). Bub1 is required for kinetochore localization of BubR1, Cenp-E, Cenp-F and Mad2, and chromosome congression. Journal of Cell Science *117*, 1577–1589.

Jones, M.H., Huneycutt, B.J., Pearson, C.G., Zhang, C., Morgan, G., Shokat, K., Bloom, K., and Winey, M. (2005). Chemical genetics reveals a role for Mps1 kinase in kinetochore attachment during mitosis. Current Biology *15*, 160–165.

Karess, R. (2005). Rod-Zw10-Zwilch: a key player in the spindle checkpoint. Trends Cell Biol. *15*, 386–392.

Kawashima, S.A., Yamagishi, Y., Honda, T., Ishiguro, K.-I., and Watanabe, Y. (2010). Phosphorylation of H2A by Bub1 prevents chromosomal instability through localizing shugoshin. Science *327*, 172–177.

Kemmler, S., Stach, M., Knapp, M., Ortiz, J., Pfannstiel, J., Ruppert, T., and Lechner, J. (2009). Mimicking Ndc80 phosphorylation triggers spindle assembly checkpoint signalling. The EMBO Journal *28*, 1099–1110.

Kim, S., Sun, H., Ball, H.L., Wassmann, K., Luo, X., and Yu, H. (2010a). Phosphorylation of the spindle checkpoint protein Mad2 regulates its conformational transition. Proc. Natl. Acad. Sci. U.S.a. *107*, 19772–19777.

Kim, Y., Holland, A.J., Lan, W., and Cleveland, D.W. (2010b). Aurora Kinases and Protein Phosphatase 1 Mediate Chromosome Congression through Regulation of CENP-E. Cell *142*, 444–455.

Kiyomitsu, T., Murakami, H., and Yanagida, M. (2011). Protein interaction domain mapping of human kinetochore protein Blinkin reveals a consensus motif for binding of spindle assembly checkpoint proteins Bub1 and BubR1. Mol. Cell. Biol. *31*, 998–1011.

Kiyomitsu, T., Obuse, C., and Yanagida, M. (2007). Human Blinkin/AF15q14 is required

for chromosome alignment and the mitotic checkpoint through direct interaction with Bub1 and BubR1. Developmental Cell *13*, 663–676.

Klebig, C., Korinth, D., and Meraldi, P. (2009a). Bub1 regulates chromosome segregation in a kinetochore-independent manner. J. Cell Biol. *185*, 841–858.

Klebig, C., Toso, A., Borusu, S., and Meraldi, P. (2009b). Analysing kinetochore function in human cells: spindle checkpoint and chromosome congression. Methods Mol. Biol. *545*, 205–220.

Kops, G.J.P.L., Foltz, D.R., and Cleveland, D.W. (2004). Lethality to human cancer cells through massive chromosome loss by inhibition of the mitotic checkpoint. Proc. Natl. Acad. Sci. U.S.a. *101*, 8699–8704.

Kraft, C., Herzog, F., Gieffers, C., Mechtler, K., Hagting, A., Pines, J., and Peters, J.-M. (2003). Mitotic regulation of the human anaphase-promoting complex by phosphorylation. The EMBO Journal *22*, 6598–6609.

Kulukian, A., Han, J.S., and Cleveland, D.W. (2009). Unattached kinetochores catalyze production of an anaphase inhibitor that requires a Mad2 template to prime Cdc20 for BubR1 binding. Developmental Cell *16*, 105–117.

Kwiatkowski, N., Jelluma, N., Filippakopoulos, P., Soundararajan, M., Manak, M.S., Kwon, M., Choi, H.G., Sim, T., Deveraux, Q.L., Rottmann, S., et al. (2010). Small-molecule kinase inhibitors provide insight into Mps1 cell cycle function. Nat. Chem. Biol. *6*, 359–368.

Lampert, F., Hornung, P., and Westermann, S. (2010). The Dam1 complex confers microtubule plus end-tracking activity to the Ndc80 kinetochore complex. J. Cell Biol. *189*, 641–649.

Lampert, F., Mieck, C., Alushin, G.M., Nogales, E., and Westermann, S. (2013). Molecular requirements for the formation of a kinetochore-microtubule interface by Dam1 and Ndc80 complexes. J. Cell Biol. *200*, 21–30.

Lampson, M.A., Renduchitala, K., Khodjakov, A., and Kapoor, T.M. (2004). Correcting improper chromosome-spindle attachments during cell division. Nature Cell Biology *6*, 232–237.

Lan, W., and Cleveland, D.W. (2010). A chemical tool box defines mitotic and interphase roles for Mps1 kinase. J. Cell Biol. *190*, 21–24.

Lauzé, E., Stoelcker, B., Luca, F.C., Weiss, E., Schutz, A.R., and Winey, M. (1995). Yeast spindle pole body duplication gene MPS1 encodes an essential dual specificity protein kinase. The EMBO Journal *14*, 1655–1663.

Lénárt, P., Petronczki, M., Steegmaier, M., Di Fiore, B., Lipp, J.J., Hoffmann, M., Rettig, W.J., Kraut, N., and Peters, J.-M. (2007). The Small-Molecule Inhibitor BI 2536 Reveals Novel Insights into Mitotic Roles of Polo-like Kinase 1. Current Biology *17*, 304–315.

Li, R., and Murray, A.W. (1991). Feedback control of mitosis in budding yeast. Cell *66*,

519–531.

Li, X., and Nicklas, R.B. (1995). Mitotic forces control a cell-cycle checkpoint. Nature *373*, 630–632.

Li, Y., Yu, W., Liang, Y., and Zhu, X. (2007). Kinetochore dynein generates a poleward pulling force to facilitate congression and full chromosome alignment. Cell Res. *17*, 701–712.

Liu, D., Vleugel, M., Backer, C.B., Hori, T., Fukagawa, T., Cheeseman, I.M., and Lampson, M.A. (2010). Regulated targeting of protein phosphatase 1 to the outer kinetochore by KNL1 opposes Aurora B kinase. J. Cell Biol. *188*, 809–820.

Liu, S.-T., Chan, G.K.T., Hittle, J.C., Fujii, G., Lees, E., and Yen, T.J. (2003). Human MPS1 kinase is required for mitotic arrest induced by the loss of CENP-E from kinetochores. Mol Biol Cell *14*, 1638–1651.

Liu, S.-T., Rattner, J.B., Jablonski, S.A., and Yen, T.J. (2006). Mapping the assembly pathways that specify formation of the trilaminar kinetochore plates in human cells. J. Cell Biol. *175*, 41–53.

Liu, X., and Winey, M. (2012). The MPS1 family of protein kinases. Annu. Rev. Biochem. *81*, 561–585.

London, N., Ceto, S., Ranish, J.A., and Biggins, S. (2012). Phosphoregulation of Spc105 by Mps1 and PP1 regulates Bub1 localization to kinetochores. Curr. Biol. *22*, 900–906.

Lu, Y., Wang, Z., Ge, L., Chen, N., and Liu, H. (2009). The RZZ complex and the spindle assembly checkpoint. Cell Struct. Funct. *34*, 31–45.

Maciejowski, J., George, K.A., Terret, M.-E., Zhang, C., Shokat, K.M., and Jallepalli, P.V. (2010). Mps1 directs the assembly of Cdc20 inhibitory complexes during interphase and mitosis to control M phase timing and spindle checkpoint signaling. J. Cell Biol. *190*, 89–100.

Maldonado, M., and Kapoor, T.M. (2011). Constitutive Mad1 targeting to kinetochores uncouples checkpoint signalling from chromosome biorientation. Nature Cell Biology *13*, 475–482.

Malureanu, L.A., Jeganathan, K.B., Hamada, M., Wasilewski, L., Davenport, J., and van Deursen, J.M. (2009). BubR1 N terminus acts as a soluble inhibitor of cyclin B degradation by APC/C(Cdc20) in interphase. Developmental Cell *16*, 118–131.

Martin-Lluesma, S., Stucke, V.M., and Nigg, E.A. (2002). Role of Hec1 in spindle checkpoint signaling and kinetochore recruitment of Mad1/Mad2. Science *297*, 2267–2270.

Maure, J.-F., Kitamura, E., and Tanaka, T.U. (2007). Mps1 kinase promotes sister-kinetochore bi-orientation by a tension-dependent mechanism. Current Biology *17*, 2175–2182.

Menant, A., and Karess, R. (2010). RZZ finds its ancestral roots. Structure *18*, 549–550.

Meraldi, P., and Sorger, P.K. (2005). A dual role for Bub1 in the spindle checkpoint and chromosome congression. The EMBO Journal *24*, 1621–1633.

Meraldi, P., Draviam, V.M., and Sorger, P.K. (2004). Timing and checkpoints in the regulation of mitotic progression. Developmental Cell *7*, 45–60.

Miranda, J.L., Wulf, P.D., Sorger, P.K., and Harrison, S.C. (2005). The yeast DASH complex forms closed rings on microtubules. Nature Structural & Molecular Biology *12*, 138–143.

Morrow, C.J., Tighe, A., Johnson, V.L., Scott, M.I.F., Ditchfield, C., and Taylor, S.S. (2005). Bub1 and aurora B cooperate to maintain BubR1-mediated inhibition of APC/CCdc20. Journal of Cell Science *118*, 3639–3652.

Musacchio, A., and Salmon, E.D. (2007). The spindle-assembly checkpoint in space and time. Nature Reviews Molecular Cell Biology *8*, 379–393.

Nilsson, J., Yekezare, M., Minshull, J., and Pines, J. (2008). The APC/C maintains the spindle assembly checkpoint by targeting Cdc20 for destruction. Nature Cell Biology *10*, 1411–1420.

Ohta, S., Bukowski-Wills, J.-C., Sanchez-Pulido, L., Alves, F. de L., Wood, L., Chen, Z.A., Platani, M., Fischer, L., Hudson, D.F., Ponting, C.P., et al. (2010). The protein composition of mitotic chromosomes determined using multiclassifier combinatorial proteomics. Cell *142*, 810–821.

Olsen, J.V., Blagoev, B., Gnad, F., Macek, B., Kumar, C., Mortensen, P., and Mann, M. (2006). Global, in vivo, and site-specific phosphorylation dynamics in signaling networks. Cell *127*, 635–648.

Olsen, J.V., de Godoy, L.M.F., Li, G., Macek, B., Mortensen, P., Pesch, R., Makarov, A., Lange, O., Horning, S., and Mann, M. (2005). Parts per million mass accuracy on an Orbitrap mass spectrometer via lock mass injection into a C-trap. Mol. Cell Proteomics *4*, 2010–2021.

Olsen, J.V., Vermeulen, M., Santamaria, A., Kumar, C., Miller, M.L., Jensen, L.J., Gnad, F., Cox, J., Jensen, T.S., Nigg, E.A., et al. (2010). Quantitative phosphoproteomics reveals widespread full phosphorylation site occupancy during mitosis. Sci Signal *3*, ra3.

Oppermann, F.S., Grundner-Culemann, K., Kumar, C., Gruss, O.J., Jallepalli, P.V., and Daub, H. (2012). Combination of chemical genetics and phosphoproteomics for kinase signaling analysis enables confident identification of cellular downstream targets. Mol. Cell Proteomics *11*, O111.012351.

Palframan, W.J., Meehl, J.B., Jaspersen, S.L., Winey, M., and Murray, A.W. (2006). Anaphase inactivation of the spindle checkpoint. Science *313*, 680–684.

Perera, D., Tilston, V., Hopwood, J.A., Barchi, M., Boot-Handford, R.P., and Taylor, S.S. (2007). Bub1 maintains centromeric cohesion by activation of the spindle checkpoint.

Developmental Cell *13*, 566–579.

Peters, J.-M. (2006). The anaphase promoting complex/cyclosome: a machine designed to destroy. Nature Reviews Molecular Cell Biology *7*, 644–656.

Pinsky, B.A., and Biggins, S. (2005). The spindle checkpoint: tension versus attachment. Trends Cell Biol. *15*, 486–493.

Pinsky, B.A., Kung, C., Shokat, K.M., and Biggins, S. (2006). The Ipl1-Aurora protein kinase activates the spindle checkpoint by creating unattached kinetochores. Nature Cell Biology *8*, 78–83.

Pinsky, B.A., Nelson, C.R., and Biggins, S. (2009). Protein phosphatase 1 regulates exit from the spindle checkpoint in budding yeast. Curr. Biol. *19*, 1182–1187.

Pomerening, J.R., Kim, S.Y., and Ferrell, J.E. (2005). Systems-level dissection of the cell-cycle oscillator: bypassing positive feedback produces damped oscillations. Cell *122*, 565–578.

Raaijmakers, J.A., Tanenbaum, M.E., Maia, A.F., and Medema, R.H. (2009). RAMA1 is a novel kinetochore protein involved in kinetochore-microtubule attachment. Journal of Cell Science *122*, 2436–2445.

Rago, F., and Cheeseman, I.M. (2013). Review series: The functions and consequences of force at kinetochores. J. Cell Biol. *200*, 557–565.

Rappsilber, J., Mann, M., and Ishihama, Y. (2007). Protocol for micro-purification, enrichment, pre-fractionation and storage of peptides for proteomics using StageTips. Nature Protocols *2*, 1896–1906.

Rieder, C.L. (1981). The structure of the cold-stable kinetochore fiber in metaphase PtK1 cells. Chromosoma *84*, 145–158.

Rieder, C.L., and Borisy, G.G. (1981). The attachment of kinetochores to the pro-metaphase spindle in PtK1 cells. Recovery from low temperature treatment. Chromosoma *82*, 693–716.

Rieder, C.L., Cole, R.W., Khodjakov, A., and Sluder, G. (1995). The checkpoint delaying anaphase in response to chromosome monoorientation is mediated by an inhibitory signal produced by unattached kinetochores. J. Cell Biol. *130*, 941–948.

Rieder, C.L., Schultz, A., Cole, R., and Sluder, G. (1994). Anaphase onset in vertebrate somatic cells is controlled by a checkpoint that monitors sister kinetochore attachment to the spindle. J. Cell Biol. *127*, 1301–1310.

Rischitor, P.E., May, K.M., and Hardwick, K.G. (2007). Bub1 is a fission yeast kinetochore scaffold protein, and is sufficient to recruit other spindle checkpoint proteins to ectopic sites on chromosomes. PLoS ONE *2*, e1342.

Rosenberg, J.S., Cross, F.R., and Funabiki, H. (2011). KNL1/Spc105 recruits PP1 to silence the spindle assembly checkpoint. Curr. Biol. *21*, 942–947.

Santaguida, S., Tighe, A., D'Alise, A.M., Taylor, S.S., and Musacchio, A. (2010). Dissecting the role of MPS1 in chromosome biorientation and the spindle checkpoint through the small molecule inhibitor reversine. J. Cell Biol. *190*, 73–87.

Santaguida, S., and Musacchio, A. (2009). The life and miracles of kinetochores. *28*, 2511–2531.

Santaguida, S., Vernieri, C., Villa, F., Ciliberto, A., and Musacchio, A. (2011). Evidence that Aurora B is implicated in spindle checkpoint signalling independently of error correction. The EMBO Journal *30*, 1508–1519.

Sauer, G., Körner, R., Hanisch, A., Ries, A., Nigg, E.A., and Silljé, H.H.W. (2005). Proteome analysis of the human mitotic spindle. Mol. Cell Proteomics *4*, 35–43.

Saurin, A.T., van der Waal, M.S., Medema, R.H., Lens, S.M.A., and Kops, G.J.P.L. (2011). Aurora B potentiates Mps1 activation to ensure rapid checkpoint establishment at the onset of mitosis. Nat Commun *2*, 316.

Schmidt, M., Budirahardja, Y., Klompmaker, R., and Medema, R.H. (2005). Ablation of the spindle assembly checkpoint by a compound targeting Mps1. EMBO Rep. *6*, 866–872.

Schmidt, J.C., Arthanari, H., Boeszoermenyi, A., Dashkevich, N.M., Wilson-Kubalek, E.M., Monnier, N., Markus, M., Oberer, M., Milligan, R.A., Bathe, M., et al. (2012). The Kinetochore-Bound Ska1 Complex Tracks Depolymerizing Microtubules and Binds to Curved Protofilaments. Developmental Cell *23*, 968–980.

Schroeder, M.J., Shabanowitz, J., Schwartz, J.C., Hunt, D.F., and Coon, J.J. (2004). A neutral loss activation method for improved phosphopeptide sequence analysis by quadrupole ion trap mass spectrometry. Anal. Chem. *76*, 3590–3598.

Screpanti, E., De Antoni, A., Alushin, G.M., Petrovic, A., Melis, T., Nogales, E., and Musacchio, A. (2011). Direct binding of Cenp-C to the Mis12 complex joins the inner and outer kinetochore. Curr. Biol. *21*, 391–398.

Sharp-Baker, H., and Chen, R.H. (2001). Spindle checkpoint protein Bub1 is required for kinetochore localization of Mad1, Mad2, Bub3, and CENP-E, independently of its kinase activity. J. Cell Biol. *153*, 1239–1250.

Shepperd, L.A., Meadows, J.C., Sochaj, A.M., Lancaster, T.C., Zou, J., Buttrick, G.J., Rappsilber, J., Hardwick, K.G., and Millar, J.B.A. (2012). Phosphodependent recruitment of Bub1 and Bub3 to Spc7/KNL1 by Mph1 kinase maintains the spindle checkpoint. Curr. Biol. *22*, 891–899.

Shimogawa, M.M., Graczyk, B., Gardner, M.K., Francis, S.E., White, E.A., Ess, M., Molk, J.N., Ruse, C., Niessen, S., Yates, J.R., et al. (2006). Mps1 phosphorylation of Dam1 couples kinetochores to microtubule plus ends at metaphase. Current Biology *16*, 1489–1501.

Sliedrecht, T., Zhang, C., Shokat, K.M., and Kops, G.J.P.L. (2010). Chemical genetic inhibition of Mps1 in stable human cell lines reveals novel aspects of Mps1 function in

mitosis. PLoS ONE *5*, e10251.

Steegmaier, M., Hoffmann, M., Baum, A., Lénárt, P., Petronczki, M., Krssák, M., Gürtler, U., Garin-Chesa, P., Lieb, S., Quant, J., et al. (2007). BI 2536, a potent and selective inhibitor of polo-like kinase 1, inhibits tumor growth in vivo. Current Biology *17*, 316–322.

Stucke, V.M., Baumann, C., and Nigg, E.A. (2004). Kinetochore localization and microtubule interaction of the human spindle checkpoint kinase Mps1. Chromosoma *113*, 1–15.

Stucke, V.M., Silljé, H.H.W., Arnaud, L., and Nigg, E.A. (2002). Human Mps1 kinase is required for the spindle assembly checkpoint but not for centrosome duplication. The EMBO Journal *21*, 1723–1732.

Sudakin, V., Chan, G.K., and Yen, T.J. (2001). Checkpoint inhibition of the APC/C in HeLa cells is mediated by a complex of BUBR1, BUB3, CDC20, and MAD2. J. Cell Biol. *154*, 925–936.

Suijkerbuijk, S.J.E., van Dam, T.J.P., Karagöz, G.E., Castelmur, von, E., Hubner, N.C., Duarte, A.M.S., Vleugel, M., Perrakis, A., Rüdiger, S.G.D., Snel, B., et al. (2012a). The vertebrate mitotic checkpoint protein BUBR1 is an unusual pseudokinase. Developmental Cell *22*, 1321–1329.

Suijkerbuijk, S.J.E., van Osch, M.H.J., Bos, F.L., Hanks, S., Rahman, N., and Kops, G.J.P.L. (2010). Molecular causes for BUBR1 dysfunction in the human cancer predisposition syndrome mosaic variegated aneuploidy. Cancer Research *70*, 4891–4900.

Suijkerbuijk, S.J.E., Vleugel, M., Teixeira, A., and Kops, G.J.P.L. (2012b). Integration of kinase and phosphatase activities by BUBR1 ensures formation of stable kinetochore-microtubule attachments. Developmental Cell *23*, 745–755.

Sundin, L.J.R., Guimaraes, G.J., and DeLuca, J.G. (2011). The NDC80 complex proteins Nuf2 and Hec1 make distinct contributions to kinetochore-microtubule attachment in mitosis. Mol Biol Cell *22*, 759–768.

Swanton, C., Marani, M., Pardo, O., Warne, P.H., Kelly, G., Sahai, E., Elustondo, F., Chang, J., Temple, J., Ahmed, A.A., et al. (2007). Regulators of mitotic arrest and ceramide metabolism are determinants of sensitivity to paclitaxel and other chemotherapeutic drugs. Cancer Cell *11*, 498–512.

Tanaka, K., Kitamura, E., Kitamura, Y., and Tanaka, T.U. (2007). Molecular mechanisms of microtubule-dependent kinetochore transport toward spindle poles. J. Cell Biol. *178*, 269–281.

Tang, Z., Bharadwaj, R., Li, B., and Yu, H. (2001). Mad2-Independent inhibition of APCCdc20 by the mitotic checkpoint protein BubR1. Developmental Cell *1*, 227–237.

Tang, Z., Shu, H., Oncel, D., Chen, S., and Yu, H. (2004). Phosphorylation of Cdc20 by Bub1 provides a catalytic mechanism for APC/C inhibition by the spindle checkpoint. Molecular Cell *16*, 387–397.

Tannous, B.A., Kerami, M., Van der Stoop, P.M., Kwiatkowski, N., Wang, J., Zhou, W., Kessler, A.F., Lewandrowski, G., Hiddingh, L., Sol, N., et al. (2013). Effects of the Selective MPS1 Inhibitor MPS1-IN-3 on Glioblastoma Sensitivity to Antimitotic Drugs. J. Natl. Cancer Inst.

Taylor, S.S., and McKeon, F. (1997). Kinetochore localization of murine Bub1 is required for normal mitotic timing and checkpoint response to spindle damage. Cell *89*, 727–735.

Taylor, S.S., Ha, E., and McKeon, F. (1998). The human homologue of Bub3 is required for kinetochore localization of Bub1 and a Mad3/Bub1-related protein kinase. J. Cell Biol. *142*, 1–11.

Terret, M.-E., Sherwood, R., Rahman, S., Qin, J., and Jallepalli, P.V. (2009). Cohesin acetylation speeds the replication fork. Nature *462*, 231–234.

Theis, M., Slabicki, M., Junqueira, M., Paszkowski-Rogacz, M., Sontheimer, J., Kittler, R., Heninger, A.-K., Glatter, T., Kruusmaa, K., Poser, I., et al. (2009). Comparative profiling identifies C13orf3 as a component of the Ska complex required for mammalian cell division. The EMBO Journal *28*, 1453–1465.

Tien, J.F., Umbreit, N.T., Gestaut, D.R., Franck, A.D., Cooper, J., Wordeman, L., Gonen, T., Asbury, C.L., and Davis, T.N. (2010). Cooperation of the Dam1 and Ndc80 kinetochore complexes enhances microtubule coupling and is regulated by aurora B. J. Cell Biol. *189*, 713–723.

Tighe, A., Staples, O., and Taylor, S. (2008). Mps1 kinase activity restrains anaphase during an unperturbed mitosis and targets Mad2 to kinetochores. J. Cell Biol. *181*, 893–901.

Tooley, J.G., Miller, S.A., and Stukenberg, P.T. (2011). The Ndc80 complex uses a tripartite attachment point to couple microtubule depolymerization to chromosome movement. Mol Biol Cell *22*, 1217–1226.

Torras-Llort, M., Moreno-Moreno, O., and Azorín, F. (2009). Focus on the centre: the role of chromatin on the regulation of centromere identity and function. The EMBO Journal *28*, 2337–2348.

Umbreit, N.T., Gestaut, D.R., Tien, J.F., Vollmar, B.S., Gonen, T., Asbury, C.L., and Davis, T.N. (2012). The Ndc80 kinetochore complex directly modulates microtubule dynamics. Proc. Natl. Acad. Sci. U.S.a. *109*, 16113–16118.

Vanoosthuyse, V., and Hardwick, K.G. (2005). Bub1 and the multilayered inhibition of Cdc20-APC/C in mitosis. Trends Cell Biol. *15*, 231–233.

Vanoosthuyse, V., and Hardwick, K.G. (2009). Overcoming inhibition in the spindle checkpoint. Genes & Development *23*, 2799–2805.

Varma, D., Wan, X., Cheerambathur, D., Gassmann, R., Suzuki, A., Lawrimore, J., Desai, A., and Salmon, E.D. (2013). Spindle assembly checkpoint proteins are positioned close to core microtubule attachment sites at kinetochores. J. Cell Biol. *202*, 735–746.

Vigneron, S., Prieto, S., Bernis, C., Labbé, J.-C., Castro, A., and Lorca, T. (2004). Kinetochore localization of spindle checkpoint proteins: who controls whom? Mol Biol Cell *15*, 4584–4596.

Villén, J., and Gygi, S.P. (2008). The SCX/IMAC enrichment approach for global phosphorylation analysis by mass spectrometry. Nature Protocols *3*, 1630–1638.

Vink, M., Simonetta, M., Transidico, P., Ferrari, K., Mapelli, M., De Antoni, A., Massimiliano, L., Ciliberto, A., Faretta, M., Salmon, E.D., et al. (2006). In Vitro FRAP Identifies the Minimal Requirements for Mad2 Kinetochore Dynamics. Current Biology *16*, 755–766.

Wainman, A., Giansanti, M.G., Goldberg, M.L., and Gatti, M. (2012). The Drosophila RZZ complex - roles in membrane trafficking and cytokinesis. Journal of Cell Science *125*, 4014–4025.

Wassmann, K., Liberal, V., and Benezra, R. (2003). Mad2 phosphorylation regulates its association with Mad1 and the APC/C. The EMBO Journal *22*, 797–806.

Weaver, B.A.A., and Cleveland, D.W. (2009). The role of aneuploidy in promoting and suppressing tumors. J. Cell Biol. *185*, 935–937.

Wei, R.R., Sorger, P.K., and Harrison, S.C. (2005). Molecular organization of the Ndc80 complex, an essential kinetochore component. Proc. Natl. Acad. Sci. U.S.a. *102*, 5363–5367.

Weiss, E., and Winey, M. (1996). The Saccharomyces cerevisiae spindle pole body duplication gene MPS1 is part of a mitotic checkpoint. J. Cell Biol. *132*, 111–123.

Welburn, J.P.I., Grishchuk, E.L., Backer, C.B., Wilson-Kubalek, E.M., Yates, J.R., and Cheeseman, I.M. (2009). The human kinetochore Ska1 complex facilitates microtubule depolymerization-coupled motility. Developmental Cell *16*, 374–385.

Welburn, J.P.I., Vleugel, M., Liu, D., Yates, J.R., Lampson, M.A., Fukagawa, T., and Cheeseman, I.M. (2010). Aurora B phosphorylates spatially distinct targets to differentially regulate the kinetochore-microtubule interface. Molecular Cell *38*, 383–392.

Westermann, S., Avila-Sakar, A., Wang, H.-W., Niederstrasser, H., Wong, J., Drubin, D.G., Nogales, E., and Barnes, G. (2005). Formation of a dynamic kinetochore-microtubule interface through assembly of the Dam1 ring complex. Molecular Cell *17*, 277–290.

Wigge, P.A., and Kilmartin, J.V. (2001). The Ndc80p complex from Saccharomyces cerevisiae contains conserved centromere components and has a function in chromosome segregation. J. Cell Biol. *152*, 349–360.

Williams, B.C., Li, Z., Liu, S., Williams, E.V., Leung, G., Yen, T.J., and Goldberg, M.L. (2003). Zwilch, a new component of the ZW10/ROD complex required for kinetochore functions. Mol Biol Cell *14*, 1379–1391.

Winey, M., Goetsch, L., Baum, P., and Byers, B. (1991). MPS1 and MPS2: novel yeast

genes defining distinct steps of spindle pole body duplication. J. Cell Biol. *114*, 745–754.

Wong, J., Nakajima, Y., Westermann, S., Shang, C., Kang, J.S., Goodner, C., Houshmand, P., Fields, S., Chan, C.S.M., Drubin, D., et al. (2007). A protein interaction map of the mitotic spindle. Mol Biol Cell *18*, 3800–3809.

Wong, O.K., and Fang, G. (2005). Plx1 is the 3F3/2 kinase responsible for targeting spindle checkpoint proteins to kinetochores. J. Cell Biol. *170*, 709–719.

Xia, G., Luo, X., Habu, T., Rizo, J., Matsumoto, T., and Yu, H. (2004). Conformation-specific binding of p31(comet) antagonizes the function of Mad2 in the spindle checkpoint. The EMBO Journal *23*, 3133–3143.

Yamagishi, Y., Yang, C.-H., Tanno, Y., and Watanabe, Y. (2012). MPS1/Mph1 phosphorylates the kinetochore protein KNL1/Spc7 to recruit SAC components. Nature Cell Biology *14*, 746–752.

Yang, M., Li, B., Tomchick, D.R., Machius, M., Rizo, J., Yu, H., and Luo, X. (2007). p31comet blocks Mad2 activation through structural mimicry. Cell *131*, 744–755.

Yang, Z., Kenny, A.E., Brito, D.A., and Rieder, C.L. (2009). Cells satisfy the mitotic checkpoint in Taxol, and do so faster in concentrations that stabilize syntelic attachments. J. Cell Biol. *186*, 675–684.

Yu, H., and Tang, Z. (2005). Bub1 multitasking in mitosis. Cc *4*, 262–265.

Zich, J., and Hardwick, K.G. (2010). Getting down to the phosphorylated "nuts and bolts" of spindle checkpoint signalling. Trends Biochem. Sci. *35*, 18–27.